GDD
Gas Detectors Development Group

The 7th International Conference on
Micro Pattern Gaseous Detectors 2022
Weizmann Institute of Science, Rehovot, Israel

MPGDs in the High Luminosity LHC ERA

E. Oliveri, CERN EP-DT-DD, Gas Detector Development (GDD) team

12 December 2022

Outline

- **High Luminosity LHC - Machine**
- **High Luminosity LHC - Experiments**
  - ALICE (TPC, **GEM**)
  - ATLAS (Muon, **MM**)
  - CMS (Muon, **GEM**)
  - LHCb (Muon, **μRWELL**)
- **Some slides shared between them…**
- **Physics Beyond Collider @ CERN waiting or during HL-LHC**
- **Summary**

Outline

- **High Luminosity LHC - Machine**
- **High Luminosity LHC - Experiments**
  - ALICE (TPC, **GEM**)
  - ATLAS (Muon, **MM**)
  - CMS (Muon, **GEM**)
  - LHCb (Muon, **μRWELL**)

.. And what has been left out

.. or temporarily postponed

- **Some slides shared between them…**
- **Physics Beyond Collider @ CERN waiting or during HL-LHC**
- **Summary and Outlook**

High Luminosity LHC - Machine

High Luminosity LHC (Run4++, ~2029++)

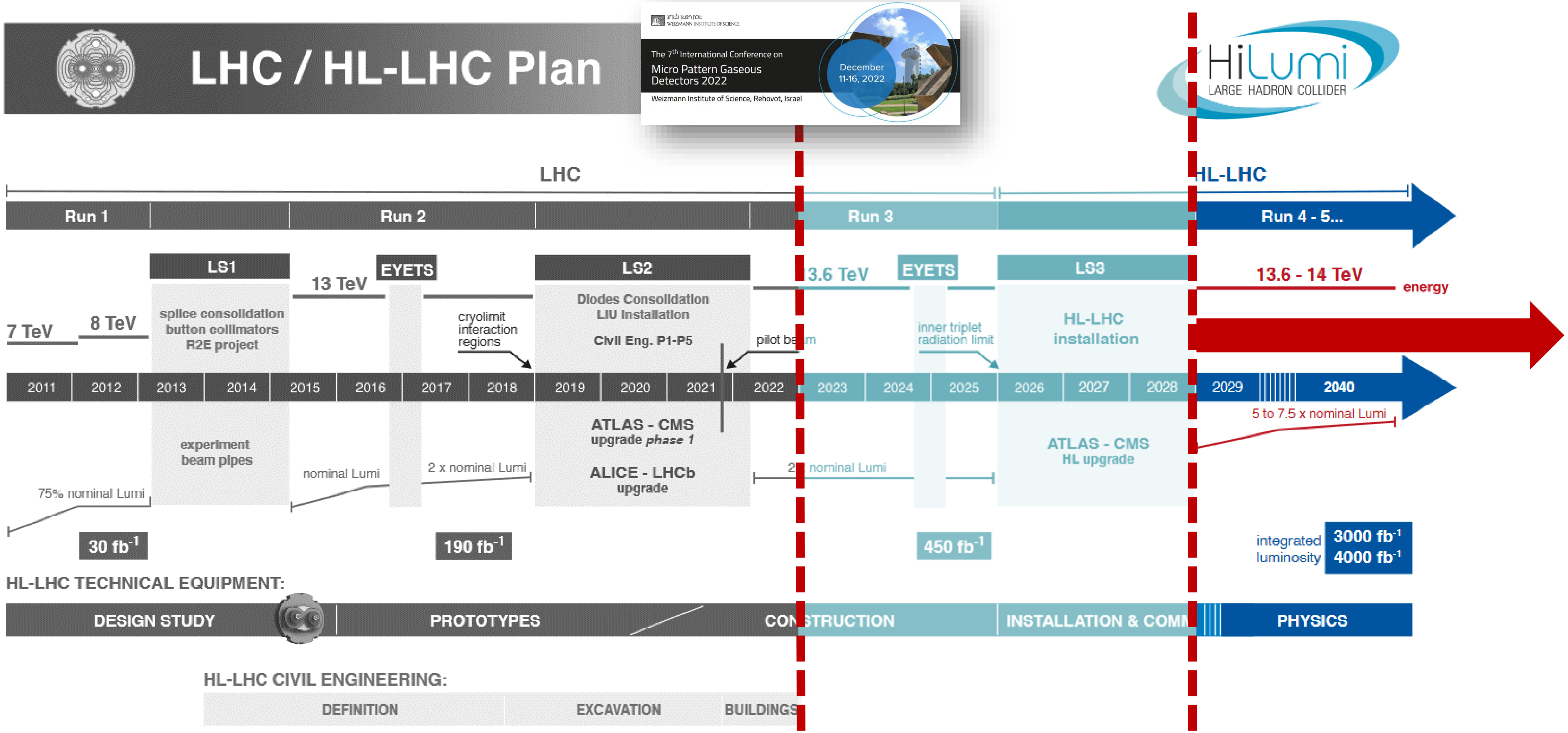

https://hilumilhc.web.cern.ch/sites/default/files/HL-LHC_Janvier2022.pdf

High Luminosity LHC

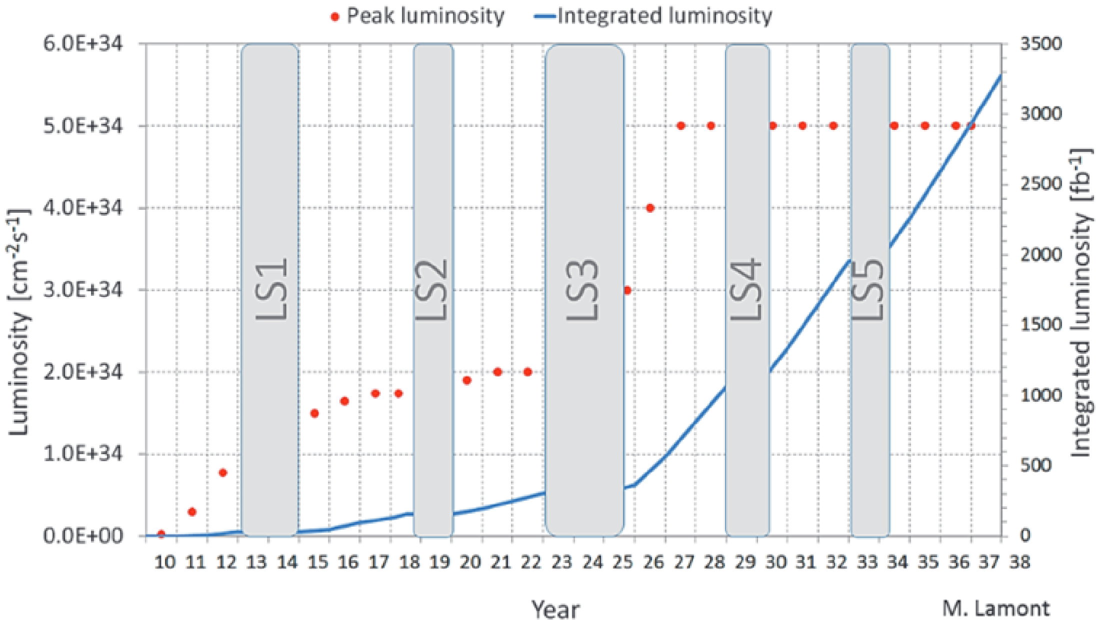

Fig. 7. Peak luminosity (red dots) and integrated luminosity (blue line) vs time till 2035.

Levelling (stable instantaneous luminosity during the run)

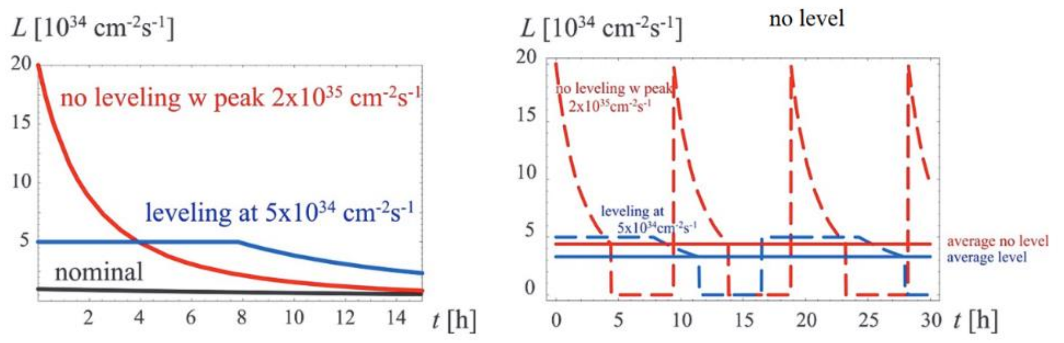

Fig. 3. Left: Luminosity profile for a single long run starting at nominal peak luminosity (black line), with upgrade no leveling (red line) with leveling (dotted line). Right: Luminosity profile with optimized run time, without and with leveling (blue and red dashed lines), and average luminosity in both cases (solid lines).

Crab Cavity (increased number of collision per crossing)

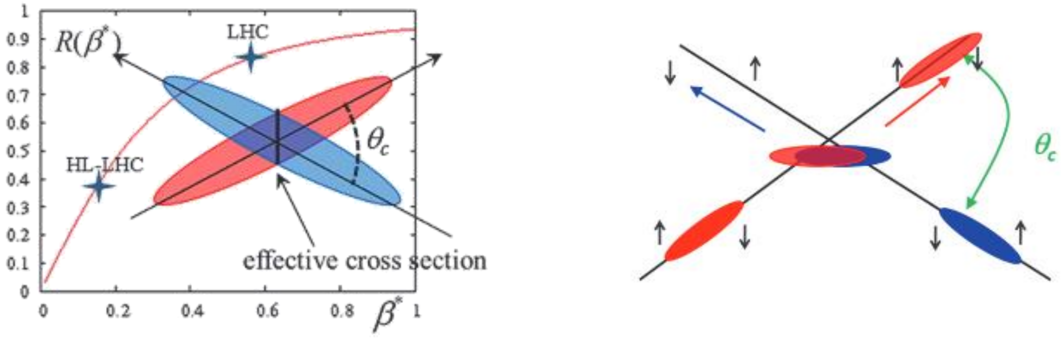

Fig. 5. Behavior of geometrical reduction factor of luminosity vs. β^* for constant normalized beam separation with indicated two operating points: Nominal LHC and HL-LHC. The sketch of bunch crossing shows the reduction mechanism.

Introduction to the HL-LHC Project Rossi , L (CERN) ; Brüning, O (CERN), Adv. Ser. Dir. High Energy Phys. 24 (2015) 1-17, The High Luminosity Large Hadron Collider, pp.1-17, DOI 10.1142/9789814675475_0001, https://cds.cern.ch/record/2130736/files/Introduction%20to%20the%20HL-LHC%20Project.pdf

High Luminosity LHC

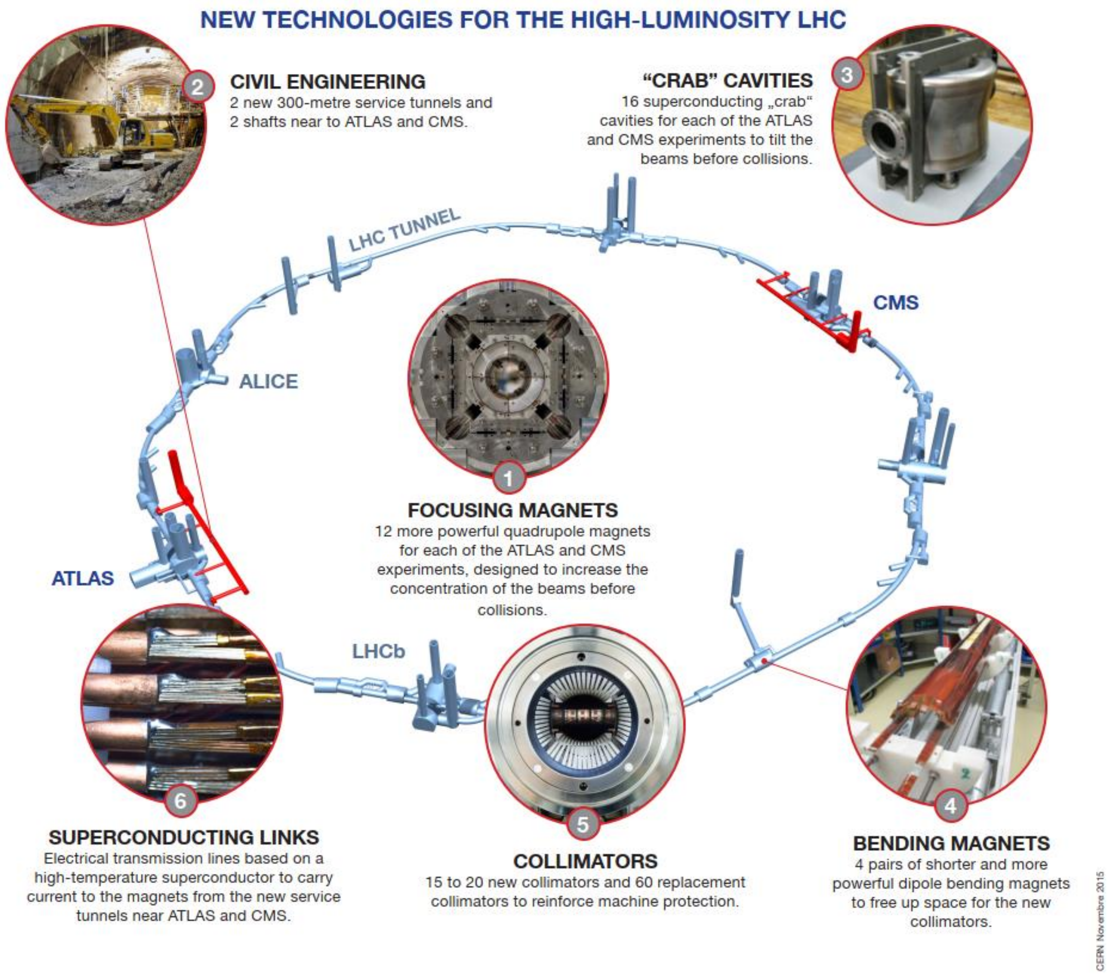

https://hilumilhc.web.cern.ch/

More powerful focusing magnets and new optics

New, more powerful superconducting quadrupole magnets will be installed on either side of the ATLAS and CMS experiments to focus the particle bunches before they meet. These magnets will be made of a superconducting compound, niobium-tin, used for the first time in an accelerator, which will make it possible to achieve higher magnetic fields than the niobium-titanium alloy used for the current LHC magnets (12 teslas as opposed to 8). Twenty-four new quadrupole magnets are currently in production. The use of niobium-tin magnets is an opportunity to test this technology for future accelerators. New beam optics (the way the beams are tilted and focused) will notably make it possible to maintain a constant collision rate throughout the lifespan of the beam.

"Crab cavities" for tilting the beams

This innovative superconducting equipment will give the particle bunches a transverse momentum before they meet, enlarging the overlap area of the two bunches and thus increasing the probability of collisions. A total of sixteen crab cavities will be installed on either side of each of the ATLAS and CMS experiments.

Reinforced machine protection

As the beams will contain more particles, machine protection will need to be reinforced. Around one hundred new, more effective collimators will be installed, replacing or supplementing the existing ones. These devices absorb particles that stray from the beam trajectory and might otherwise damage the machine.

More compact and powerful bending magnets

Two of the current bending magnets will be replaced with two pairs of shorter bending magnets and two collimators. Made of the superconducting niobium-tin compound, these new dipole magnets will generate a magnetic field of 11 teslas, compared with the 8.3 teslas of today's dipole magnets, and will thus bend the trajectory of the protons over a shorter distance.

Innovative superconducting links

Innovative superconducting power lines will connect the power converters to the accelerator. These cables, which are around one hundred metres long, are made of a superconducting material, magnesium diboride, that works at a higher temperature than that of the magnets. They will be able to carry currents of record intensities, up to 100 000 amps!

An upgraded accelerator chain

The HL-LHC's performance will also rely upon the injector chain, i.e. the four machines that pre-accelerate the beams before sending them into the 27-kilometre ring. This accelerator chain is being upgraded. A new linear accelerator, Linac4, the first link in the chain, is in the testing phase before replacing today's Linac2. Upgrades are also planned for the three other links in the accelerator chain: the PS Booster, the PS and the SPS.

High Luminosity LHC - Experiments

Detector Challenges: Increased (Luminosity) rates

e.g. Forward Muon detectors… MHz/cm2

LHCb M Stations

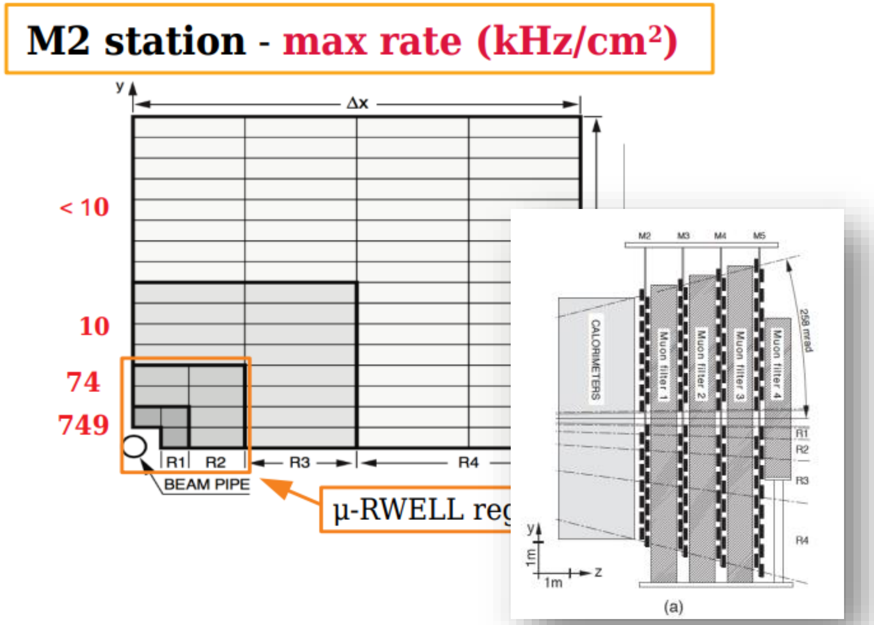

CERN-LHCC-2021-012 ; LHCB-TDR-023, Framework TDR for the LHCb Upgrade II - Opportunities in flavour physics, and beyond, in the HL-LHC era, https://cds.cern.ch/record/2776420/

CMS ME0

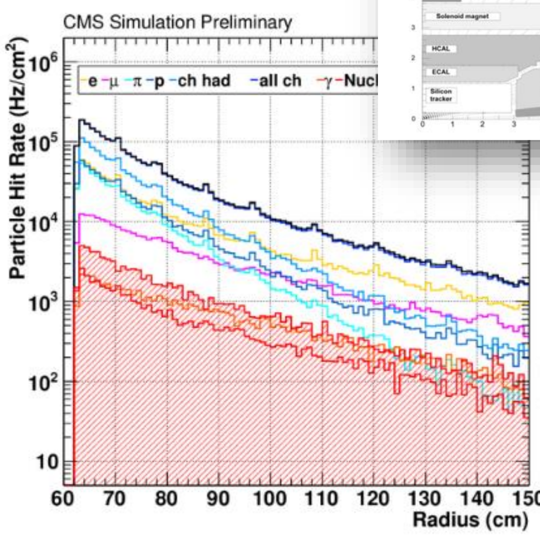

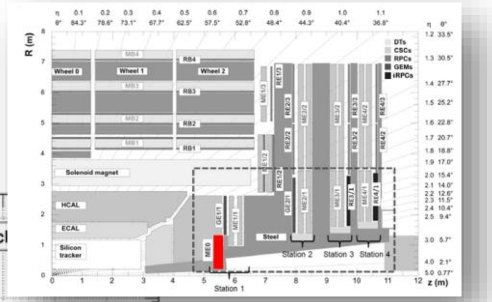

Fig. 2. Expected background flux in the ME0 environment as a function of the distance from the LHC beam line.

Rate capability of large-area triple-GEM detectors and new foil design for the innermost station, ME0, of the CMS endcap muon system, arXiv:2201.09021

ATLAS high-η-tagger

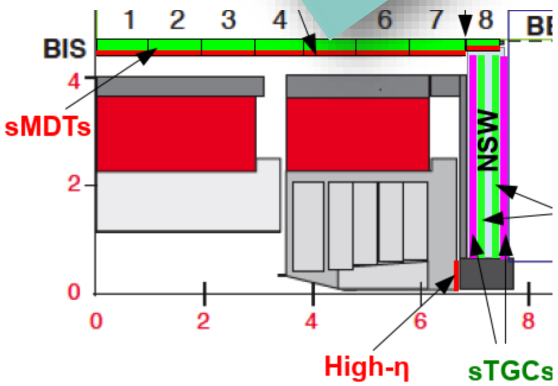

Rate Capability (@ inner radius R = 25 cm): up to 10 MHz/cm2)

CERN-LHCC-2017-017 ; ATLAS-TDR-026, Technical Design Report for the Phase-II Upgrade of the ATLAS Muon Spectrometer, http://cds.cern.ch/record/2285580/

Drastic increase in the rates often linked to the increase in the acceptance in the forward region

Detector Challenges: Radiation

Annual ***dose*** *delivered to the detector* ***per year*** *in the HL-LHC era will be similar to the* ***total dose of all operations from the beginning of the LHC program to the start of LS3***

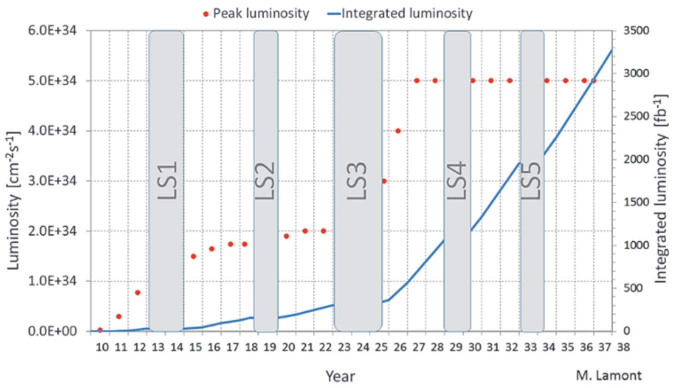

Main source of radiation is from the particles produced in the pp collisions. Mixed field of very ***low energy neutrons, photons, and electrons*** *(without any correlation with the bunch structure and relatively uniform in space and time).*

Burkhard Schmidt 2016 J. Phys.: Conf. Ser. 706 022002
https://iopscience.iop.org/article/10.1088/1742-6596/706/2/022002/pdf

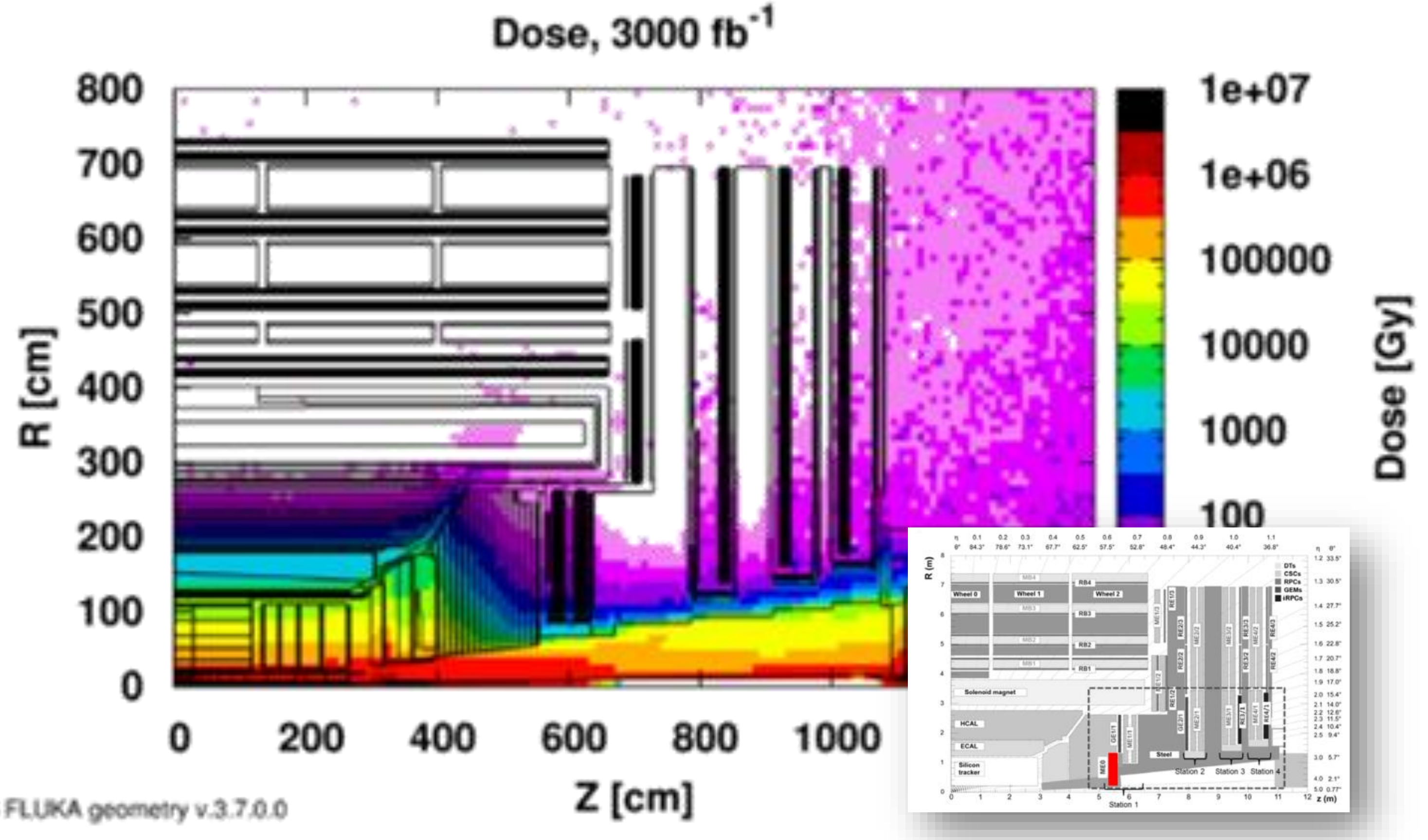

Figure 11: Absorbed dose in the CMS cavern after an integrated luminosity of 3000/fb. R is the transverse distance from the beamline and Z is the distance along the beamline from the Interaction Point at Z=0.

Drastic increase often linked to the increase of the acceptance in the forward region

Detector Challenges: Pileup

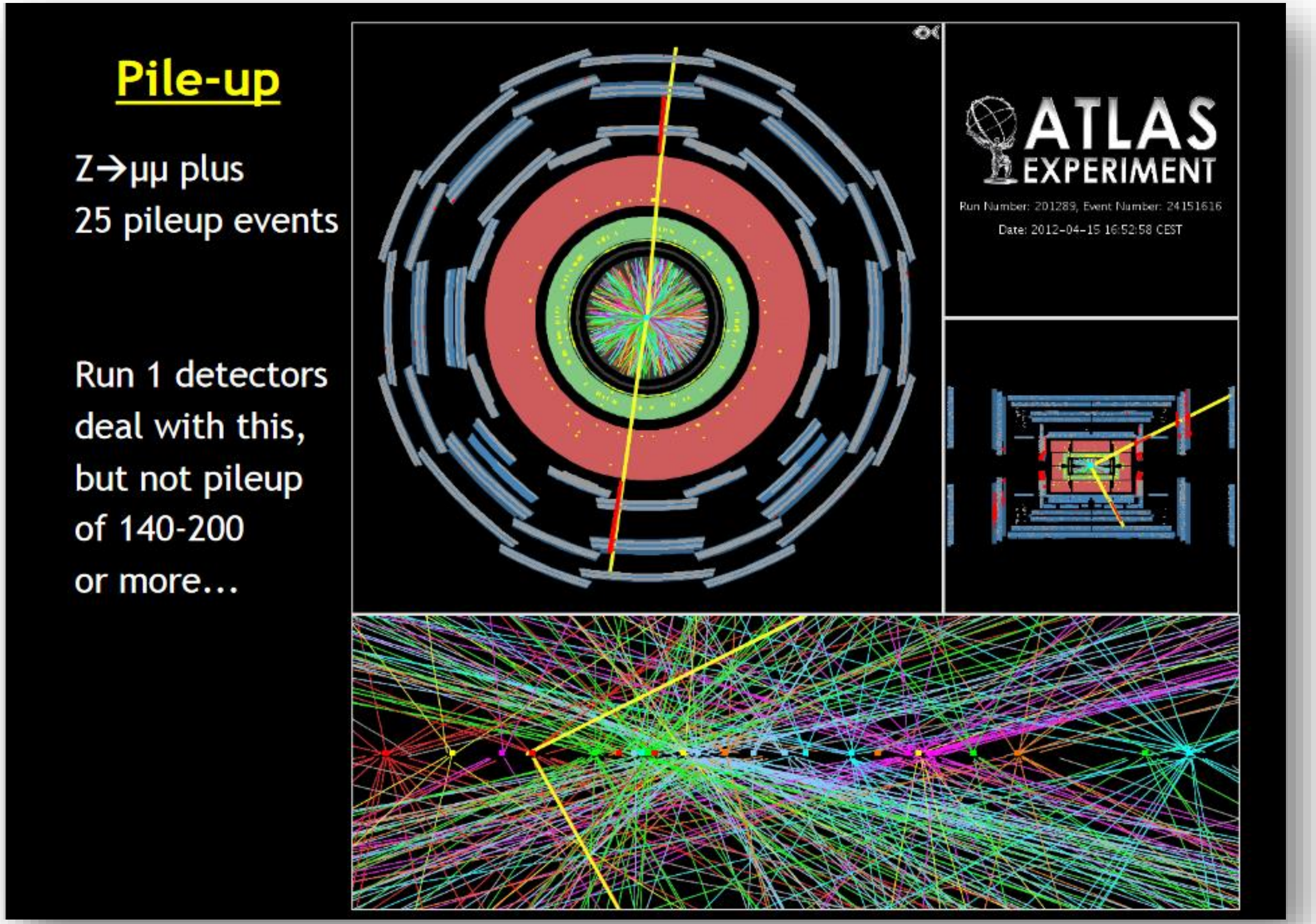

Pileup impacts track identification and reconstruction, adds extra energy to the calorimeter, hide "isolated" leptons, impact trigger and offline reconstruction,..

At the nominal luminosity of the HL-LHC, the average number of interactions in a single crossing is approximately 140. Most are "soft" or "peripheral" collisions, a relatively small fraction are "hard" collisions that contain high transverse momentum particles that may come from new high mass objects.

Key words/Flagships…

- **Granularity in space (tens of μm)…**
- **Granularity in time (tens of ps)…**
- **Low material budget (central region)**

ATL-PHYS-SLIDE-2014-753, Pileup Mitigation at the HL-LHC, P. Wells, https://cds.cern.ch/record/1957370/files/ATL-PHYS-SLIDE-2014-753.pdf
Burkhard Schmidt 2016 J. Phys.: Conf. Ser. 706 022002 https://iopscience.iop.org/article/10.1088/1742-6596/706/2/022002/pdf

ALICE

Rossi, ALICE upgrades for LHC Run 4 and beyond, https://indico.cern.ch/event/868940/contributions/3813867/attachments/2080982/3495681/Rossi_ICHEP2020_UpgradeALICE_v5.pdf
Burkhard Schmidt, 2016 J. Phys.: Conf. Ser. 706 022002 https://iopscience.iop.org/article/10.1088/1742-6596/706/2/022002/pdf

ALICE towards HL-LHC

Run3 (now)

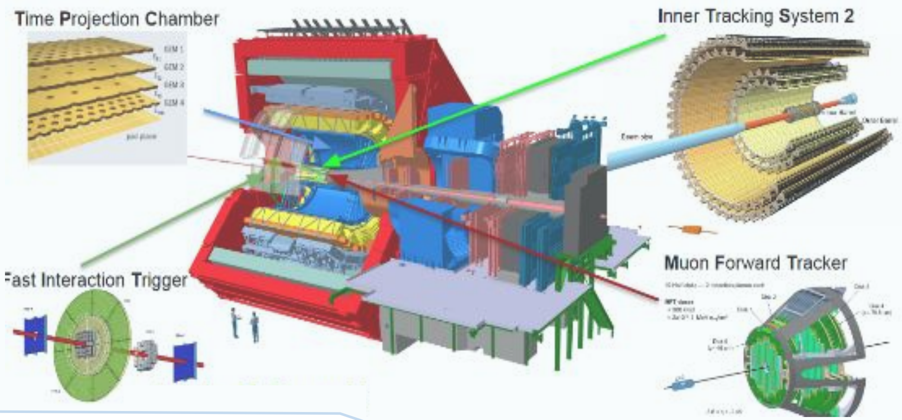

RUN3 (now)

- ALICE O^2 Offline-Online computing system (50 kHz recording).
- Inner Tracker ITS/MAPS(ALPIDE): 22.4mm from beam (before 39mm), 0.3% X0 (1.14), 30x30µm^2 (50x425), 6 (7) layers
- Muon Forward Tracker MFT: silicon pixel (ITS technology)
- **Time-Projection Chamber (TPC): GEM**

Run4 (HL-LHC)

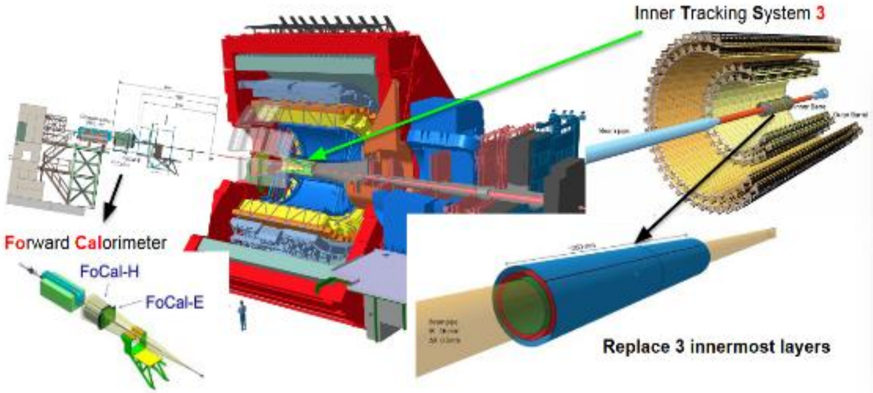

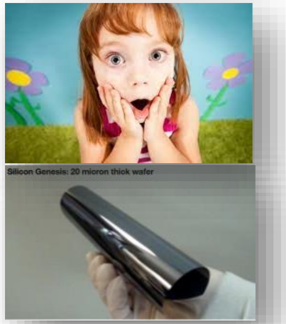

Run 5, "next-generation" possibilities: Compact, **all-silicon** "nearly massless" detector with excellent low-pT tracking capabilities

Run5 (HL-LHC)

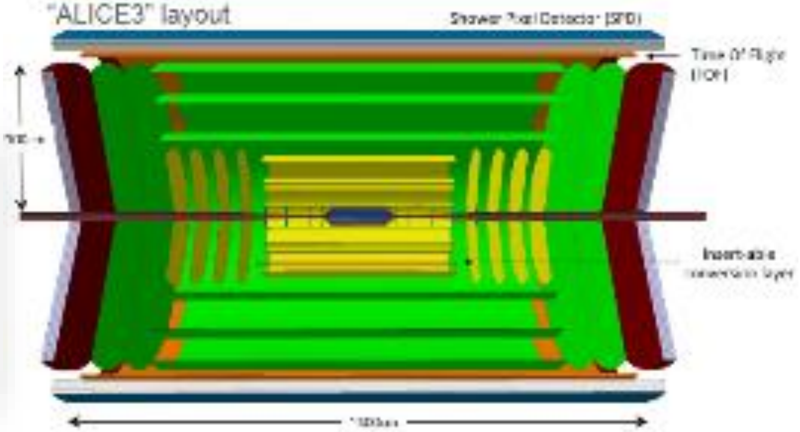

@MPGD 2002: Development of wafer-scale, monolithic CMOS pixel sensors for particle detection, Magnus Mager, CERN (Wed. 11:30)

ALICE TPC, RUN 3++

Gated operation used in run 1 & 2 becomes inacceptable after run 3 (current run)
Mandatory to identify a stable amplification stage with reduced IBF and good energy resolution

GATED OPERATION IN RUN 1 & RUN 2

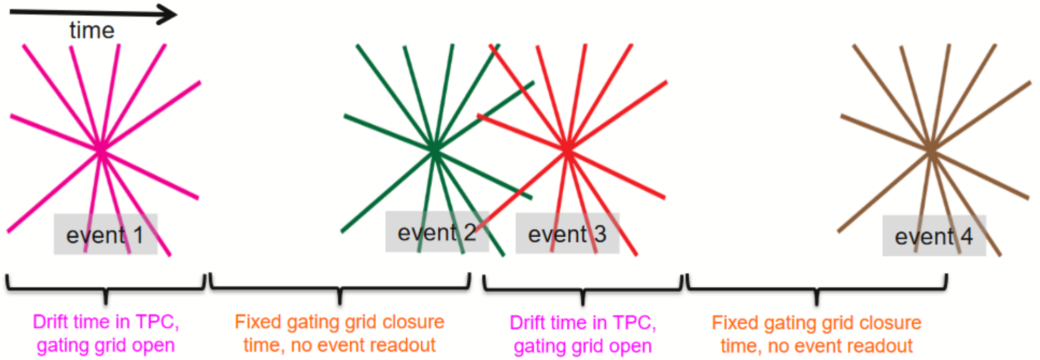

- **Multi Wire Proportional Chamber readout**
- A pulsed gating grid is used to prevent back-drifting ions from the amplification stage to distort the drift field (ion backflow (IBF) suppression ~10^{-5})
- 100 μs electron drift time + 200/400 μs gate closed (Ne/Ar) to minimize ion backflow and drift-field distortions
- **300/500 μs** in total limits the maximal readout rate to **few kHz** (in pp)
- Limitation of readout electronics: ~kHz in Run 2 **(2017 pp: 2040 Hz)**

CONTINUOUS OPERATION IN RUN 3 AND BEYOND

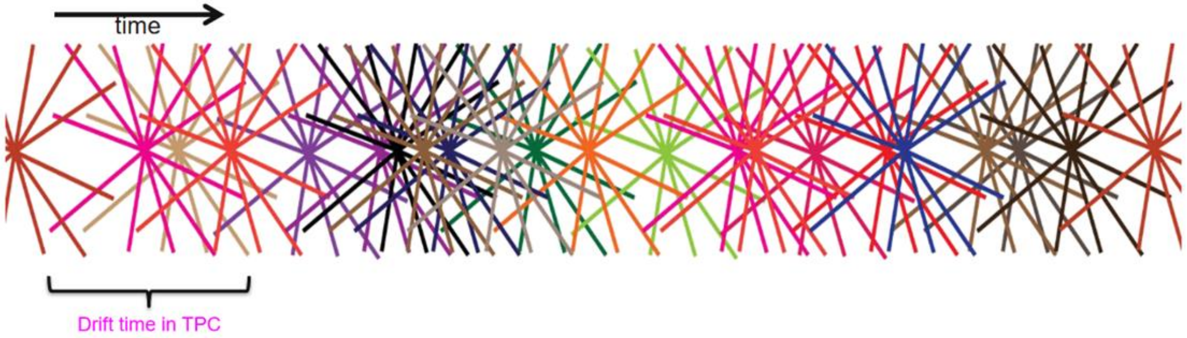

- Maximum drift time of electrons in the TPC: ~100 μs
- Average event spacing: ~20 μs
- Event pileup: 5 on average
- Triggered operation not efficient
- Minimize IBF without the use of a gating grid

R. H. Munzer, Continuous data taking with the upgraded ALICE GEM-TPC, CERN EP Detector Seminar, 24/6/2022, https://indico.cern.ch/event/1172978/

ALICE GEM TPC

2012

https://indico.cern.ch/event/181036/contributions/1450386/attachments/242092/338935/ALICE_upgrade_task-force.pdf

2013

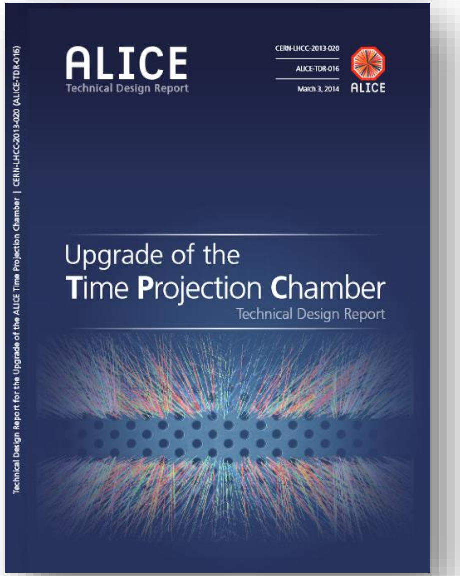

CERN-LHCC-2013-020 ; ALICE-TDR-016, Upgrade of the ALICE Time Projection Chamber, https://cds.cern.ch/record/1622286

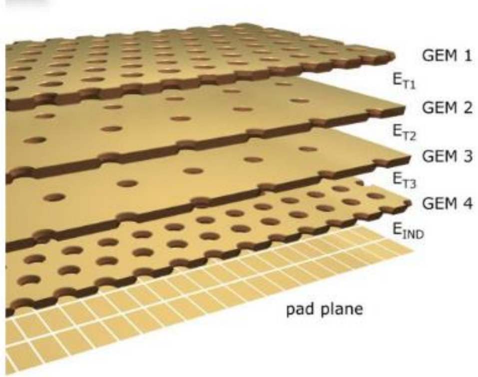

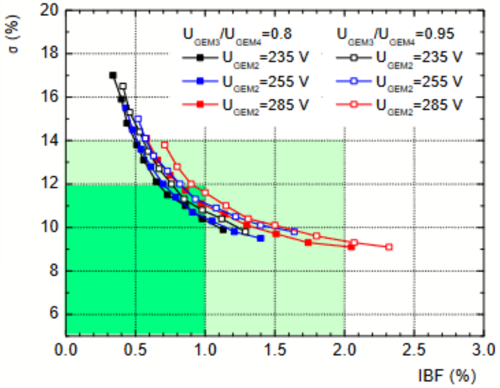

Performance with optimised HV configuration
IBF = Ion BackFlow
σ = energy resolution for ^{55}Fe

2020

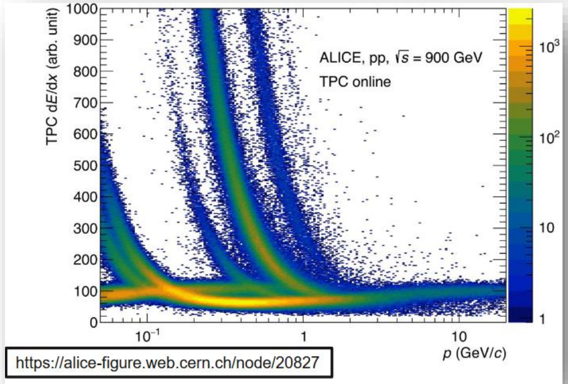

2021

R. H. Munzer, Continuous data taking with the upgraded ALICE GEM-TPC, CERN EP Detector Seminar, 24/6/2022, https://indico.cern.ch/event/1172978/

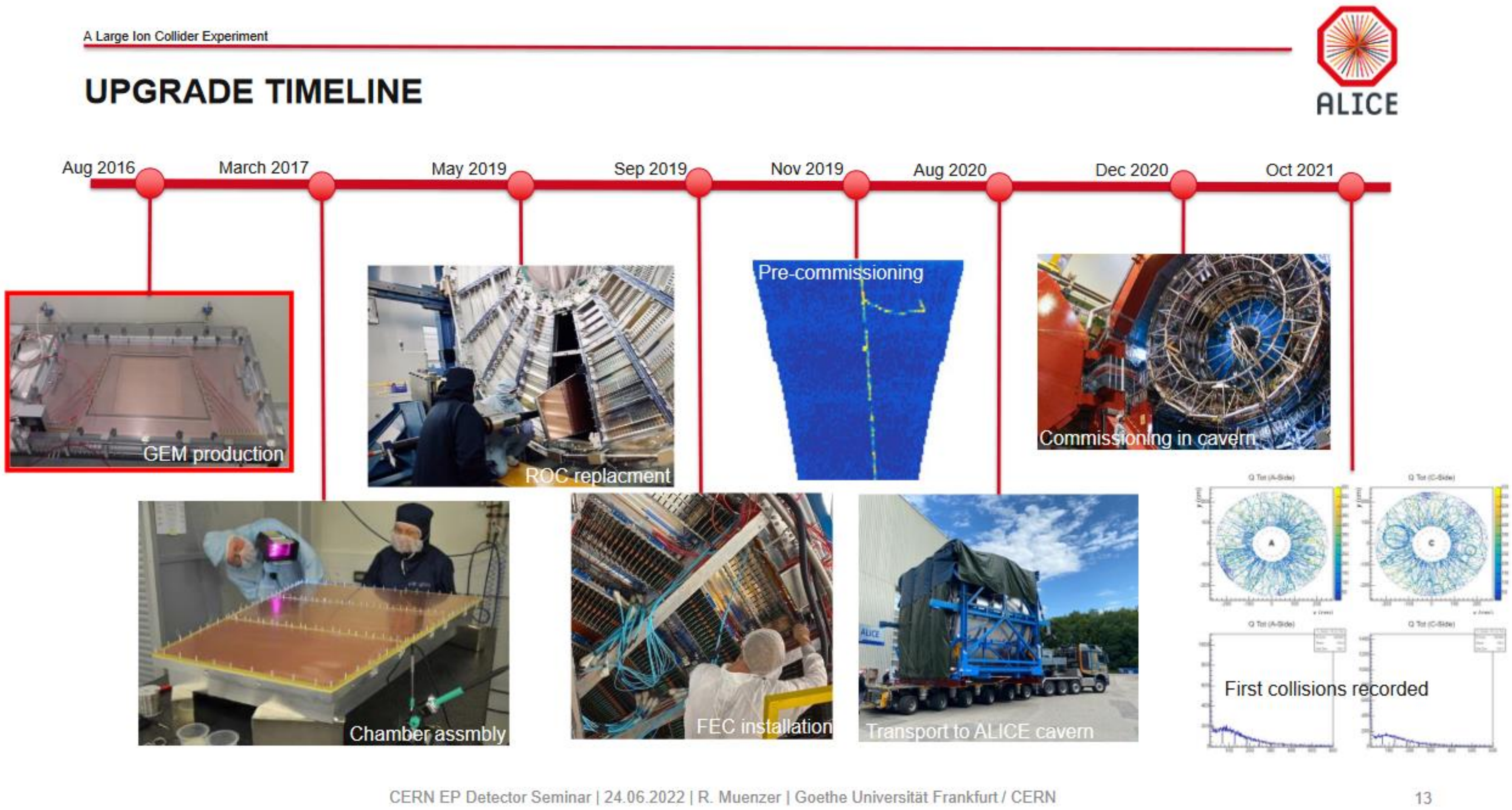

R. H. Munzer, Continuous data taking with the upgraded ALICE GEM-TPC, CERN EP Detector Seminar, 24/6/2022, https://indico.cern.ch/event/1172978/

ALICE GEM TPC, PILOT beam

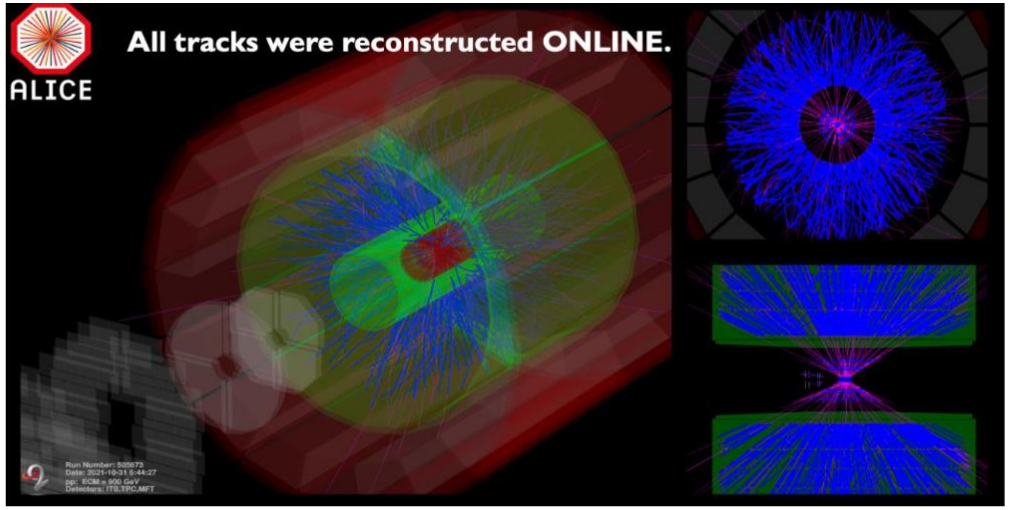

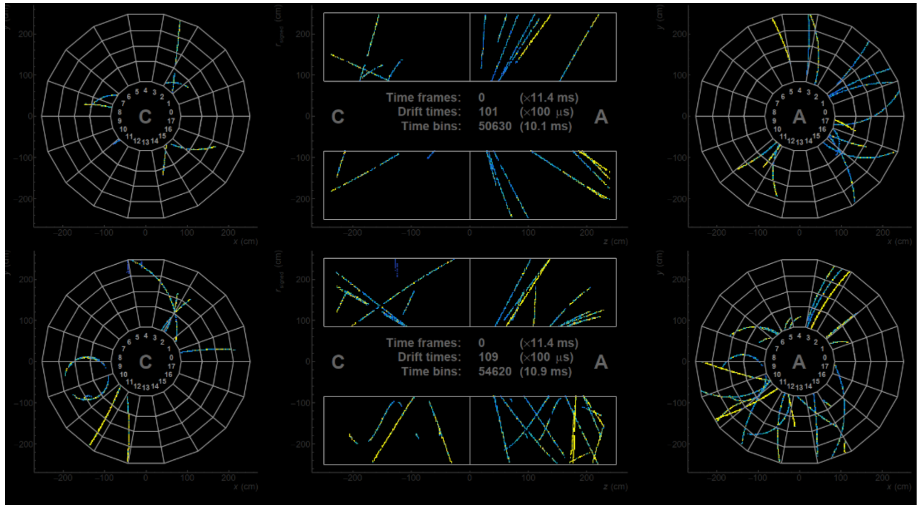

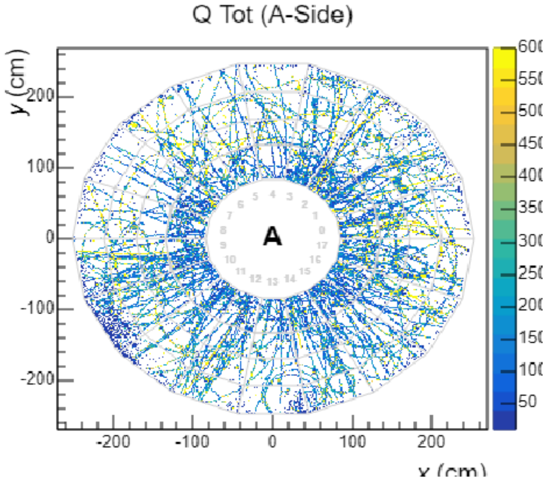

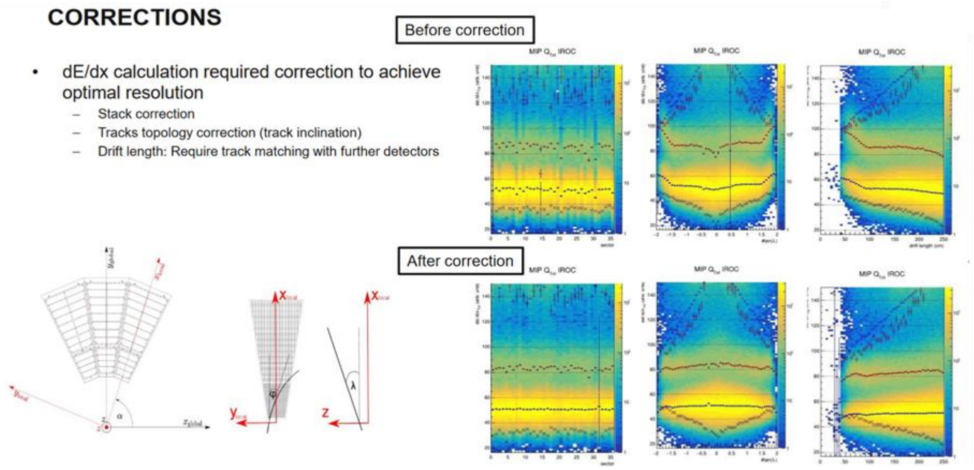

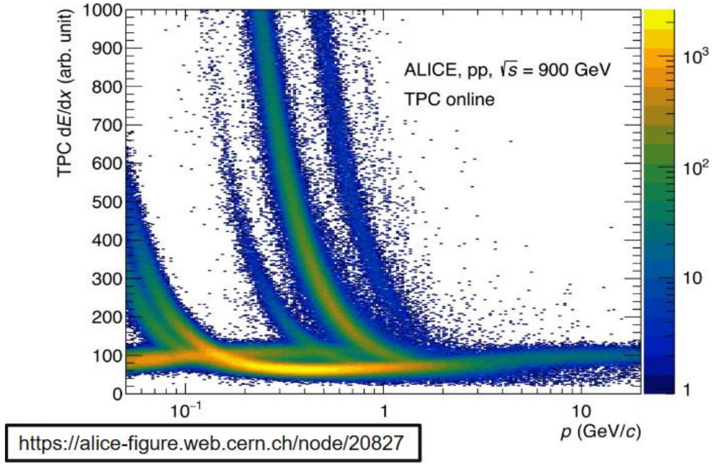

R. H. Munzer, Continuous data taking with the upgraded ALICE GEM-TPC, CERN EP Detector Seminar, 24/6/2022, https://indico.cern.ch/event/1172978/

RUN3

ALICE PERFORMANCE IN 13.6 TeV pp

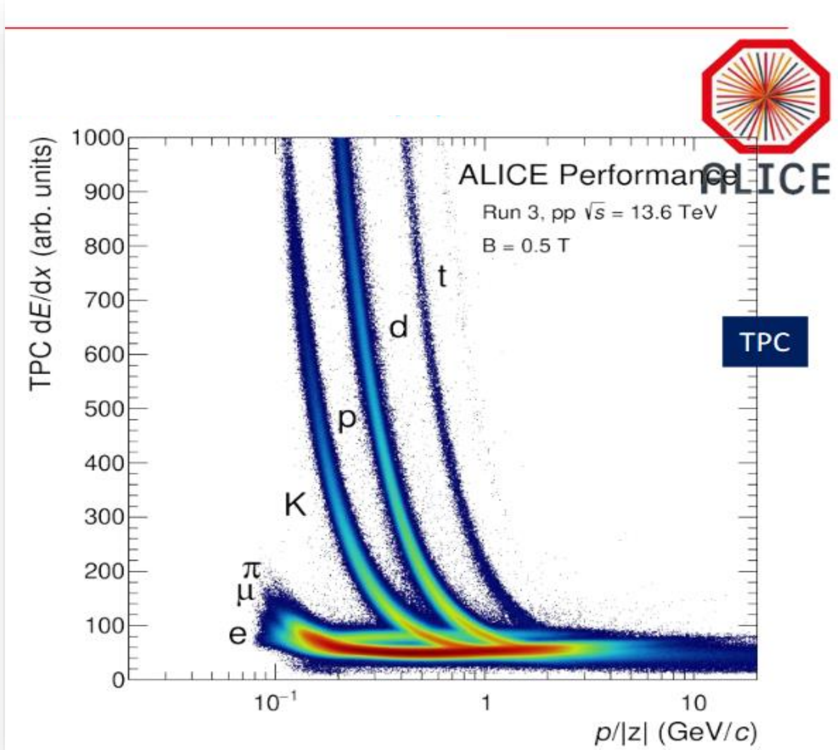

151st LHCC Meeting - OPEN Session, ALICE Status Report by F. Ronchetti
https://indico.cern.ch/event/1219913/contributions/5132247/attachments/2556873/4406273/ALICE_RC_2022_11_30-LHCC-OPEN.pdf

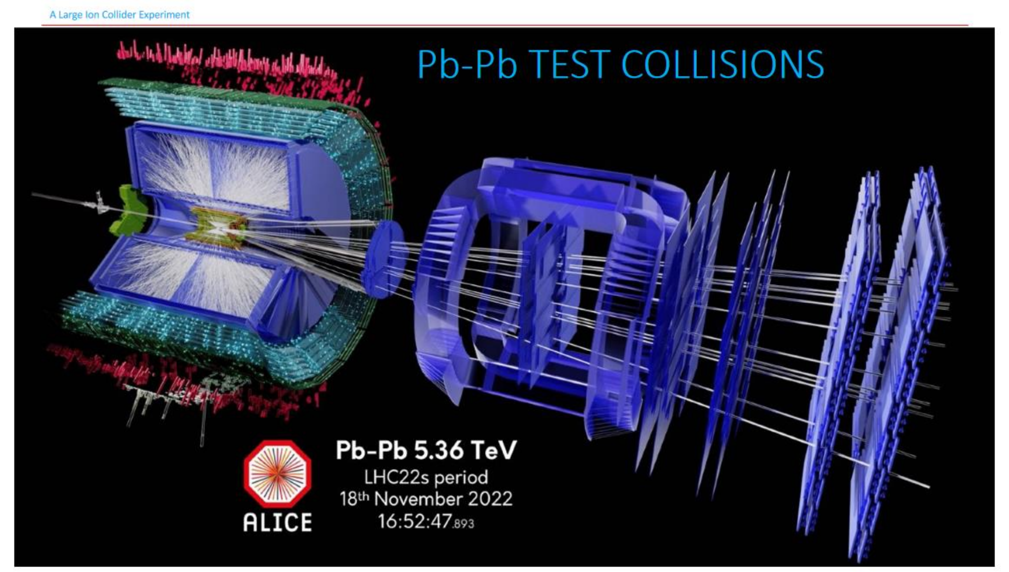

Pb-Pb: ASYNCHRONOUS PERFORMANCE

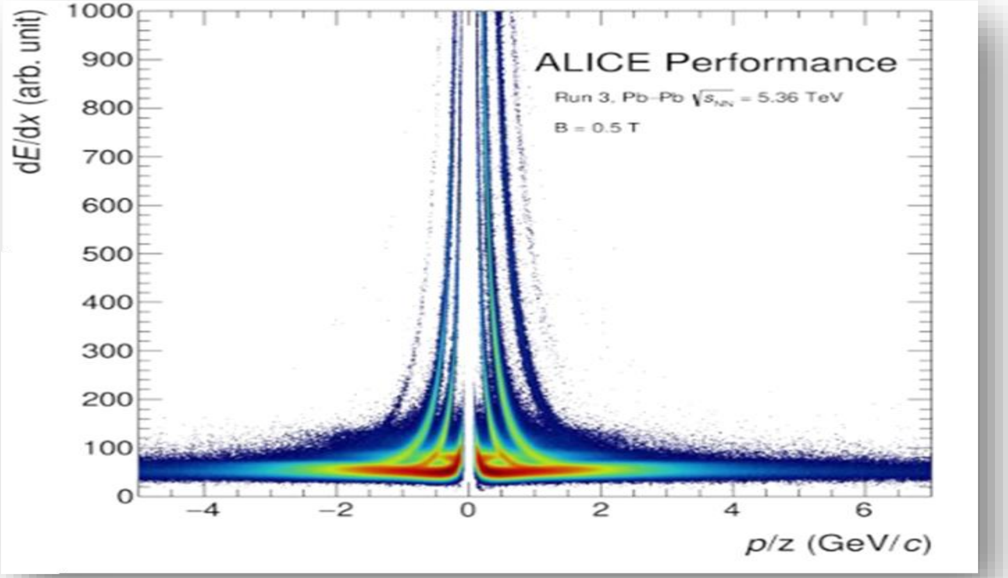

ALICE GEM TPC / Calibrations

PULSER SYSTEM

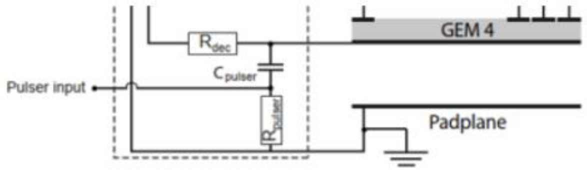

- Pad response measurement
- Common Mode calibration

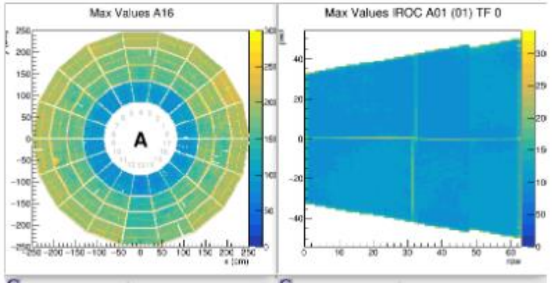

LASER SYSTEM

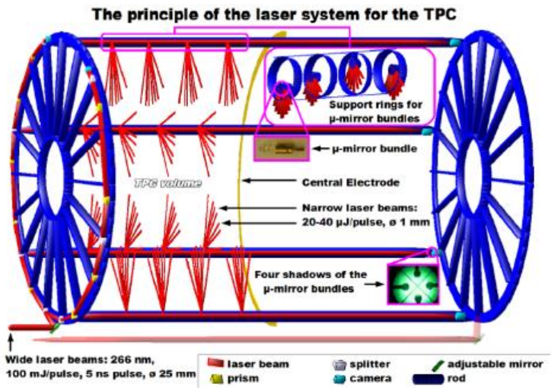

- Alignment
- Drift velocity measurement
- Drift field distortions
- Common Mode calibration

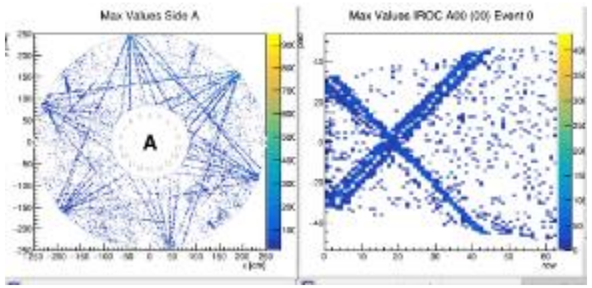

X-RAY

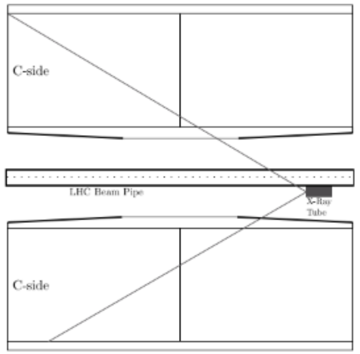

- Full gain map
- Stability

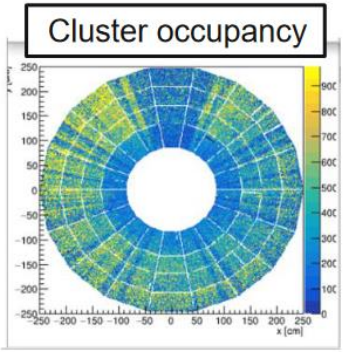

KRYPTON

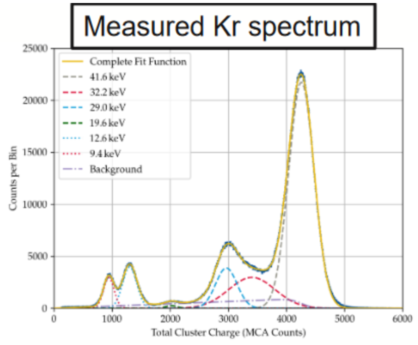

- Energy resolution: σE/E = 12% @ K(α) of 55Fe corresponds to: σE/E = 4.5% @ 41.6 keV (Krypton main peak)
- Gain Equalization

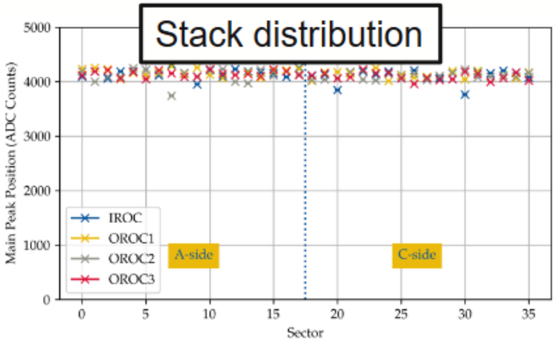

R. H. Munzer, Continuous data taking with the upgraded ALICE GEM-TPC, CERN EP Detector Seminar, 24/6/2022, https://indico.cern.ch/event/1172978/

Discharges & propagation

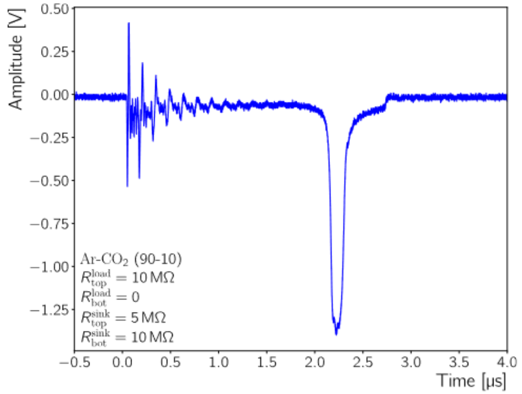

Fig. 2. Readout anode signal of a discharge followed by a secondary discharge. The waveform is recorded with a single GEM set-up. After the readout anode the signal is passed through a 32 dB attenuator, which provides R_{anode} of about 10 Ω.

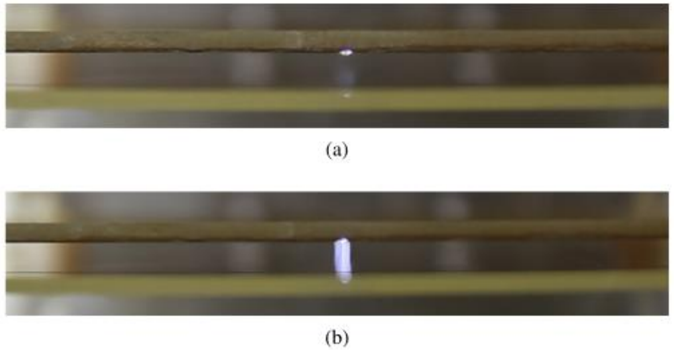

Fig. 5. Side view on the induction gap. In both photographs the GEM (upper structure) and the readout anode (lower structure) are visible. Photo (a) shows a primary discharge while photo (b) shows a secondary discharge between GEM and readout anode.

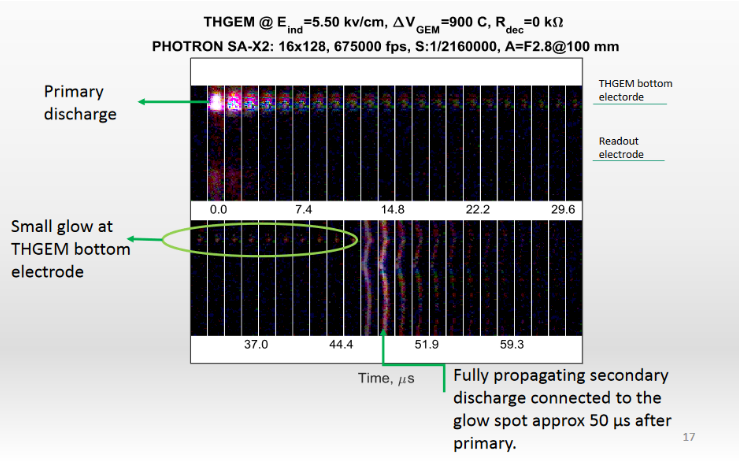

A. Utrobicic et al.
https://indico.cern.ch/event/709670/contributions/3027853/

A. Deisting et al., Nuclear Inst. and Methods in Physics Research, A 937 (2019) 168–180, https://doi.org/10.1016/j.nima.2019.05.057

https://indico.cern.ch/event/709670

New recipe: Protection Resistor on bottom gem

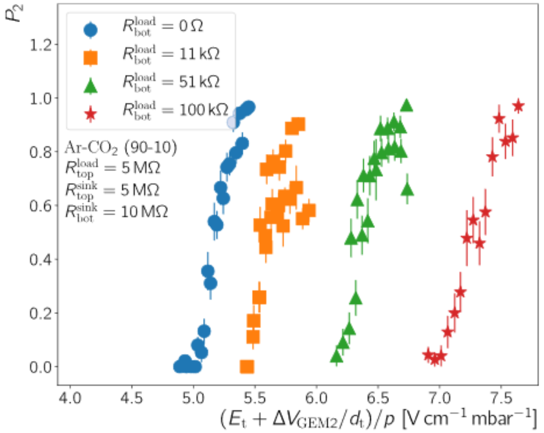

(a)

@ MPGD2022

- **P. Gasik**, Impact of the gas choice and the geometry on the breakdown limits in MPGD detectors
- **B. Ulukutlu**, New (TH)GEM coating materials characterised using spectroscopy methods
- **H. Fribert**, Studying the impact of humidity on the performance of MPGDs

ATLAS

ATLAS towards HL-LHC

Phase-0 main upgrades:
- inner pixel Insertable B-Layer (IBL)

Phase-I main upgrades :
- **New Small Wheels ,**
- BIS78 (RPC,SMDT pilot)
- Level-1 LAr Calorimeter Electronics,
- Trigger and Data Acquisition

Phase-II main upgrades :
- **Inner tracker** entirely replaced:
  - gas-based TRT removed
  - new, all-silicon Inner Tracker (ITk) with pixel sensors at the inner radii surrounded by microstrip sensors.
  - up to $|\eta| = 4$, higher granularity (x5, design-cooling-serial powering), lighter (x0.5), more rad-hard(n-in-p & 3D) up to NIEL $\simeq 2 \times 10^{16}$ 1 MeV n_{eq} /cm2 and TID of 1 GRad)
- New **timing layer** (HGTD): LGAD
- **Muon spectrometer** (RPC, MDT and TGC, **high η-tagger(?)**)
- Muon and electron **trigger** upgrades

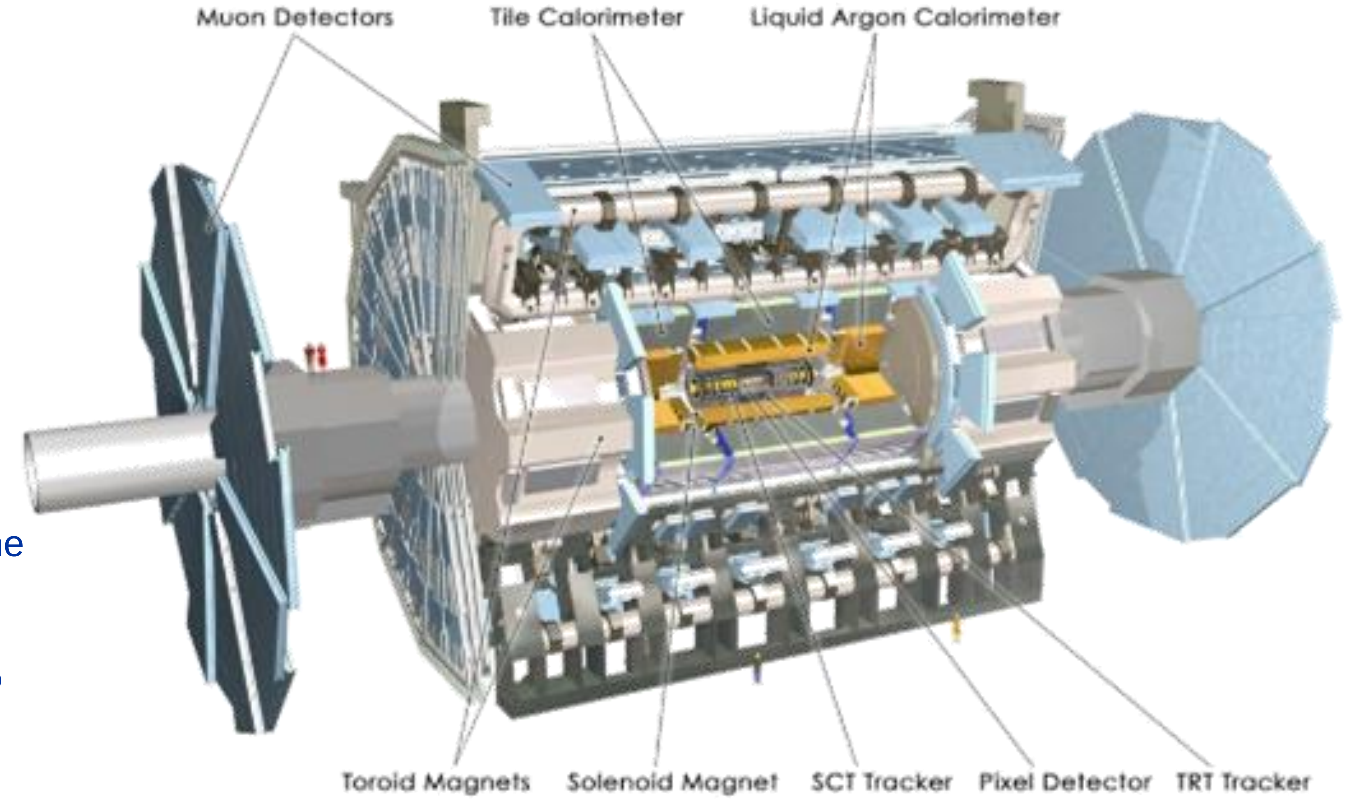

Figure 13: Schematic view of the ATLAS detector with the various sub-systems. The dimensions of the detector are 25m in height and 44m in length. The overall weight of the detector is about 7000 tons.

Burkhard Schmidt 2016 J. Phys.: Conf. Ser. 706 022002 https://iopscience.iop.org/article/10.1088/1742-6596/706/2/022002/pdf
C. Lacasta, DETECTOR UPGRADES FOR THE HL-LHC, XIII CPAN days, https://indico.ific.uv.es/event/6457/contributions/17779/attachments/10004/13374/Detector.Upgrades.CPAN22.pdf

ATLAS NSW

Complementary technologies are used for triggering and for track reconstruction.

- ***sTGC:** better bunch crossing assignment with high radial resolution and rough φ resolution from pads;*
- ***Micromegas:** even better offline radial resolution and a good φ coordinate due to its stereo strips. But: poorer bunch crossing and radial resolution for triggering.*

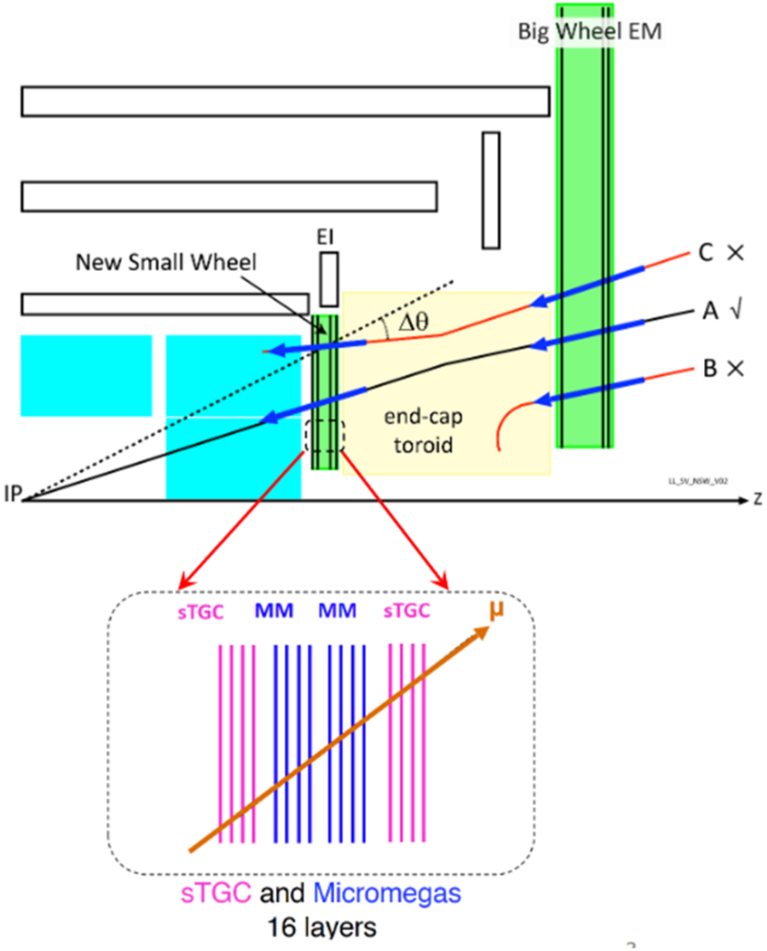

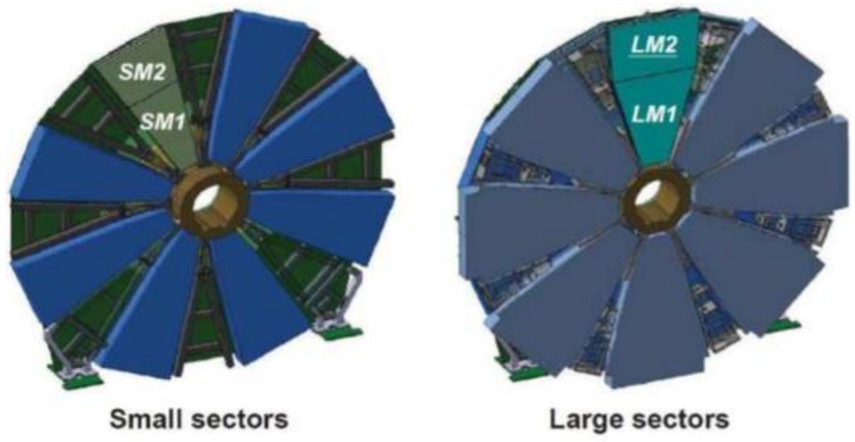

1200 m^2 MM + 1200m^2 sTGC

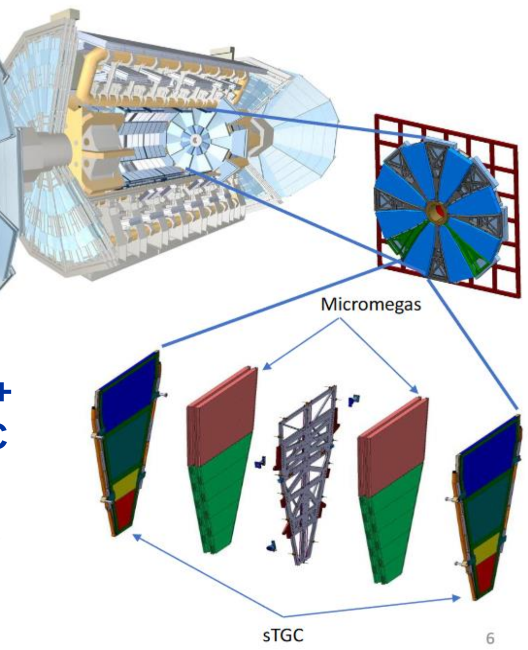

L. Levinson , Overview and innovations of the electronics of the New Small Wheel of the ATLAS Muon Spectrometer, Weizmann Institute of Science, Israel on behalf of the ATLAS Muon Spectrometer system, 11th International Conference on New Frontiers in Physics, September 2022, http://cdsweb.cern.ch/record/2842618/files/ATL-MUON-SLIDE-2022-625.pdf

NSW/Micromegas

The MAMMA*) R&D activity

- Using the micromegas technology to build muon chambers for the ATLAS upgrade was first suggested in an ATLAS Muon Collaboration brainstorming meeting back in 2007 by I. Giomataris (CEA Saclay)
  - By this time MMs had been successfully used in several experiments at very high rates (COMPASS, NA48) but the largest chambers did not exceed 0.4 x 0.4 m^2
  - The idea looked intriguing to some of us
- Profiting from the know-how of the CERN PCB workshop, the first prototype chamber, 0.4 x 0.5 m^2 in size, was built still in 2007; it worked very nicely
- By 2009 the excellent performance of MMs and their potential for large-area muon detectors was demonstrated
- 2010 was dedicated to making micromegas spark resistant
- 2011 the first resistive large-area chambers successfully built and tested

2007-2011

*) Muon ATLAS MicroMegas Activity

PH Det. seminar, 18 Nov 2011 Joerg Wotschack (CERN) 3

https://indico.cern.ch/event/149008/attachments/148102/209890/MM_Det_seminar_20111118.pdf

Resistive Micromegas

T. Alexopoulos et al. / Nuclear Instruments and Methods in Physics Research A 640 (2011) 110–118 111

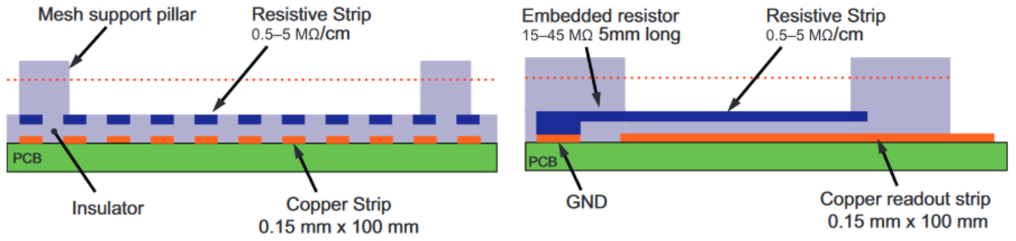

Fig. 1. Sketch of the detector principle (not to scale), illustrating the resistive protection scheme; (left) view along the strip direction, (right) side view, orthogonal to the strip direction.

T. Alexopoulos et al., A spark-resistant bulk-Micromegas chamber for high-rate applications Nucl. Instr. Meth. A 640 (2011) 110

Floating mesh (m^2 detectors)

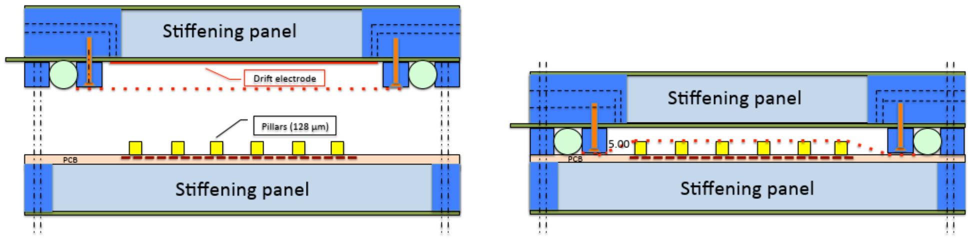

Figure 8.4: Schematics of a single MM plane assembly showing the drift and readout panels in open (left) and closed (right) position.

Resistive layers re-introduced, starting with screen printing and evolving today in different flavor of materials and resistivity… (e.g. DLC), used for protection mainly but as well for charge spreading (position resolution) …

NSW/MM from proto to final…

MM DW Integration - Performance of OLD_Double Wedge A13

- The first Large MM DW that was assembled in BB5 showed very bad results in the Cosmic stand.
- Motivated the study of the $Ar:CO_2:iC_4H_{10}$ (93:5:2) as gas mixture of choice.
- WG : study long term behavior & perform ageing studies at GIF++ (gamma) and LMU Munich (neutrons).
- Irradiation studies ongoing.
- Results : Positive – **CERN accepted the change of gas mixture.**

$Ar:CO_2$ 93:7 vol%
nom. HV: 570 V

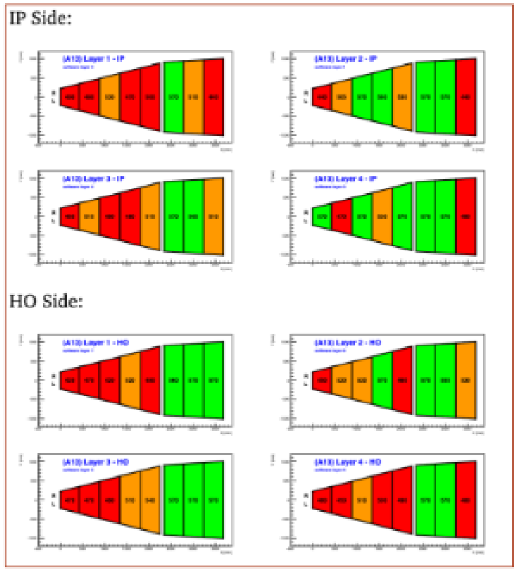

insufficient performance

green: sector is on nominal HV

red: sector is below nominal HV

-2% of CO2

+2% of Isob.

non-burning non-explosive gas-mixture

$Ar:CO_2:iC_4H_{10}$ 93:5:2 vol%
HV: 500 V

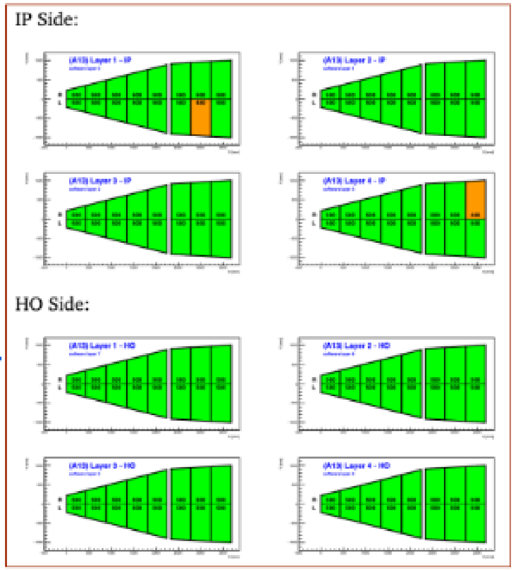

almost perfect performance
similar efficiency @ cosmics

OLD A13 (not passivated) -> REJECTED
Demonstration on a DW of the improvement given by $Ar:CO_2:iC_4H_{10}$ (93:5:2)

Change of gas mixture introducing hydrocarbons (iC4H10)

Several studies performed in the available time with positive results.

Unsafe to operate with the nominal mixture

To be monitored and further studies to be performed

@ **MPGD 2022 P. Iengo**, Accelerated longevity test of Resistive Micromegas detectors operated with and without small amount of hydrocarbons.

27

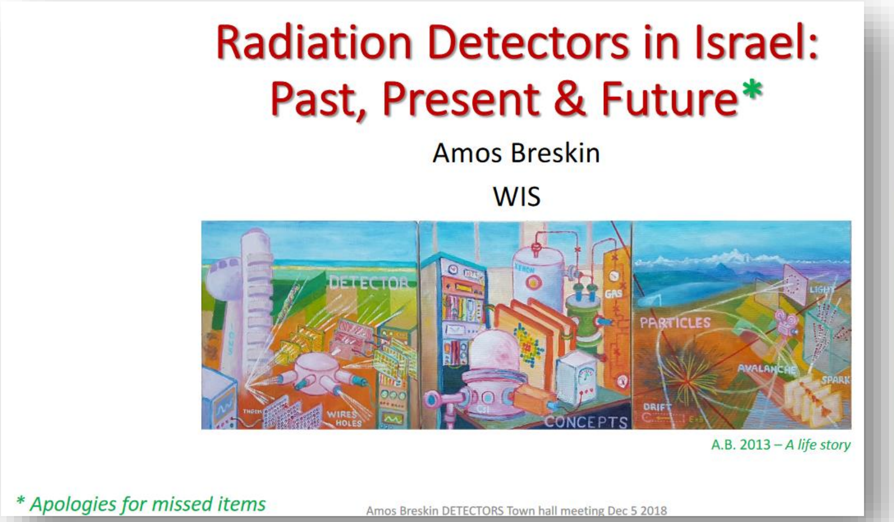

50µm gold-plated tungsten wires, 1.8mm pitch.

Cathode planes at a distance of 1.4mm from the wire plane, made of a graphite-epoxy mixture (100kΩ/ sq) on a 100µm thick G-10 plane…

Readout strips (perpendicular to the wires), 3.2mm pitch (“s” of sTGC)
Pads (covering large rectangular surfaces)

Both on 1.6mm thick PCB with the shielding ground on the opposite side..

https://indico.cern.ch/event/778319/contributions/3238311/attachments/1765600/2867530/Radiation_Detectors_in_Israel_for_IL_HEP_Dec_2018_03_12.pdf

ATLAS-IL

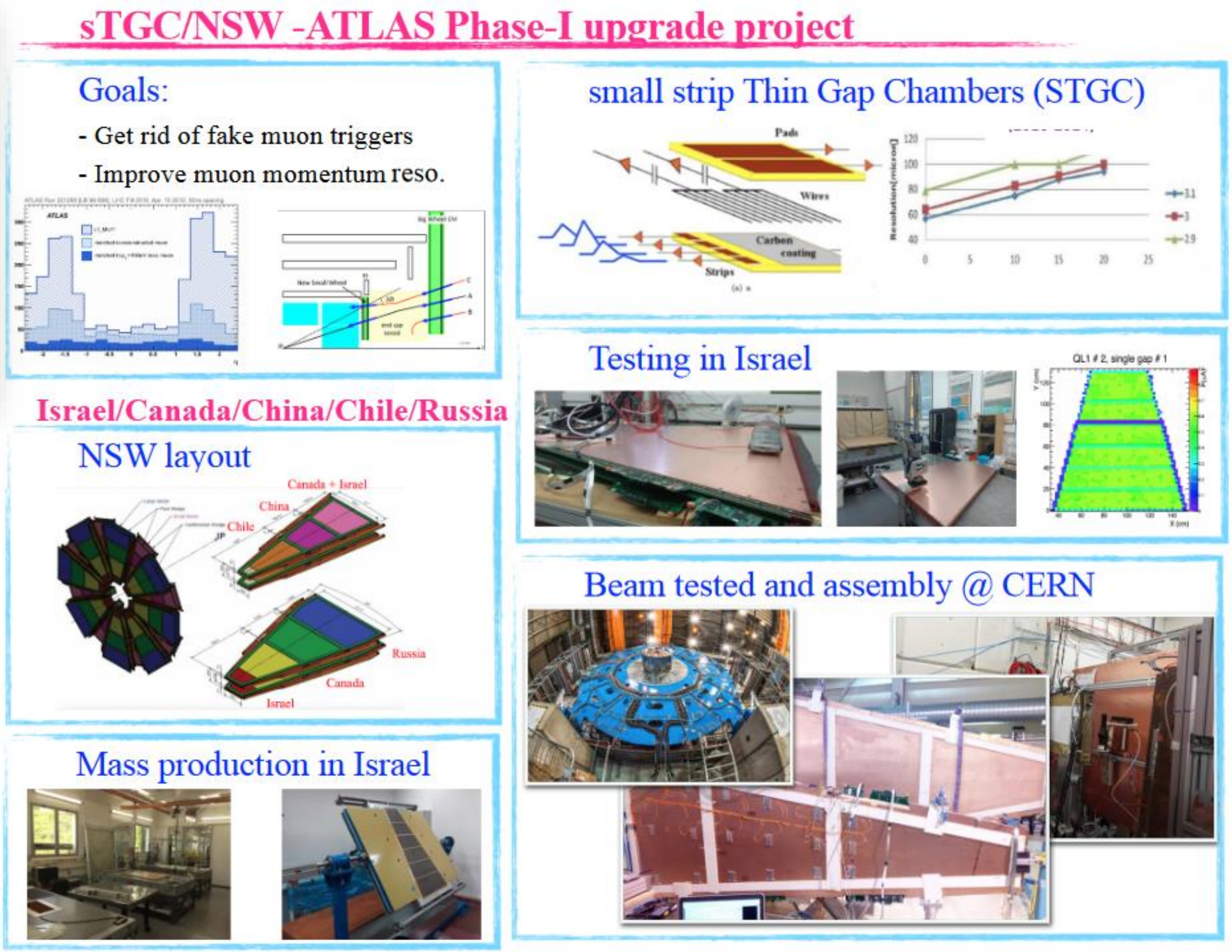

CERN-LHCC-2017-017 ; ATLAS-TDR-026, Technical Design Report for the Phase-II Upgrade of the ATLAS Muon Spectrometer, http://cds.cern.ch/record/2285580/

NSW (Phase I Upgrade)

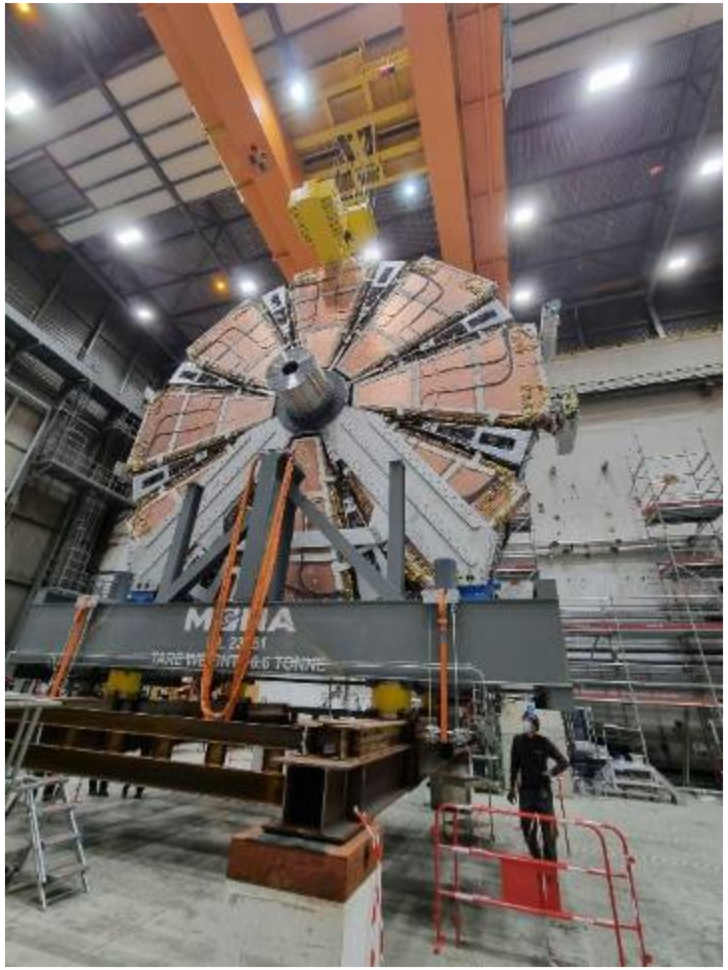

T. Vafeiadis, The New Small Wheel project of ATLAS, CERN EP Detector Seminar 17/6/2022, https://indico.cern.ch/event/1168778/attachments/2464624/4227403/_2022_06_17-TV-DetSeminar.pdf

Run3/NSW

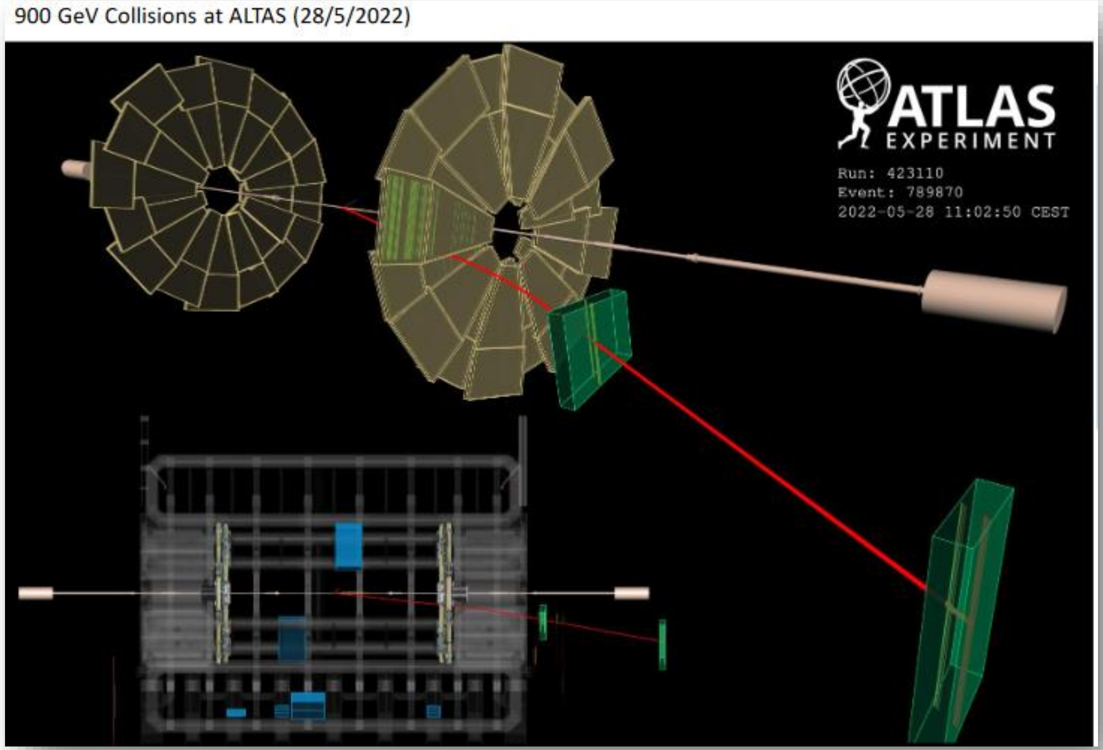

T. Vafeiadis, The New Small Wheel project of ATLAS, CERN EP Detector Seminar 17/6/2022, https://indico.cern.ch/event/1168778/attachments/2464624/4227403/_2022_06_17-TV-DetSeminar.pdf

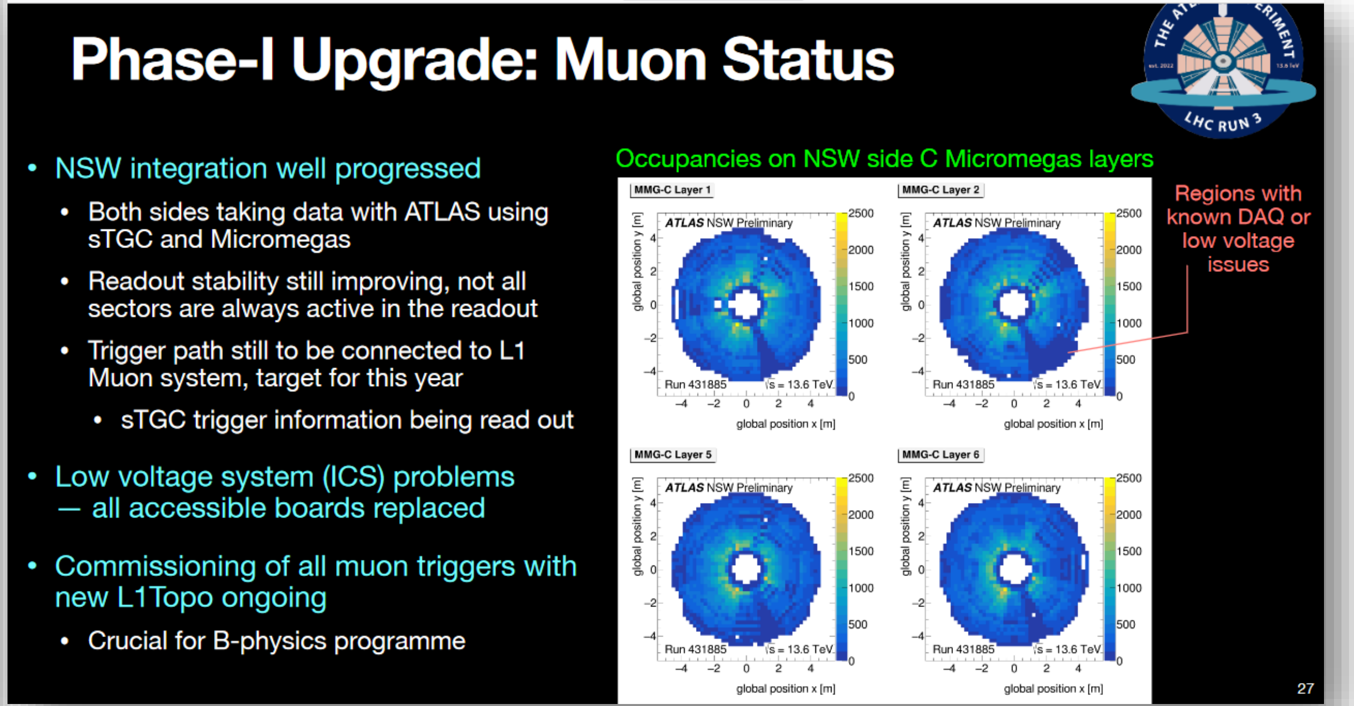

New detector, new electronics and new DAQ

151st LHCC Meeting - OPEN Session, ATLAS Status Report by T. J. Khoo, https://indico.cern.ch/event/1192325/contributions/5012980/attachments/2507852/4309670/LHCC_20220914.pdf

ATLAS/Muon spectrometer Phase-II upgrades

The muon spectrometer Phase-II upgrade comprises the installation of new chambers, the replacement of some existing chambers by new ones, and the replacement of a large part of the front-end and trigger and readout electronics.

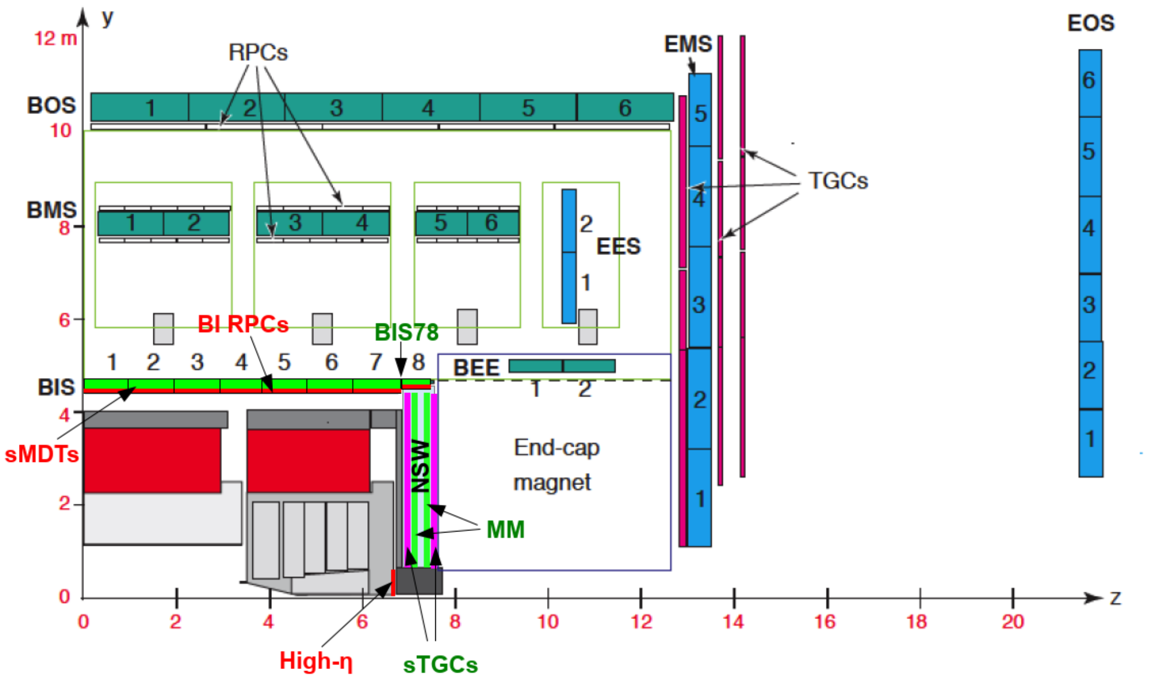

R-Z views of the small sector Phase-II ATLAS muon spectrometer layout

CERN-LHCC-2017-017 ; ATLAS-TDR-026, Technical Design Report for the Phase-II Upgrade of the ATLAS Muon Spectrometer, http://cds.cern.ch/record/2285580/

- **Upgrade of trigger and readout electronics** for all legacy (Phase0) muon system.

- **MDT and RPC chambers upgrade in the inner barrel:**
  - Old RPC at reduced performance (i.e. efficiency) to limit currents and integrated charge
  - new BI RPC chambers with increased rate capability will be installed on the inner (BI) MDT chambers of the barrel to maintain a high trigger efficiency.
  - new BI sMDT in small sector to fit in new RPC
  - BIS78/Phase I: pilot project for the future BI iupgarde (8 sMDT+RPC small chamber).

- **TGC chamber upgrade in the barrel-endcap transition region**
  - TGC triplets with finer readout granularity to obtain a uniform level of purity for triggered muons in the endcap
  - Trigger coincidence between BW and NSW/BIS78

- **High-η tagger (?)**
  - Following ITK extension up to |η|<4. Silicon or MPGD. Identify muons that penetrate the endcap calorimeter matching an ITk track

CMS

CMS towards HL-LHC

Phase II Detector Upgrade:

- New tracker (x4 granularity and lighter)
- New forward calorimeter: High Granularity Calorimeter (HGC) ILC/CALICE concepts for 3D measurement of shower Topologies. Si & Si/Scint-SiPM mixed layers.
- New Timing Layers (barrel/LYSO+SiPM and endcap/LGAD)
- Enhanced muon systems (endcaps):
    - **$1.5 < |\eta| < 2.4$ with GEM on station 1(Ph. I) & 2,** and low-resistivity RPC (3&4)
    - **Up to $|\eta|$~3 with GEM (ME0)**
- Beam radiation protection and luminosity measurement

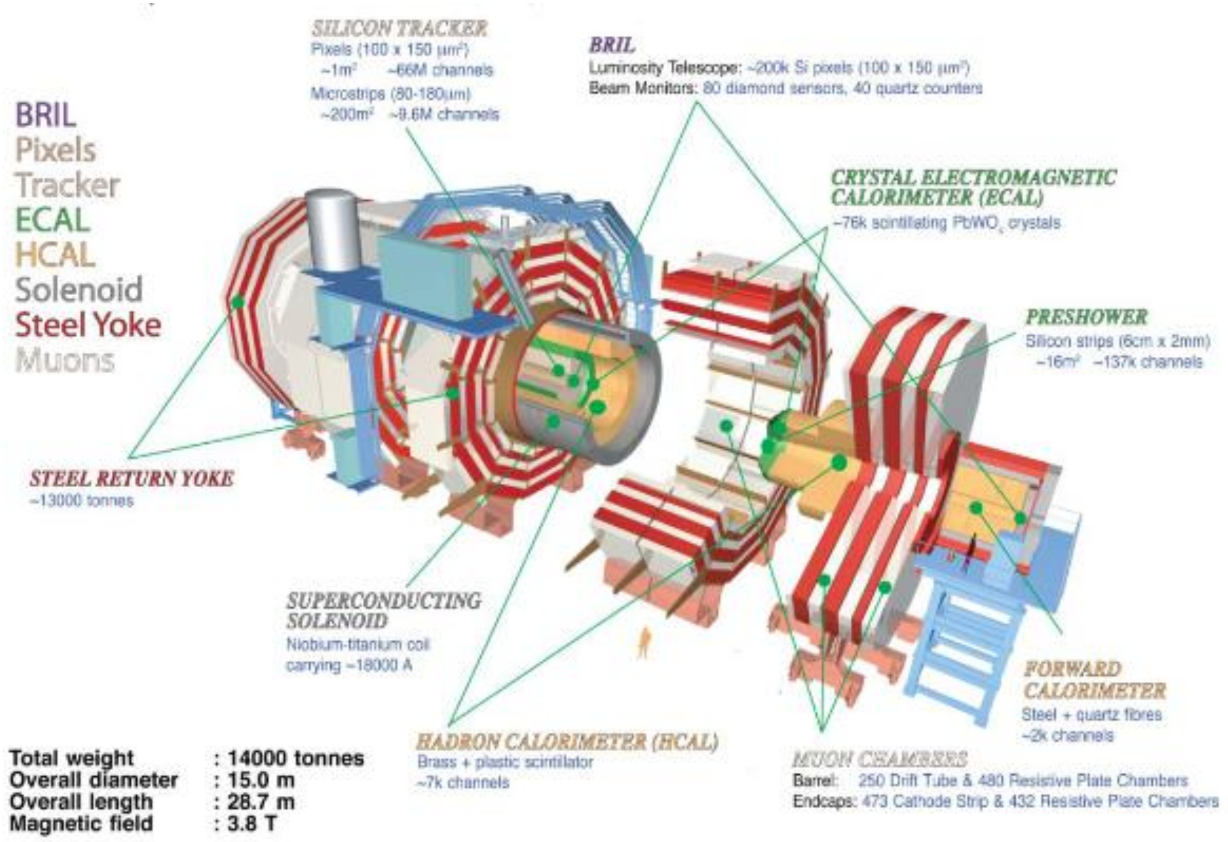

- Radiation: Tracker and the endcap calorimeter to be replaced.
- Pile-up mitigation: particle-flow event reconstruction (increased tracker granularity, new endcap calorimeter with optimized segmentation and energy resolution)
- Upgrades in the forward regions: maximize the physics acceptance
- Trigger and readout electronics upgrade (event selection, PU, rate,..)

Burkhard Schmidt 2016 J. Phys.: Conf. Ser. 706 022002
https://iopscience.iop.org/article/10.1088/1742-6596/706/2/022002/pdf

CMS GEM upgrade timeline

- Existing Detectors compatible with HL-LHC expected rates and dose
- New detectors to extend acceptance and resolution (GEM and RPC)
- Electronics changed to improve trigger

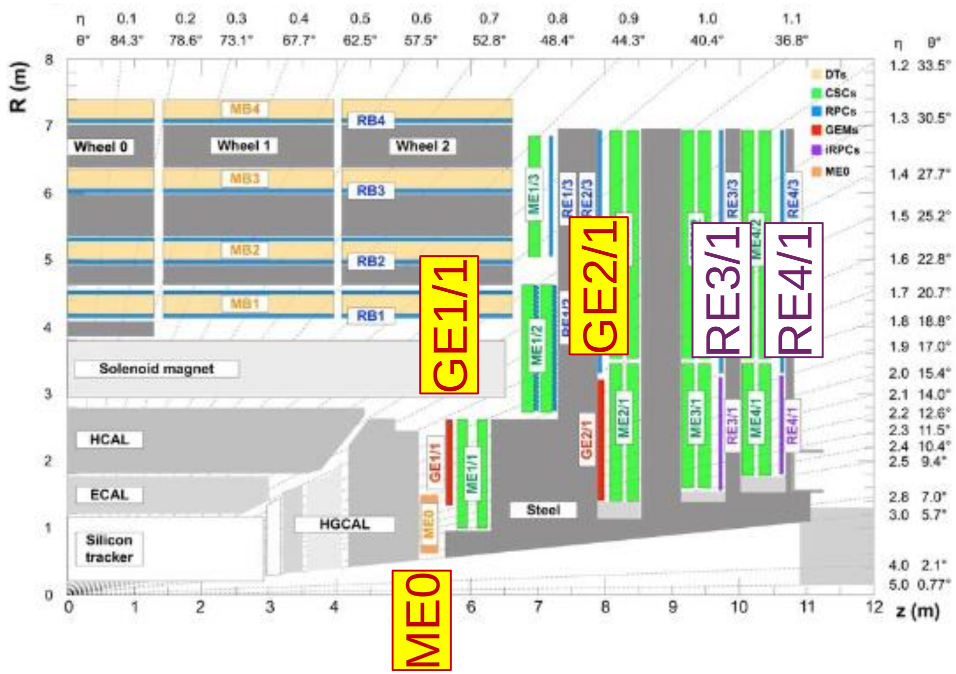

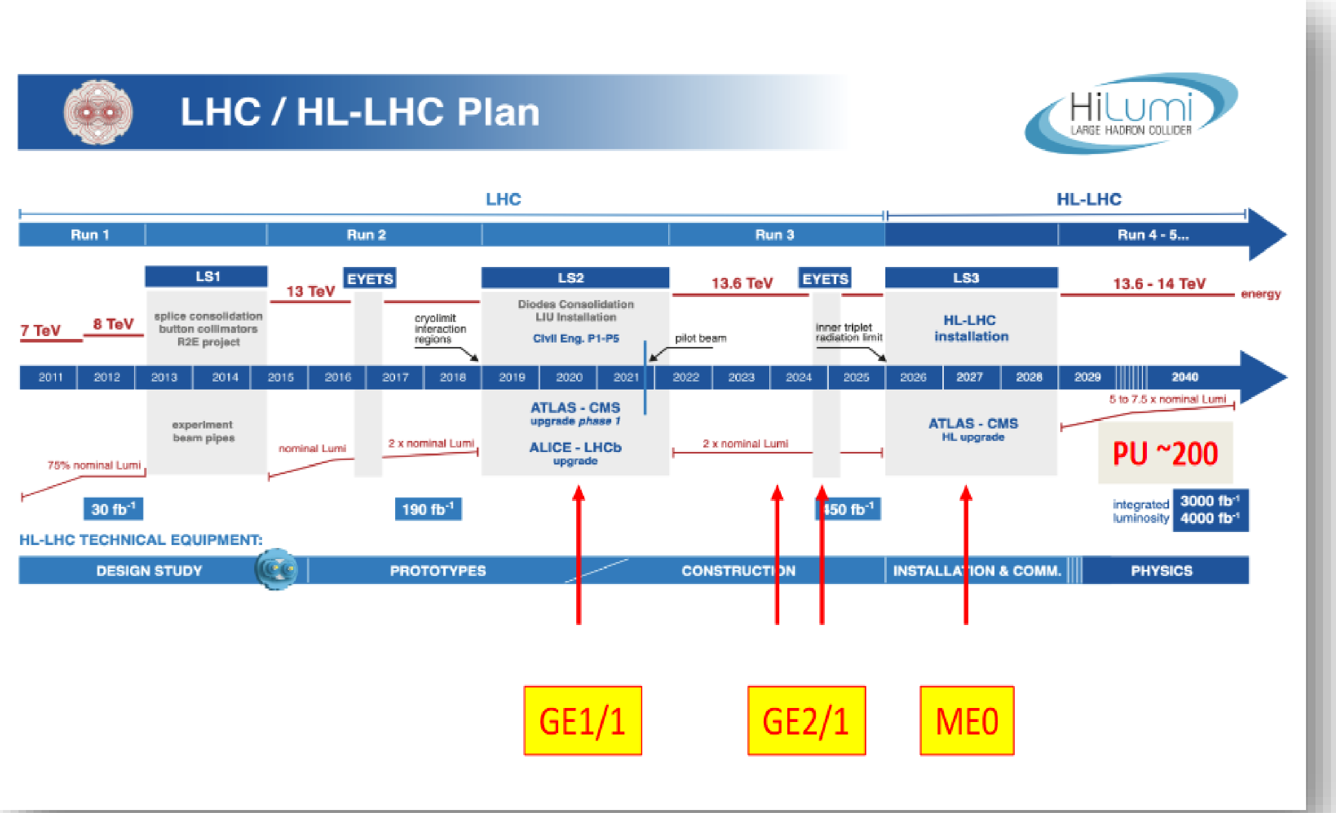

M. Bianco, The GEM detectors within the CMS Experiment, CERN EP Detector Seminar, 8/7/2022, https://indico.cern.ch/event/1175363/

CMS Muons , GEM

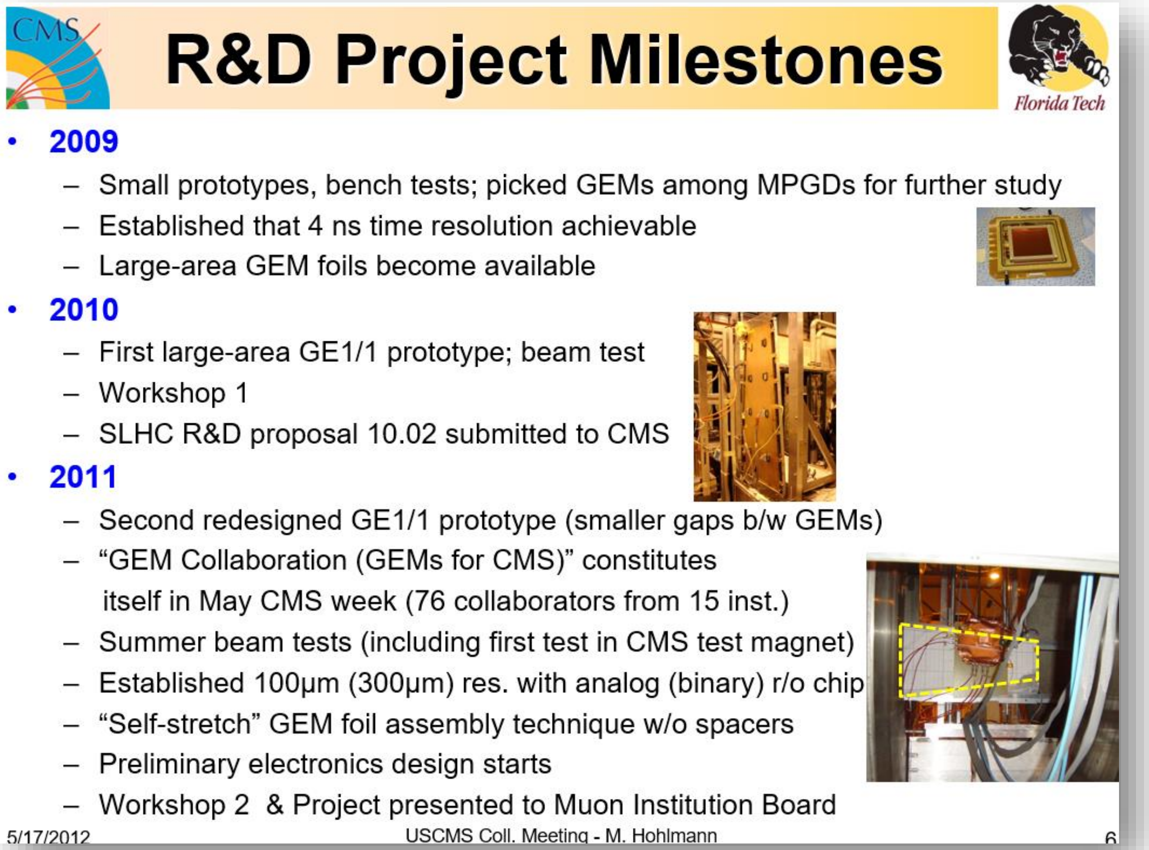

R&D Project Milestones

- **2009**
  - Small prototypes, bench tests; picked GEMs among MPGDs for further study
  - Established that 4 ns time resolution achievable
  - Large-area GEM foils become available
- **2010**
  - First large-area GE1/1 prototype; beam test
  - Workshop 1
  - SLHC R&D proposal 10.02 submitted to CMS
- **2011**
  - Second redesigned GE1/1 prototype (smaller gaps b/w GEMs)
  - "GEM Collaboration (GEMs for CMS)" constitutes itself in May CMS week (76 collaborators from 15 inst.)
  - Summer beam tests (including first test in CMS test magnet)
  - Established 100µm (300µm) res. with analog (binary) r/o chip
  - "Self-stretch" GEM foil assembly technique w/o spacers
  - Preliminary electronics design starts
  - Workshop 2 & Project presented to Muon Institution Board

5/17/2012 USCMS Coll. Meeting - M. Hohlmann 6

M. Hohlmann, *USCMS Collaboration Meeting, Boulder, CO, May 17, 2012*

Large Area (single mask) GEM

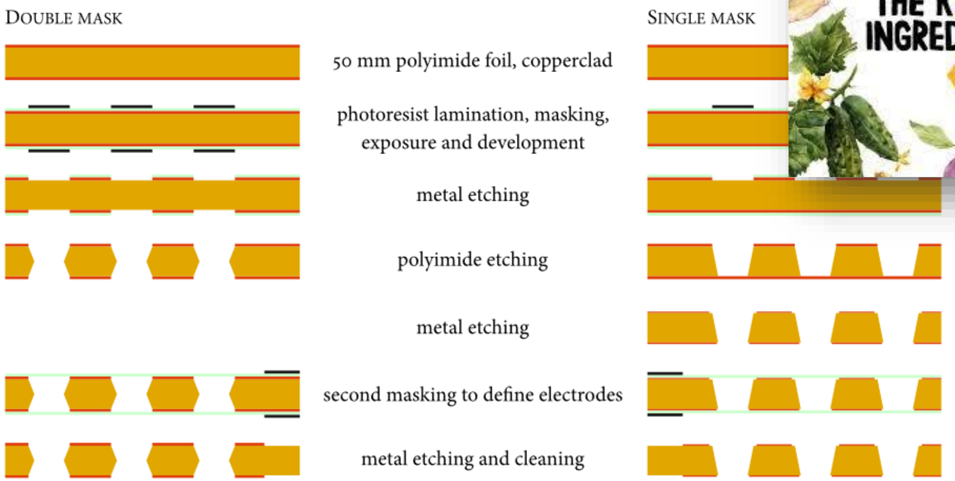

Figure 1. Schematic comparison of procedures for fabrication of a double-mask GEM (left) and a single-mask GEM (right).

S Duarte Pinto *et al* 2009 *JINST* **4** P12009 **DOI** 10.1088/1748-0221/4/12/P12009

CERN Micro Pattern Technology (MPT) Workshop

M. Bianco, CERN EP Detector Seminar, 8/7/2022, https://indico.cern.ch/event/1175363/

Key developments for what shown before (ALICE TPC)

CMS GEM

NS2 (*no- spacer*, *no*-stretch) Technique

J. Merlin, PHD thesis, https://cds.cern.ch/record/2155685/files/CERN-THESIS-2016-041.pdf

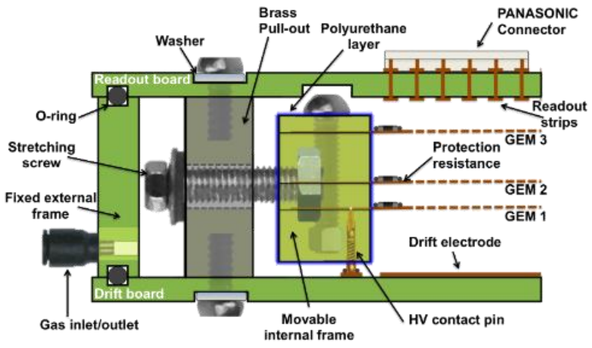

FIGURE 5.6: Cross-section of a single GE1/1 detector showing the main components and the self-stretching structure.

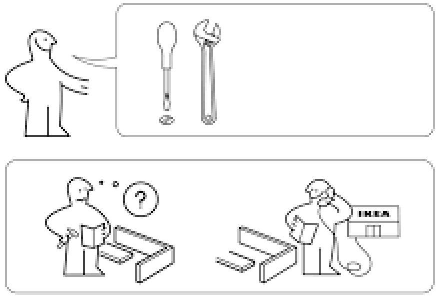

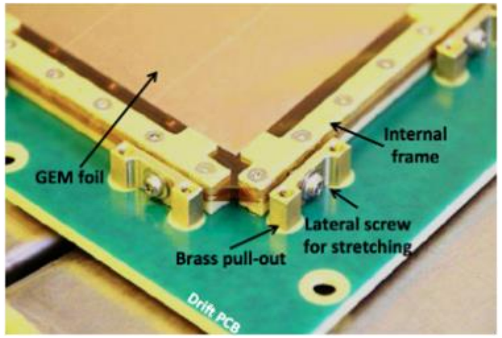

FIGURE 5.7: Bottom left corner of a GE1/1 detector during the assembly showing the self-stretching structure.

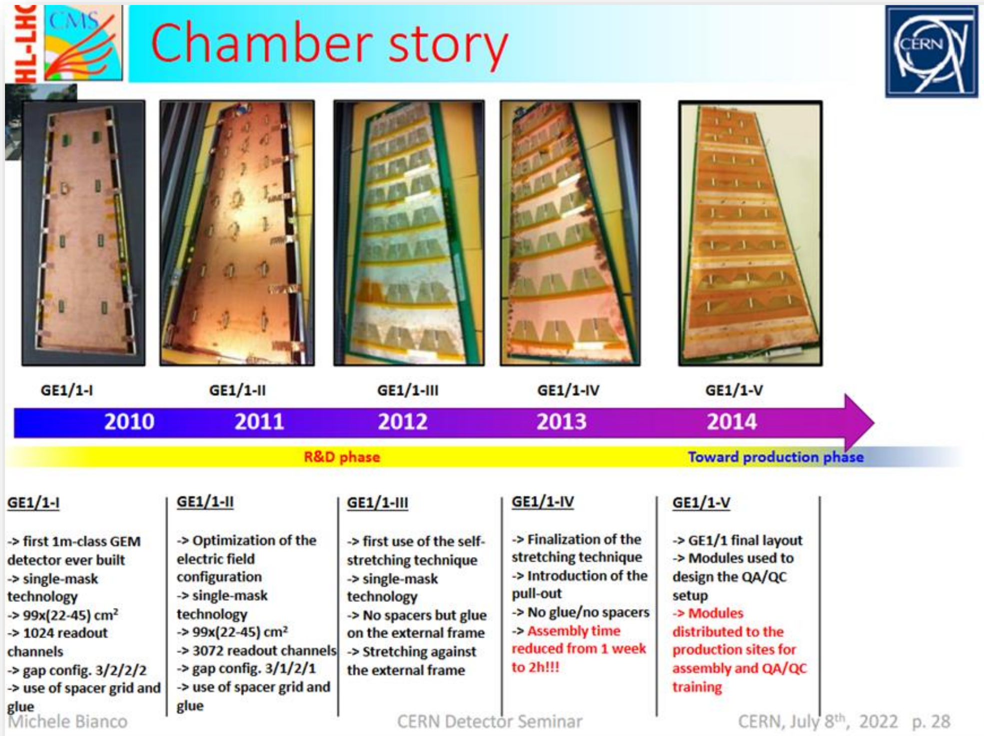

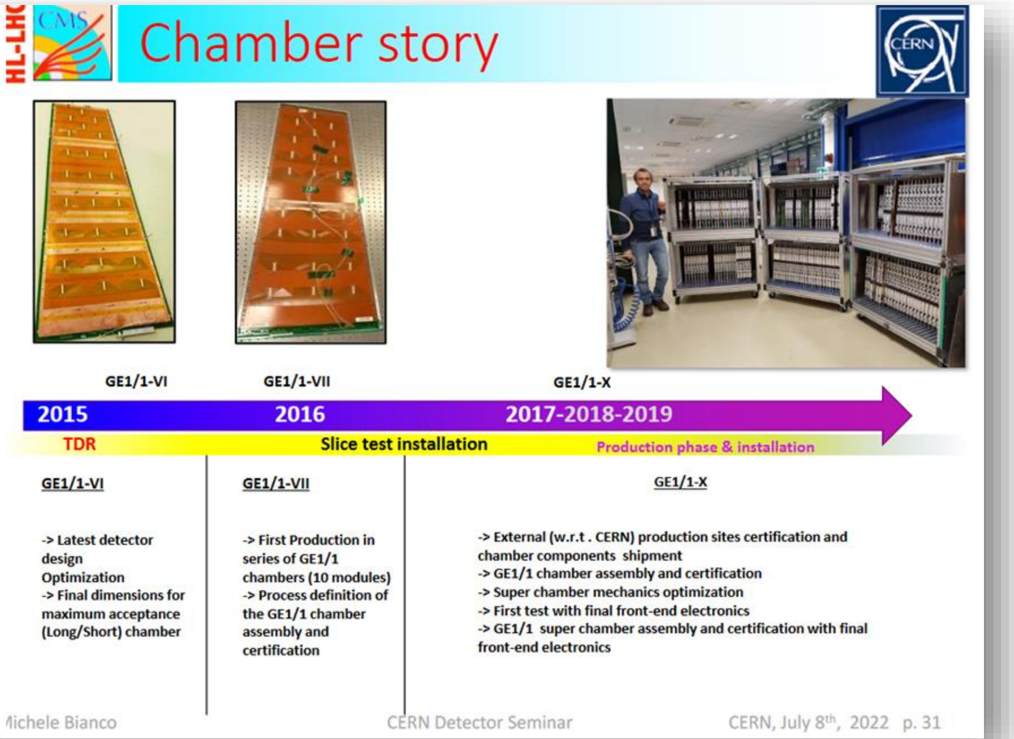

Pro/Cons to be considered

Pro: assembly

Main Cons: gaps uniformity

M. Bianco, CERN EP Detector Seminar, 8/7/2022, https://indico.cern.ch/event/1175363/

CMS Muons (ME0)

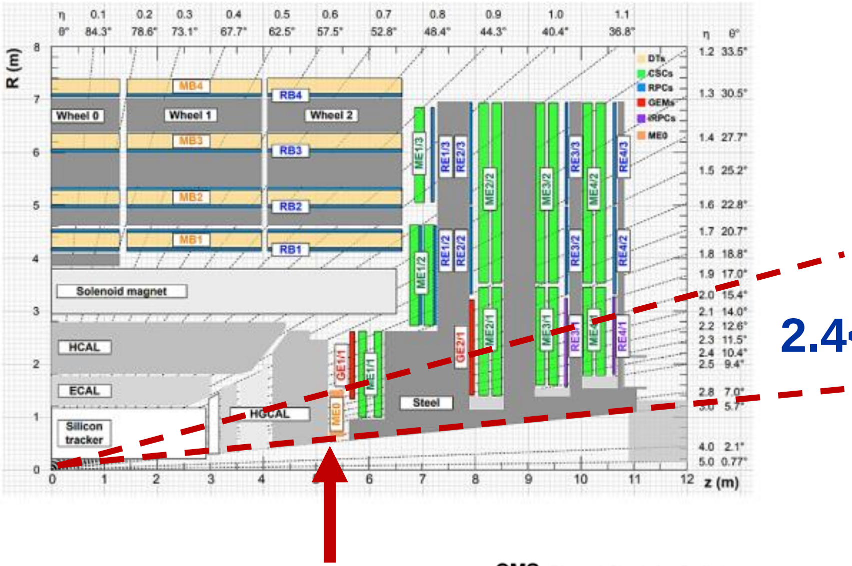

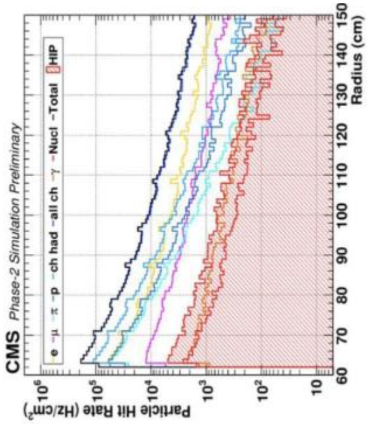

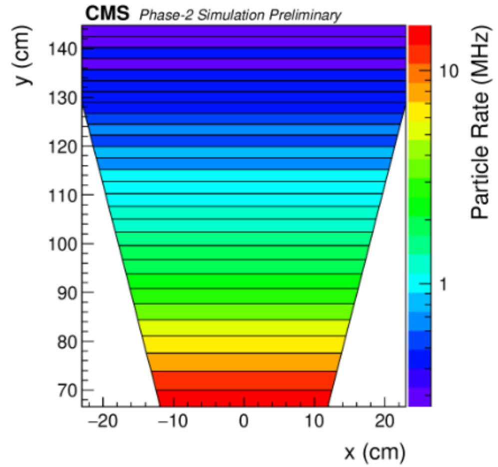

M. Bianco et al., arXiv:2201.09021, https://cds.cern.ch/record/2801251/

Random sectorization to minimize distortion (F. Sauli/GDD)

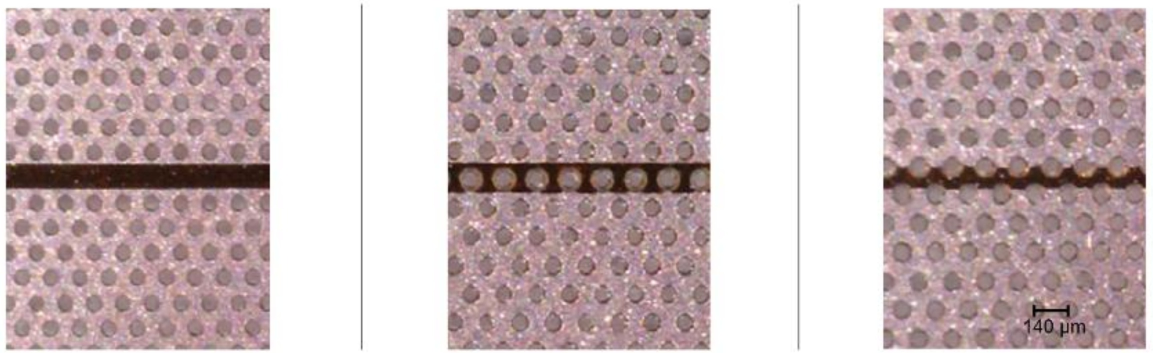

A.P. Marques et al., Nuclear Inst. and Methods in Physics Research, A 961 (2020) 163673, https://doi.org/10.1016/j.nima.2020.163673

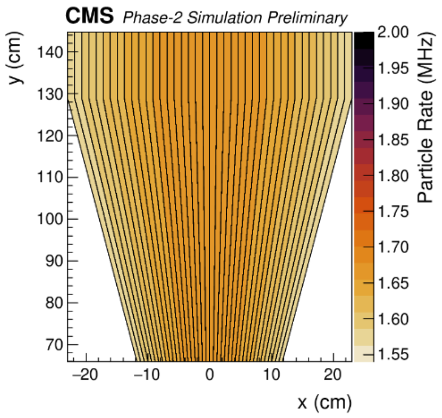

Fig. 10. Design of the adopted azimuthal segmentation for the ME0 detectors, showing the expected background particle rate per sector in the CMS environment.

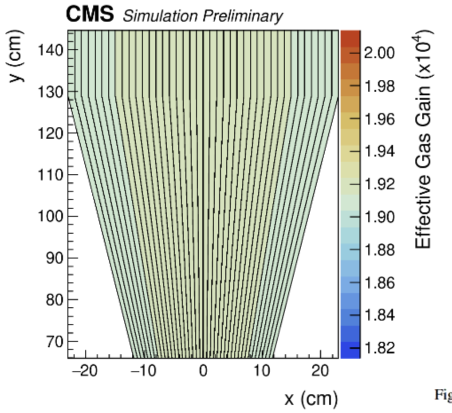

Fig. 12. Expected gain of the ME0 detectors with azimuthal segmentation for each GEM foil sector under irradiation in the CMS environment.

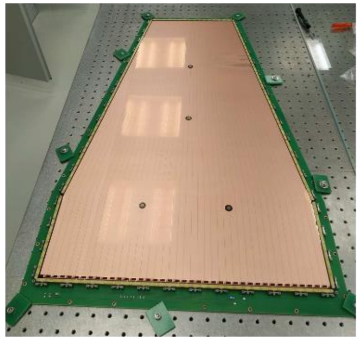

Fig. 13. Picture of the first GEM foil produced with azimuthal segmentation.

*@ **MPGD 2022 Antonello Pellecchia**, Michele Bianco, Production and characterization of random electrode sectorization in GEM foils*

Discharges & propagation

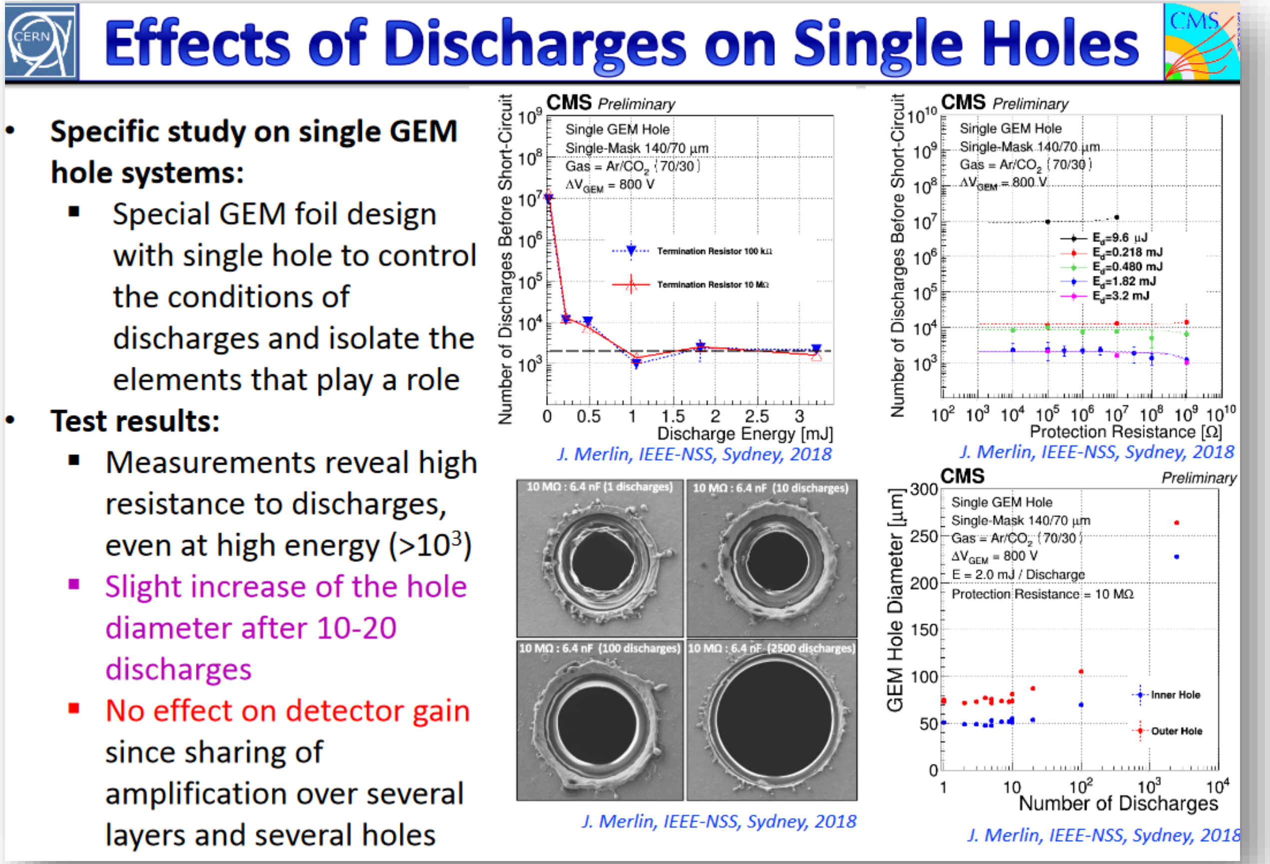

New recipe: Double Segmented Foils

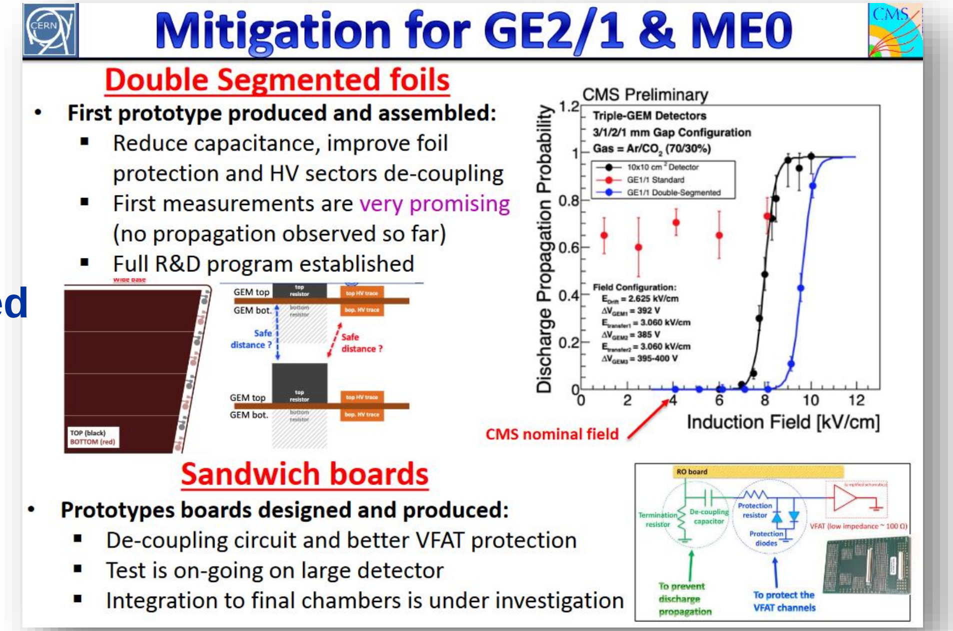

Not applicable to last GEM foil (coupling)

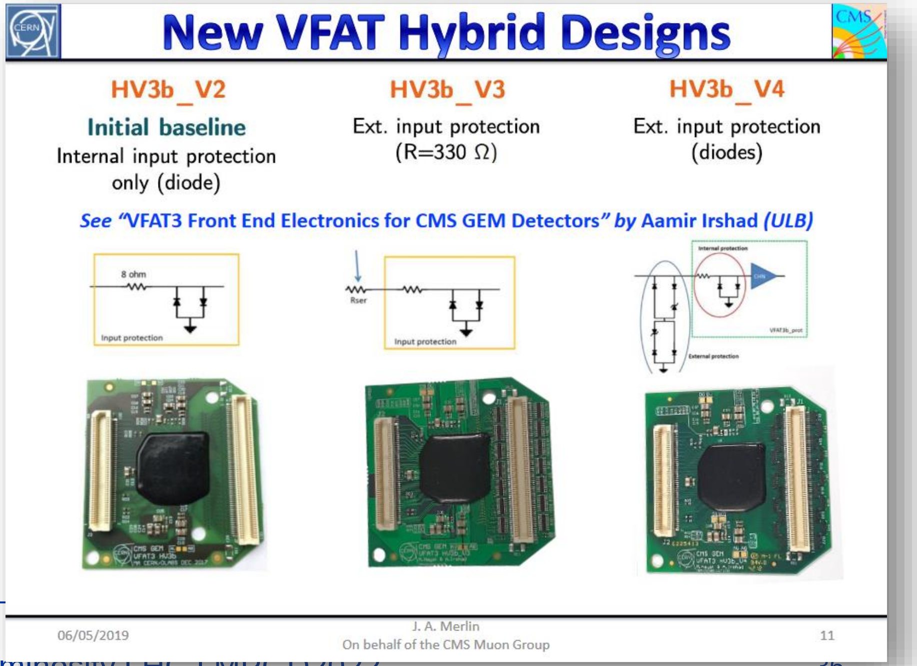

MicroPattern Gaseous Detectors Conference 2019

J. Merlin, Study of discharges and their effects in GEM detectors, https://indico.cern.ch/event/757322/contributions/3396501/

CMS GEM GE1/1 (LS2)

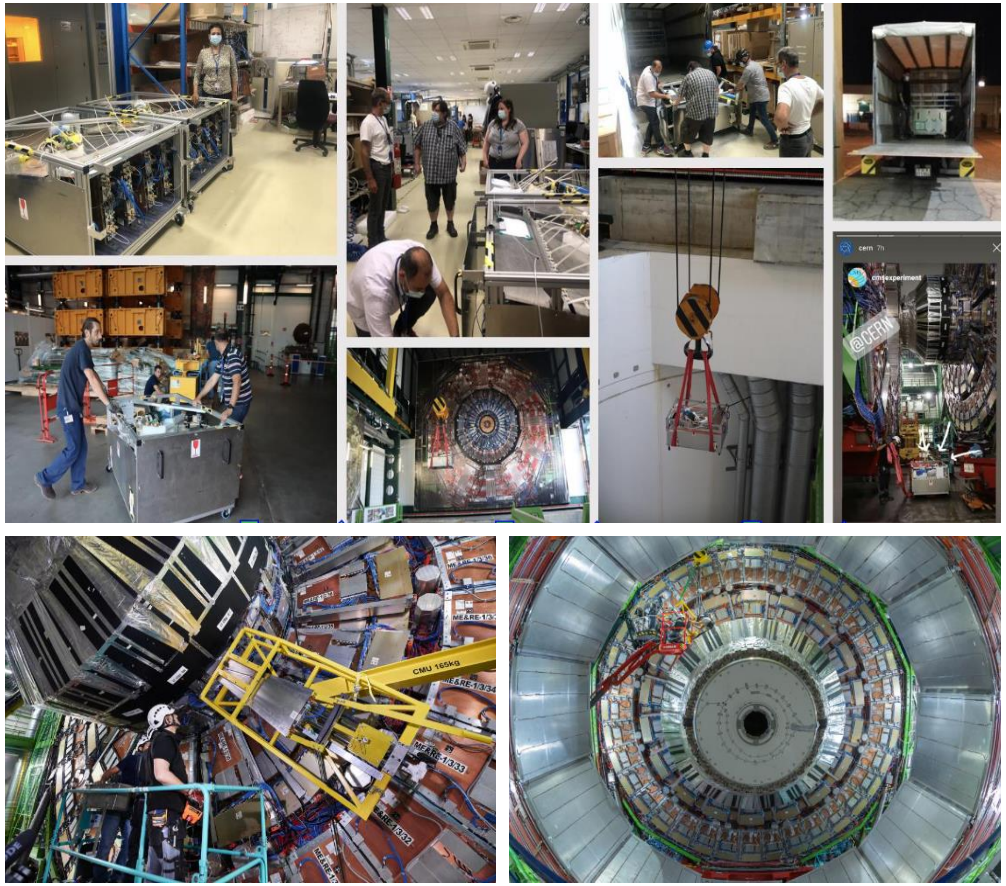

http://cds.cern.ch/record/2684028, https://www.youtube.com/watch?v=fU0ujGWbeQ0&feature=youtu.be

M. Bianco, The GEM detectors within the CMS Experiment, CERN EP Detector Seminar, 8/7/2022, https://indico.cern.ch/event/1175363/

CMS GE2/1 & iRPC Demonstrators (LS2)

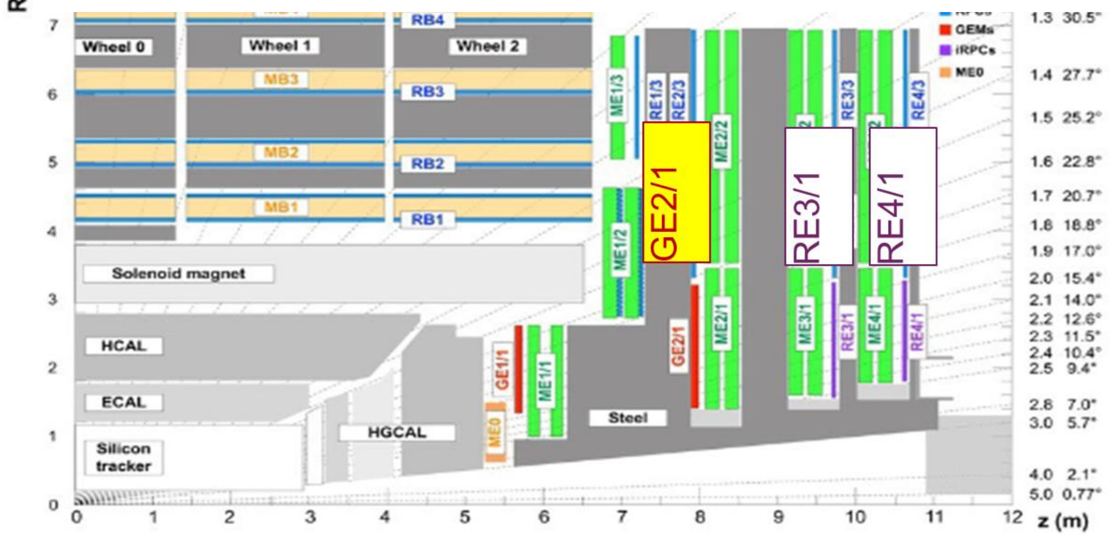

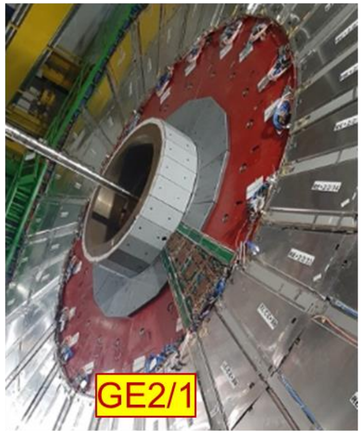

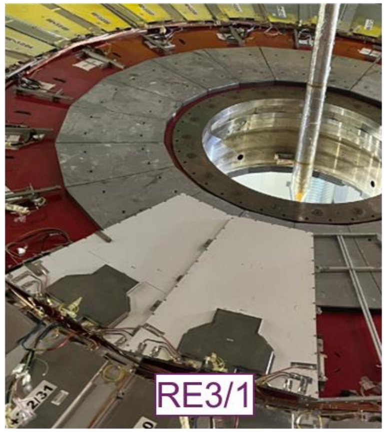

CMS GEM GE1/1 (LS2)

2021 TEST COLLISION DI-MUON IN GEM (+CSC +RPC)

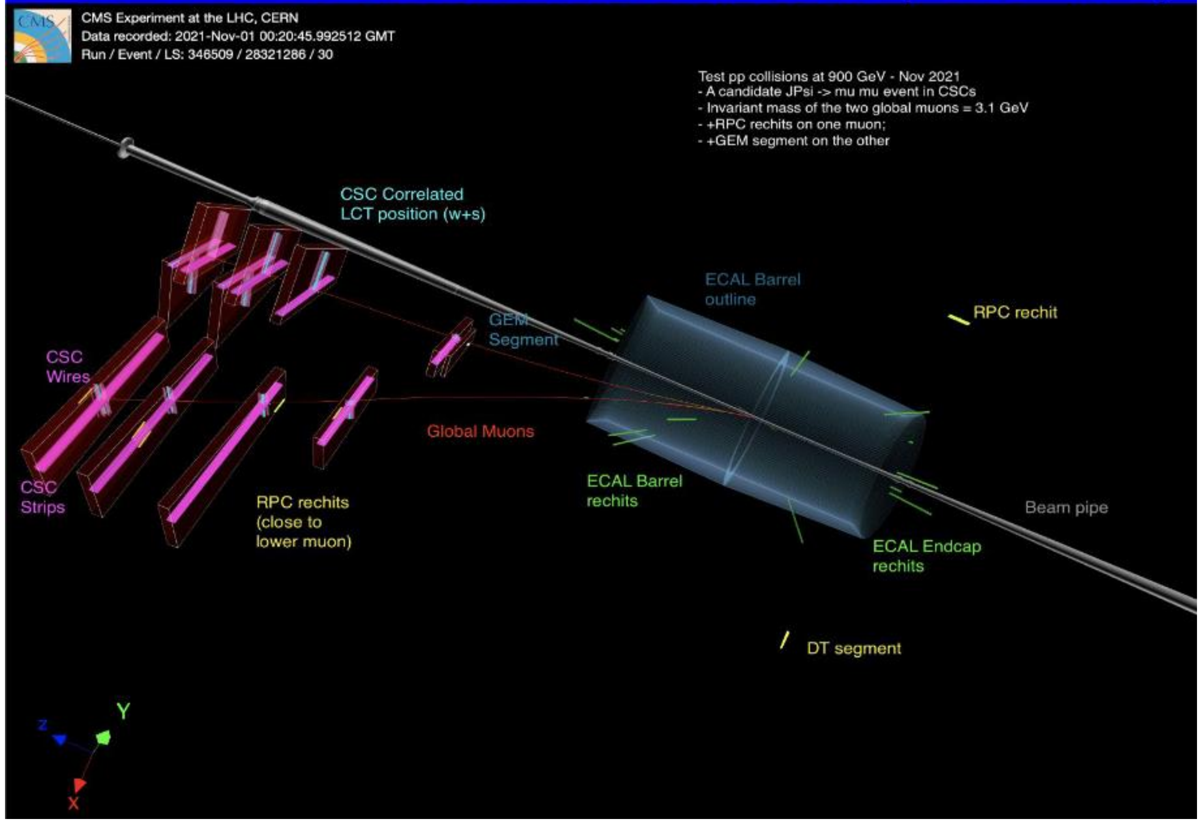

2022 CRAFT MUON IN GEM (+CSC +RPC)

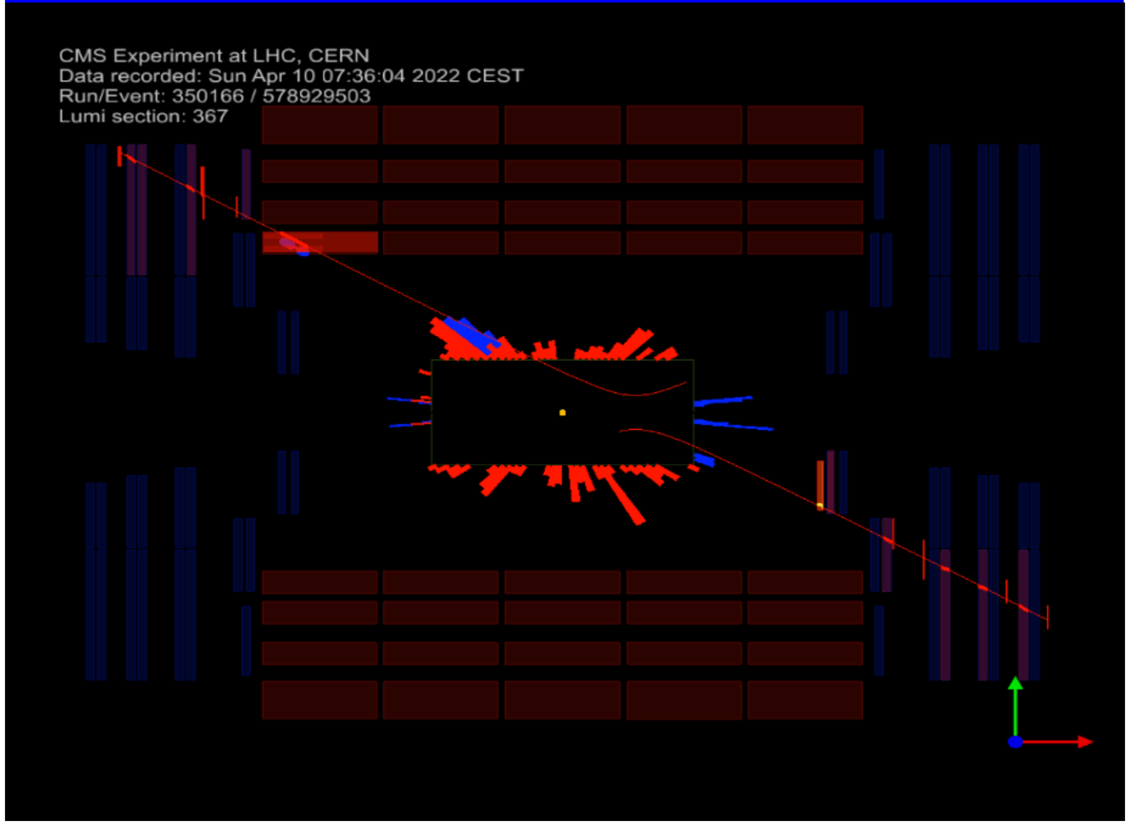

M. Bianco, The GEM detectors within the CMS Experiment, CERN EP Detector Seminar, 8/7/2022, https://indico.cern.ch/event/1175363/

LHCb

Burkhard Schmidt, 2016 J. Phys.: Conf. Ser. 706 022002
https://iopscience.iop.org/article/10.1088/1742-6596/706/2/022002/pdf

C. Lacasta, DETECTOR UPGRADES FOR THE HL-LHC XIII CPAN days, March 2022, Huelva,
https://indico.ific.uv.es/event/6457/contributions/17779/attachments/10004/13374/Detector.Upgrades.CPAN22.pdf

LHCb towards HL-LHC

LHCb Upgrade I (LS2)

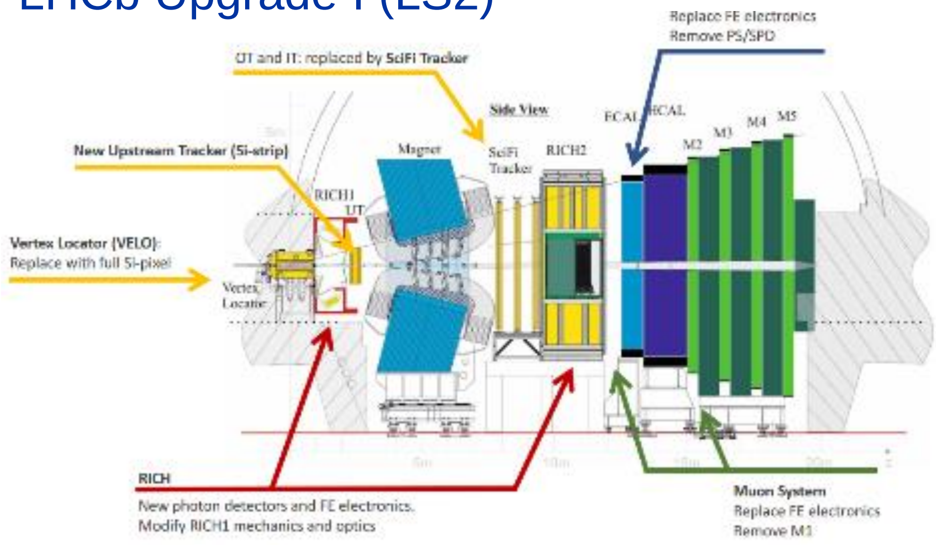

LHCb Upgrade II (LS4 -2033/2034)

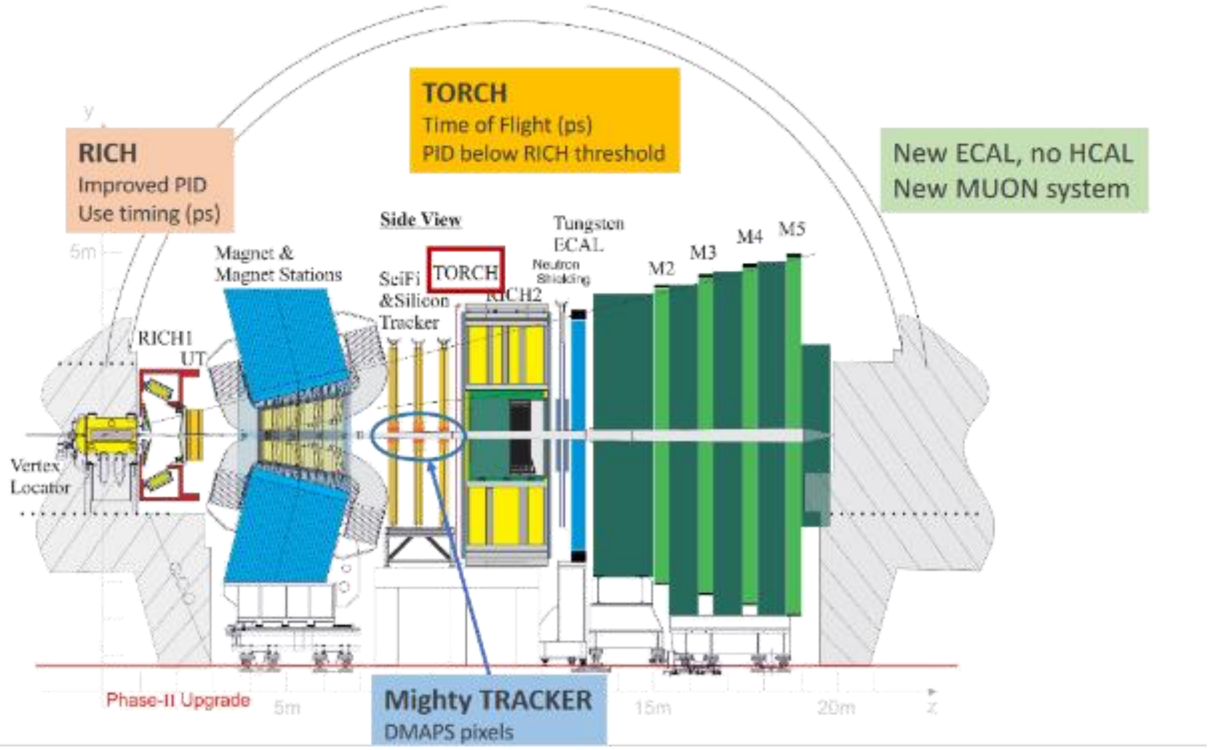

- Tracker Upgrade:
  - VELO: 55x55μm^2 pixels (before strips), 3.5mm (5.5mm) inner radius, , 40MHz readout, rad-hard (>5x10^15 MeV n eq cm^2), on-chip zero suppression, new CO2 based cooling.
  - UT: silicon micro-strip with higher segmentation and acceptance, 300μm (before 500μm) thick;
  - SciFi: fibers with SiPM readout (defore Si strips and straw), higher segmentation, higher acceptance, lower material budget.

- Particle Identification System
  - RICH: mult-anode istead of hybrid (HPD) photodetectors
  - Calorimeter: PMT gain reduced, Preshower(PS) and Scintillating Pad Detector (SPD) removed (HW trigger), electronics upgrade for trigger-less readout.
  - **Muon system: removal of M1 station (L0 trigger) & upgrade of M2-M5**

- **Full software trigger (upgrade of FE/BE electronics)**

New MUON system → μRWELL

LHCb

~1 MHz/cm²

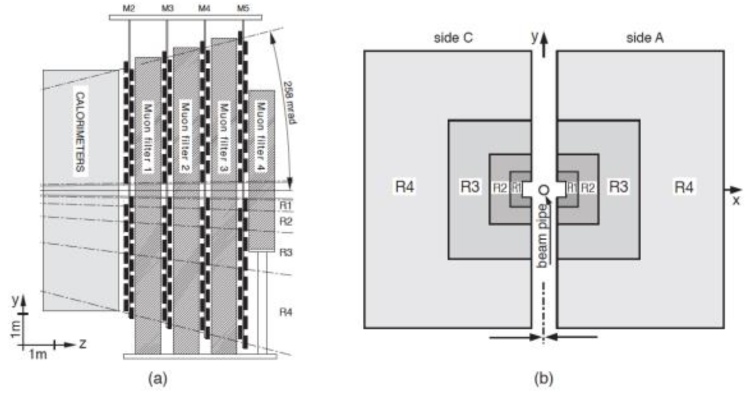

Figure 4.15: (a) Side view of the LHCb muon system for the Phase-I Upgrade. (b) Station layout with the four regions R1–R4 indicated.

M2 station - max rate (kHz/cm²)

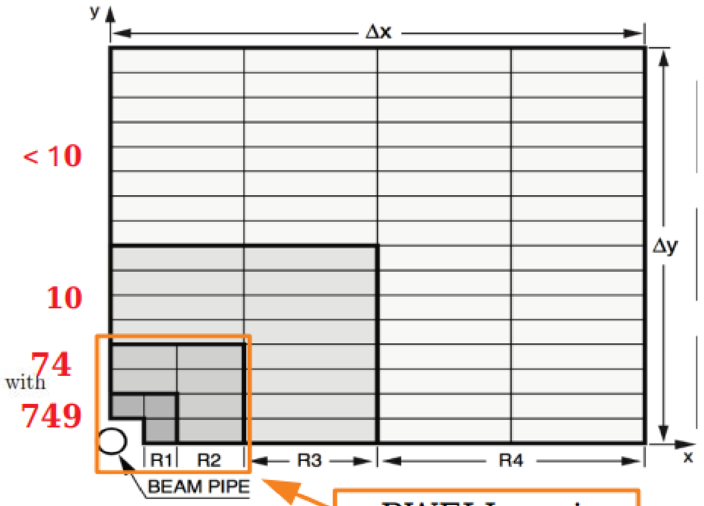

μ-RWELL region

Rates (kHz/cm²)	M2	M3	M4	M5
R1	749	431	158	134
R2	74	54	23	15
R3	10	6	4	3
R4	8	2	2	2

Area (m²)	M2	M3	M4	M5
R1	0.9	1.0	1.2	1.4
R2	3.6	4.2	4.9	5.5
R3	14.4	16.8	19.3	22.2
R4	57.6	67.4	77.4	88.7

R1/R2 μRWELL **(4 gaps/chamber - redundancy)**
R3/R4 MWPC (alternative solutions for R4 are RPC or Scintillating-tile+WLS+SiPM)

R1÷R2: 576 detectors, size 30x25 to 74x31 cm², 90 m² detector (130 m² DLC)

LHCb muon apparatus Run5 – Run6 requirements

- Rate up to **1 MHz/cm²** on detector single gap
- Rate up to **700 kHz** per electronic channel
- Efficiency quadrigap >=99% within a BX (25 ns)
- Stability up to **1C/cm²** accumulated charge in 10y at M2R1, G=4000

CERN-LHCC-2017-003, Expression of Interest for a Phase-II LHCb Upgrade: Opportunities in flavour physics, and beyond, in the HL-LHC era, https://cds.cern.ch/record/2244311/

CERN-LHCC-2021-012 ; LHCB-TDR-023, Framework TDR for the LHCb Upgrade II - Opportunities in flavour physics, and beyond, in the HL-LHC era, https://cds.cern.ch/record/2776420/

High Rate (HR) µRWELL

Rate vs protection

The avenue of the charge evacuation (*)

Table 1. Resistive and geometrical parameters of the HR-layouts compared with the low rate baseline option (SRL). For the SG models the ground-pitch is the grid-pitch.

Layout	ρ (MΩ/□)	ground-pitch (mm)	dead-zone (mm)	DOCA (mm)	geometric acceptance (%)	Ω_{eff} (MΩ)
SG1	70	6	2	0.85	66	134
SG2	65	12	1.2	0.45	90	209
SG2++	64	12	0.6	0.25	95	200
DRL	54	6	0	7	100	270
SRL	70	100	0	5.5	100	1947

Single-Resistive Layout

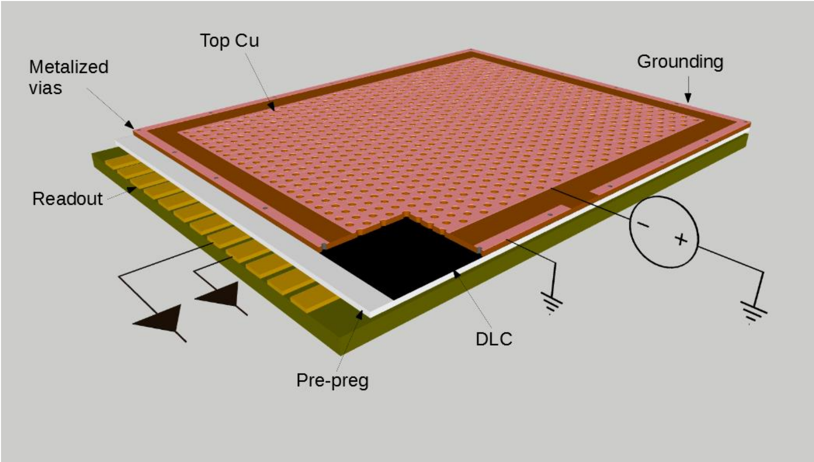

Double-Resistive Layout

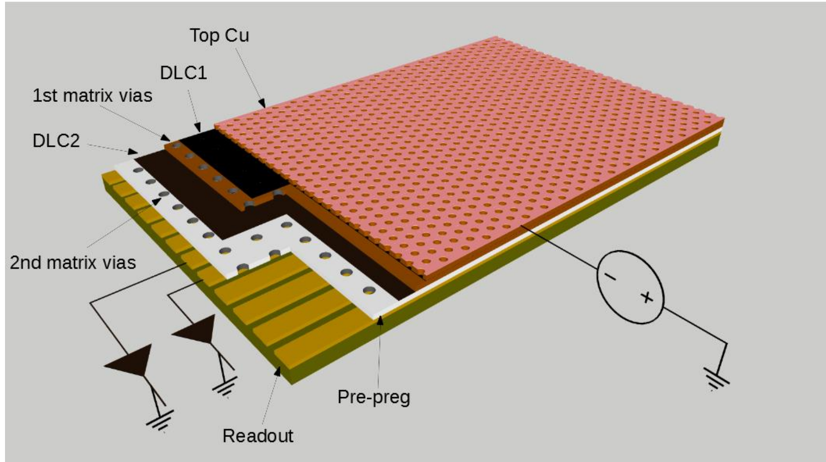

Silver-Grid Layout

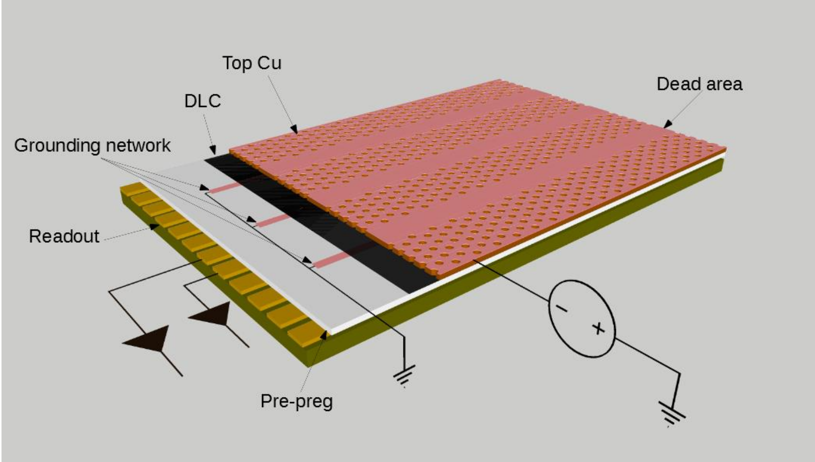

G. Bencivenni *et al* 2019 *JINST* 14 P05014, The µ-RWELL layouts for high particle rate DOI 10.1088/1748-0221/14/05/P05014, https://iopscience.iop.org/article/10.1088/1748-0221/14/05/P05014/pdf

(*) A. Teixeira Micromegas Pad Resistive Read-Out with Embedded Protection Resistor Production, https://indico.cern.ch/event/356113/contributions/1766894/

High Rate (HR) µRWELL

G. Bencivenni *et al* 2019 *JINST* 14 P05014, The µ-RWELL layouts for high particle rate
DOI 10.1088/1748-0221/14/05/P05014, https://iopscience.iop.org/article/10.1088/1748-0221/14/05/P05014/pdf

Ar/CO2/CF4 (45/15/40)

Table 1
Summary of the features of the new single-resistive high-rate (HR) versions of the µ-RWELL together with the Double Layer (DL) [5], the first high-rate-oriented µ-RWELL realized.

HR scheme	n. layers	pitch	type	Geom. accept.
SG v1	Single	6 mm	cond. grid	66%
SG v2	Single	12 mm	cond. grid	90%
RG	Single	6 mm	resist. grid	–
DL	Double	6 + 6 mm	cond. vias	–

Gain up to ~10^4

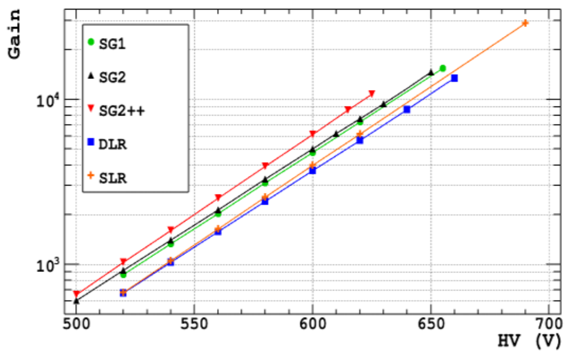

Rate capability up to 10 –20 MHz/cm²

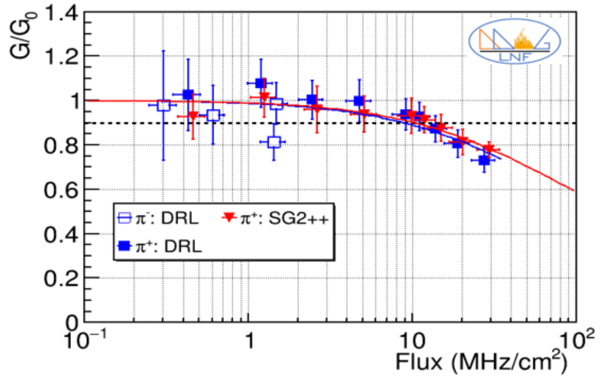

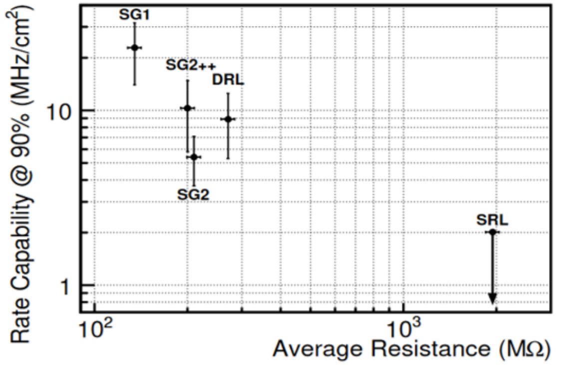

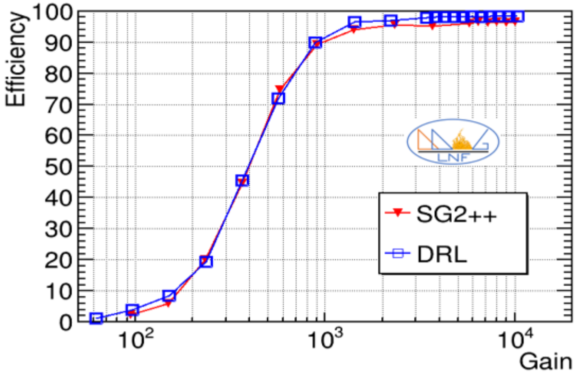

Efficiency ~97%

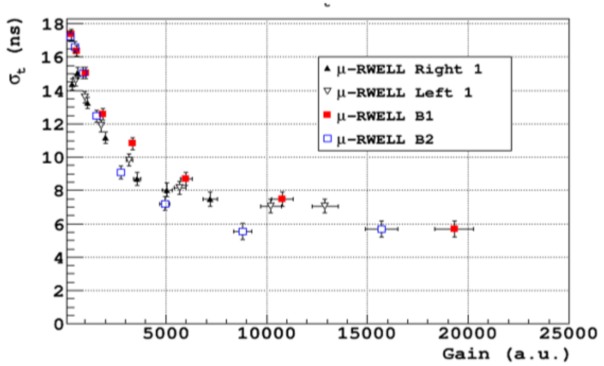

Time resolution 5-6 ns

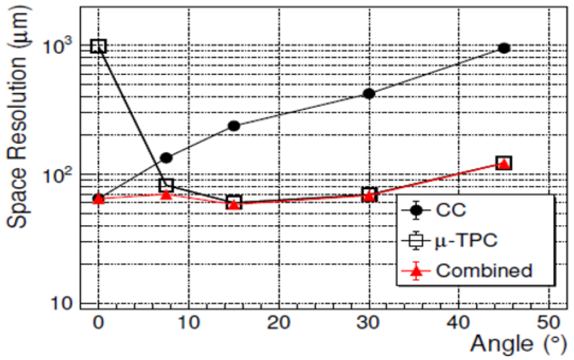

Space resolution down to 60 µm

The HR layout

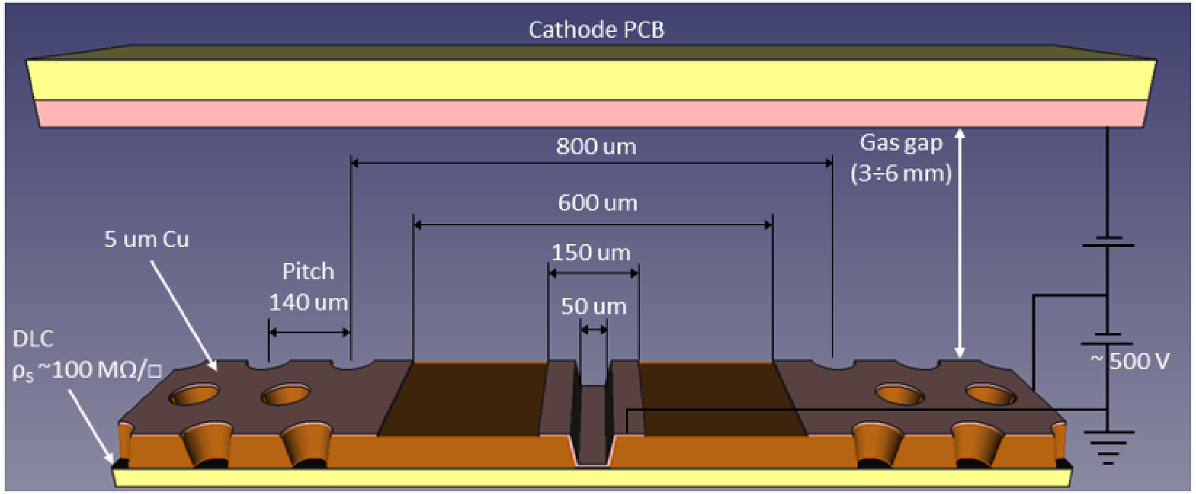

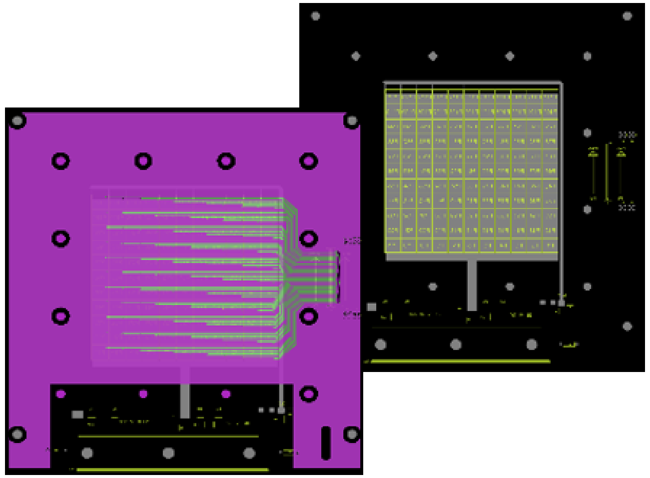

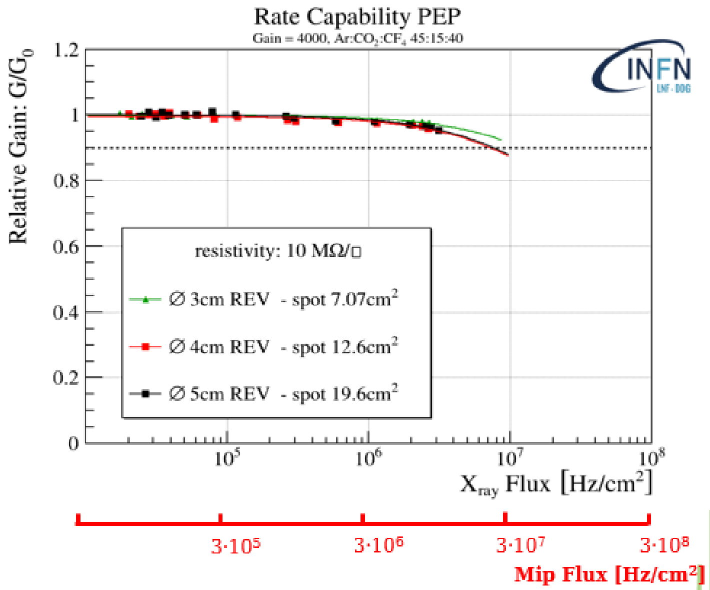

The **PEP** layout (Patterning – Etching – Plating) is the **state of art** of the **high rate** layout of the μ-RWELL developed **for LHCb**

- **Single DLC** layer
- **Grounding line from top** by kapton etching and plating (pitch down to 1/cm)
- **No alignment** problems
- **High rate** capability
- **Scalable to large size** (up to 1.2x0.5 m for the upgrade of CLAS12)

G. Bencivenni, The micro-RWELL for R1/R2, LHCb Italia meeting - 15 Nov 2022
G. Morello, The micro-RWELL detector for the LHCb Muon system phase-2 upgrade, ICHEP 2022, https://agenda.infn.it/event/28874/contributions/169584/

μRWELL, R&D (on) Production

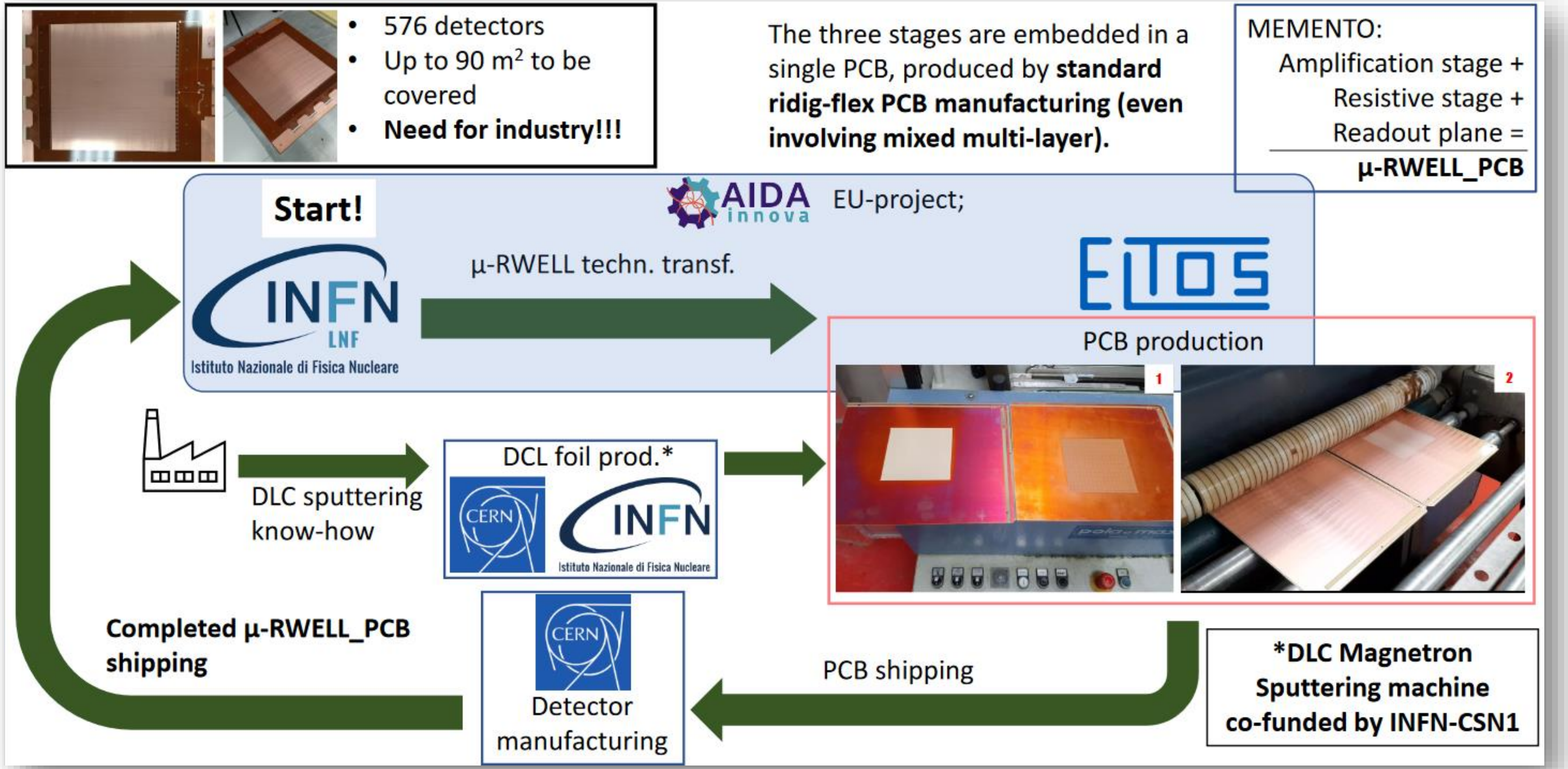

G. Morello, The micro-RWELL detector for the LHCb Muon system phase-2 upgrade, ICHEP 2022, https://agenda.infn.it/event/28874/contributions/169584/

CID: the CERN-INFN DLC machine

- **Flexible substrates, coating** areas **up to 1.7 m** × **0.6 m**
- **Rigid substrates, coating** areas up to **0.2 m** × **0.6 m**
- **Five cooled target holders,** arranged as two pairs face to face and one on the front, equipped with five shutters
- **Sputtering & co-sputtering different materials,** in order to create a coating layer by layer or an adjustable gradient in the coating
- **Installation,** week 43
- **Commissioning** & **training** of the CERN-INFN teams, week 44
- **Test runs**, week 47
- **1 week/month** joint CERN-INFN test runs

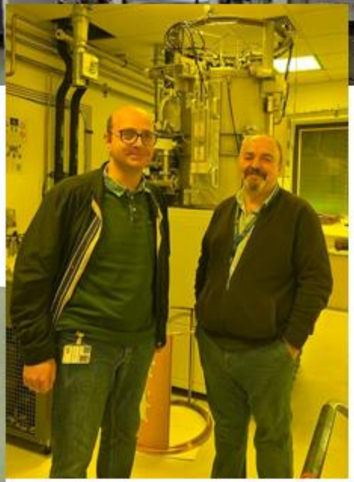

G. Bencivenni, The micro-RWELL for R1/R2, LHCb Italia meeting - 15 Nov 2022

.. and now what has been left out or postponed

… interesting ideas and approaches

ALICE TPC / explored alternative (MPGD) options…

Triple GEM/Cobra

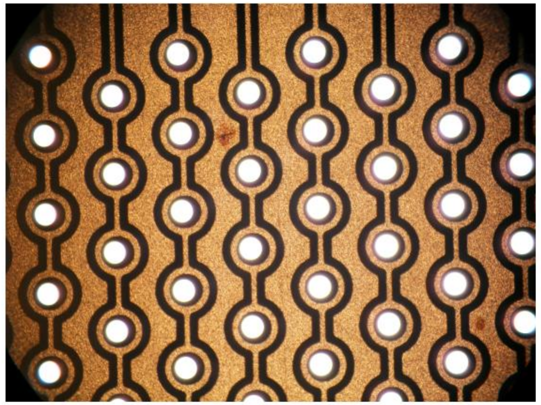

Figure 9.1: Photograph of COBRA 1 showing the GEM (around the holes) and COBRA electrodes.

Used as second and/or third GEM in the stack. Good IBF but worse energy resolution

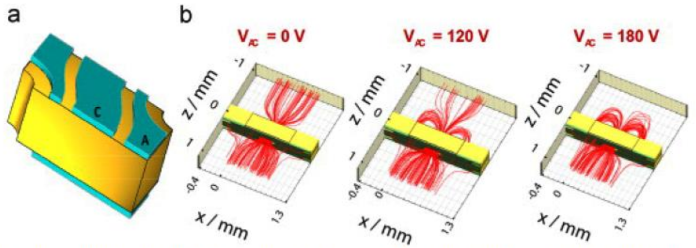

Figure 9.2: (a) COBRA GEM unit cell built in the simulation program ANSYS (b) ion drift lines in a COBRA GEM with three different potential differences ΔU_{AC} between GEM electrode (A) and COBRA electrode (C). Image from [1].

	thickness (μm)	hole size (ø) (μm)	pitch (μm)	rim size (μm)	insulator
COBRA 1	400	300	1000	100	FR5
COBRA 2	200	150	500	50	FR5
COBRA 3	100	100	400	0	LCP
GEM 50	50	70	140	0	LCP
GEM 100	100	70	140	0	LCP

Table 9.1: Geometries of COBRA GEMs and standard GEMs used for the measurements.

2 GEM + micromegas

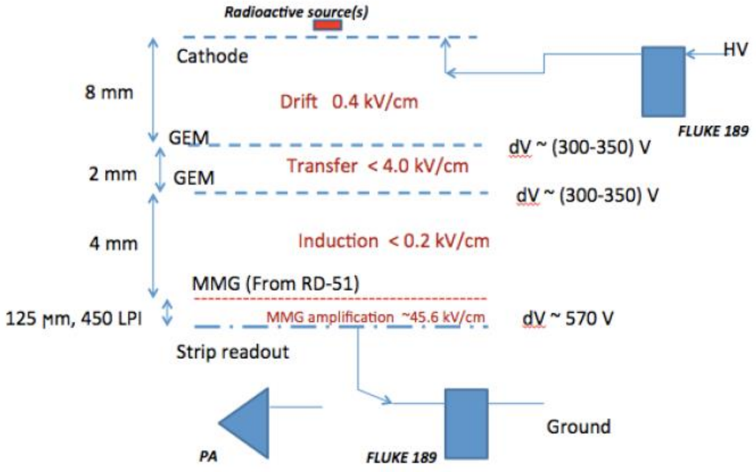

Figure 9.14: Setup used for preliminary ion backflow measurement for the hybrid 2 GEM + MMG system.

Worse discharge stability compared to quadrupole GEM measured at Super Proton Synchrotron (SPS) and Proton Synchrotron (PS) test beam at CERN

CERN-LHCC-2013-020 ; ALICE-TDR-016, Upgrade of the ALICE Time Projection Chamber, https://cds.cern.ch/record/1622286

High-η tagger

MPGDs regarded as the likely baseline solution.
A silicon-pixel option is also considered.
Technologies may also be combined for separate optimization of e.g. the inner and outer regions.

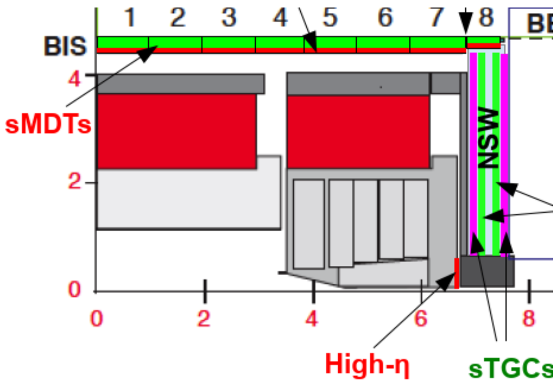

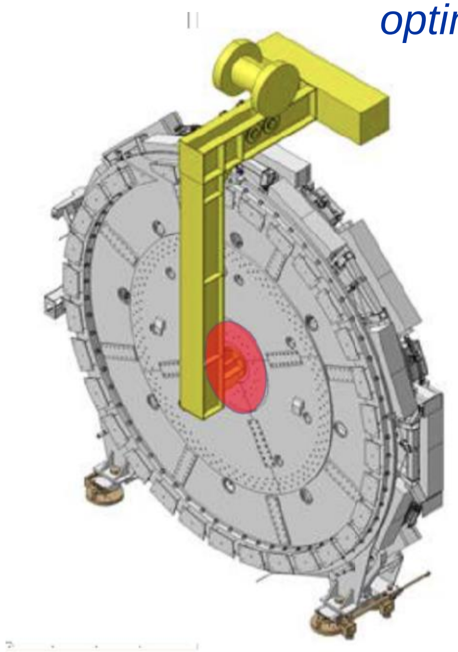

5 cm deep cavity of 2 m diameter is implemented at the centre of JD as the space for housing the high-η tagger.

a) **Resistive pixelated Micromegas** (Small Pad Resistive Micromegas)
b) **Micro-Pixel Chamber (μ-PIC)**
c) **Micro-resistive WELL (μ-RWELL)**
d) **Fast timing Micromegas (PICOSEC micromegas)**

All the mentioned MPGD technologies implement a **resistive spark protection layer** (either in full plane or patterned). Recent common developments employ Diamond Like Carbon (DLC) layers formed by carbon sputtering for high-quality resistive layers, and engineering towards a large-size detector.

Integration of front-end electronics in MPGD: All MPGD will employ highly segmented readout elements, for which the signal routing to the front-end electronics is a challenge.

Rate Capability (@ inner radius R = 25 cm): up to 10 MHz/cm^2)
Granularity (@ inner radius R = 25 cm): mm^2
Spatial resolution: around 0.5 mm.
Radiation Hardness (@ inner radius R = 25 cm and 3000 fb−1): 900 kGy for TID and 5.4x10^{15} 1-MeV n_{eq} cm^{-2}

CERN-LHCC-2017-017 ; ATLAS-TDR-026, Technical Design Report for the Phase-II Upgrade of the ATLAS Muon Spectrometer, http://cds.cern.ch/record/2285580/

High-η tagger (potential candidates/MPGD)

Resistive pixelated Micromegas

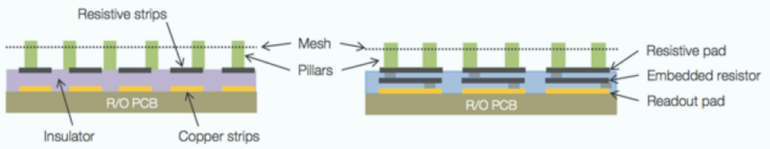

Figure 9.4: Left: The resistive Micromegas used for the NSW. Right: Pads Micromegas with an embedded resistor structure on top of the anode readout pads.

M. Iodice, Towards Large Size Pixelized Micromegas for operation beyond 1 MHz/cm2
(started as an option for the high-eta-tagger)

Though not all linked to the eta-tagger, three of the four technologies well represented at MPGD 2022

Micro-resistive WELL (μ-RWELL)

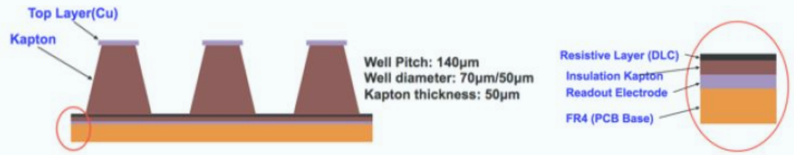

Figure 9.16: Zoom into the μ-RWELL PCB. The PCB consists of (from top to bottom) a kapton foil coated with copper on top and etched with a well pattern, a resistive layer for discharge suppression and spark protection, and a readout PCB.

K. Gnanvo, Development of Large Area μRWELL Detectors for CLAS12 High Luminosity Upgrade at Jefferson Lab
L. Shekhtman, Performance of the large-area micro-RWELL detectors
M. Poli Lener, The state of art of the μRWELL technology
(all for tracking, with relatively large area)

Micro-Pixel Chamber (μ-PIC)

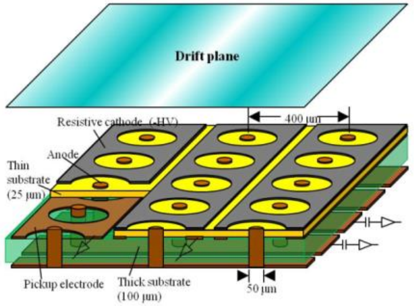

Figure 9.11: Structure of μ-PIC with resistive cathode. Cathodes are made of a resistive material (surface resistivity is a few MΩ/□). Signals from the cathodes are read out from pick-up electrodes as induced charge.

Fast timing Micromegas (PICOSEC micromegas)

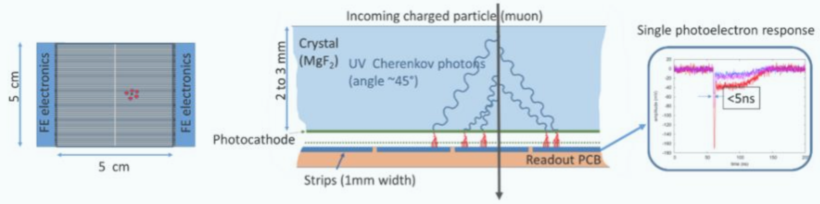

Figure 9.20: Example of a prototype of a multi-strip detector for the high-η tagger. The Cherenkov photons are emitted at an angle of about 45° in the MgF_2 crystal. An average of 10 photoelectrons are collected in the pre-amplification stage. The figure on the right shows the response to a single photoelectron. Using an adequate pre-amplifier, the fast-electron peak sticks out clearly over the slow ions signal.

A. Utrobicic, A large area 100 channel PICOSEC Micromegas detector with sub 20 ps time resolution
M. Lisowska, Towards robust PICOSEC Micromegas precise timing detectors

CERN-LHCC-2017-017 ; **ATLAS-TDR-026**, Technical Design Report for the Phase-II Upgrade of the ATLAS Muon Spectrometer, http://cds.cern.ch/record/2285580/

μRWELL proposal for CMS

L. Borgonovi, Study of the μ-RWELL detector technology
for the CMS forward muon system upgrade,
https://indico.ihep.ac.cn/event/7389/contributions/93815/attachments/49668/57191/Lisa_poster_Pechino_2.pdf

The μ-RWELL technology

The micro-Resistive WELL (μ-RWELL) is a compact single amplification stage intrinsically spark protected Micro Pattern Gaseous Detector (MPGD)

The detector structure

The μ-RWELL detector is composed of only two elements: the μ-RWELL PCB and the drift cathode.

They are separated by a drift gap of 4-7 mm.
The μ-RWELL PCB is the core of the detector and it is realized by coupling:

1. A WELL patterned kapton foil (50 μm) as single amplification stage: conical channels 70 μm (50 μm) top (bottom) in diameter and 140 μm pitch), created using a chemical etching process.
2. A resistive layer (R ~100 MΩ/□) for discharge suppression and current evacuation realized in the DLC (Diamond Like Carbon) technology (high mechanical and chemical resistant material).
3. A rigid PCB readout electrode.

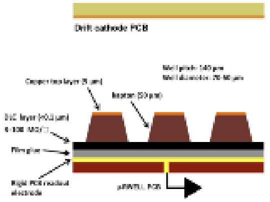

The detector advantages

- High spatial and time resolutions
- High rate capabilities, spark safe
- Radiation hardness
- Single amplification stage
- Versatility:
  - ➡ Low-rate particle scheme (LR) about 100 kHz/cm² (CMS-Phase II upgrade, SHIP);
  - ➡ High-rate particle scheme (HR) > 1 MHz/cm² (LHCb Muon upgrade, FCC-ee/hh, CepC, CepC)
- Simple production and assembly procedure: mass producible by industry; no stretching of kapton foils
- Reduction of costs and time to realize large area detectors

Beam tests @ CERN

CMS-GE1/1 size prototype

A CMS-GE1/1 μ-RWELL prototype was tested at the CERN H8 beam line during 2016 test beam campaign with 150 GeV/c muons and pions.

- ❖ Resistive DLC surface resistivity: about 70 MΩ/□ (LR configuration)
- ❖ Strips pitch = 800 μm
- ❖ Drift gap: 7 mm
- ❖ VFAT2 FE electronics
- ❖ Gas mixture: Ar/CO_2/CF_4 (45/15/40)

The results obtained from efficiency and time resolution tests have been compared with the performance of small μ-RWELL prototypes (10x10 cm², HR configuration): the behavior of all three prototypes is very similar.

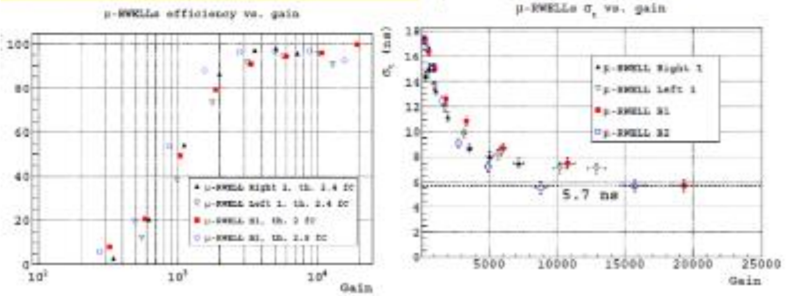

JINST 12 (2017) no.06, C06027: G. Bencivenni, R. De Oliveira, P. De Simone, G. Felici, M. Gatta, G. Morello, A. Ochi, M. Poli Lener, L. Benussi, L. Borgonovi, P. Giacomelli, A. Ranieri, M. Ressegotti, I. Vai, V. Valentino

CMS-GE2/1 M4 size prototype

A CMS-GE2/1 20° sector equipped with two large area M4 μ-RWELL detectors was assembled and exposed to a 150 GeV/c muon beam at the CERN H4 beam line. The GE2/1 sector was flushed with an AR/CO_2 70/30 gas mixture. The detector was placed on a remotely controllable moving platform in order to allow to scan the surface of the detector across the muon beam.

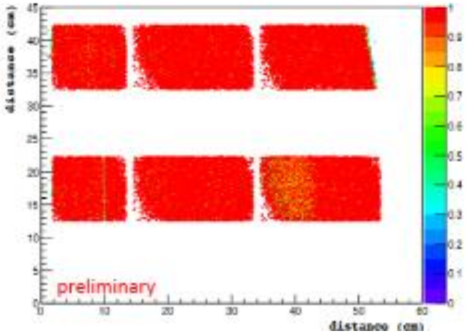

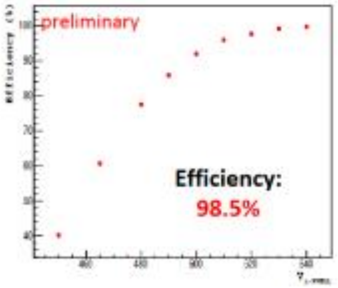

Ageing tests @ GIF++

From April 2017, the **GE1/1 size μ-RWELL** prototype (Ar/CO_2 70/30) has been exposed to the Gamma Irradiation Facility (GIF++) high-intensity source in the closest position to the source, together with two smaller prototypes:
High Rate μ-RWELL (Ar/CO_2/CF_4) 10x10 cm²
Reference μ-RWELL (Ar/CO_2) 5x5 cm²

Up to now, the CMS-GE1/1 has integrated more than 75 mC/cm² without any relevant change in performances (expected dose for GE1/1 in 10 years HL-LHC with safety factor 3: 18 mC/cm²)

Integrated charge vs time

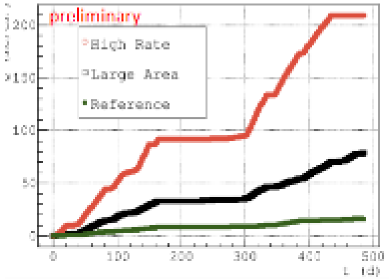

Current and applied voltage vs time for the GE1/1 size

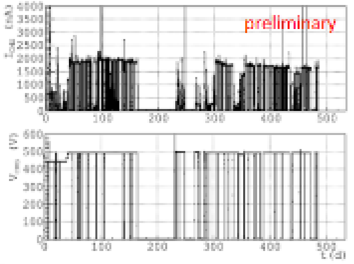

CMS Calorimeter / SCREAM

Sampling Calorimetry with Resistive Anode Micromegas

Resistive Micromegas for Particle Flow (sampling) calorimetry

→ at future linear colliders (ILC, CLIC)

HCAL with 1x1 cm2 pads, 4-5 lambda, 40 layers, W or Fe absorbers
Constrains on power-consumption (power pulsing), low noise (self-triggering)
High channel density (ASIC on PCB), active layer thickness (< 1 cm)

Advantage of resistive layer: removes spark protection diodes on PCB (→ cf. existing prototypes next slide)
(simpler design, more reliable, probably more cost effective)

→ at high-luminosity LHC (CMS)

Tail catcher of calorimetric system in forward region (completes Si-W ECAL+HCAL), upgrade for 2022 running
Constrains on rate capability, ageing, radiation hardness

Advantage of resistive layer: suppress or attenuate sparks, no or negligible dead time

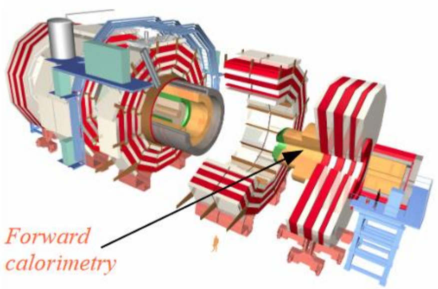

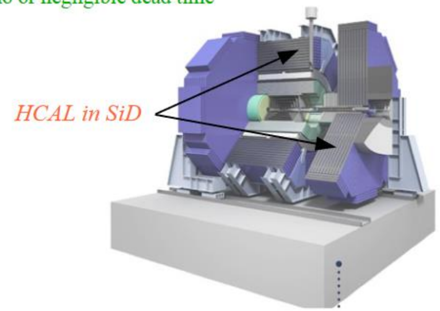

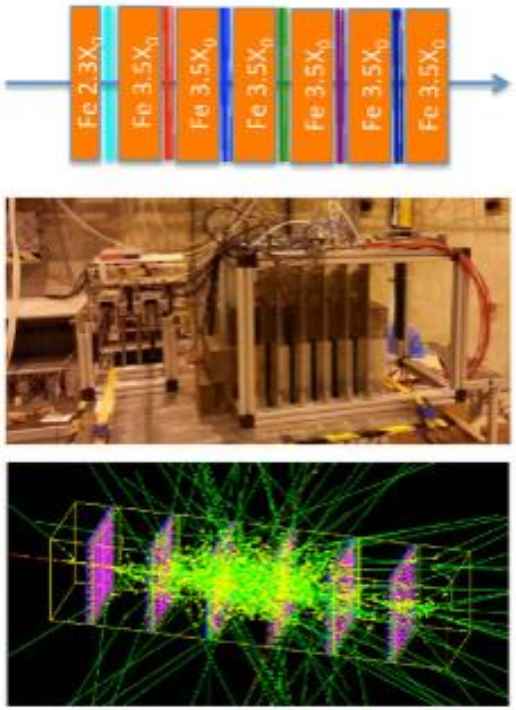

Figure 7. Prototype Calorimeter: setup schematic (top), picture of the apparatus (middle) and Geant simulated event (bottom).

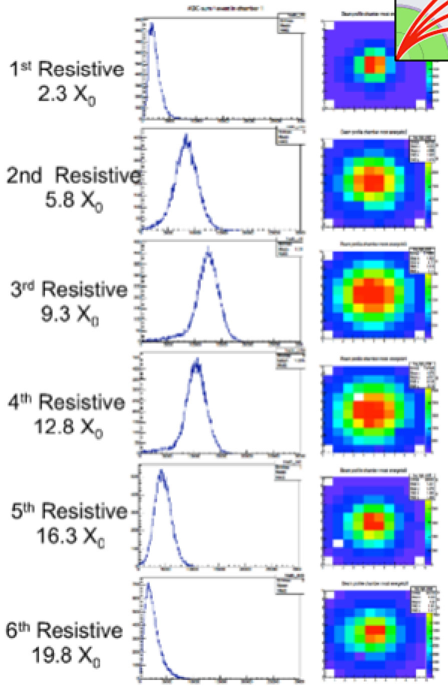

Figure 8. Spectra of energy deposited on every calorimeter layer (left) and the corresponding hit map (right) for 200 GeV e^-.

EPJ Web of Conferences 174, 01017 (2018) , https://doi.org/10.1051/epjconf/201817401017

M. Chefdeville, ANR proposal: SCREAM Sampling Calorimetry with REsisive Anode Micromegas, 11/10/2013, LAPP, https://indico.in2p3.fr/event/9015/contributions/48118/attachments/38670/47822/scream_slides.pdf
F.Ferri, Upgrade Phase II – CMS, CSTS du SPP – November 13, 2013, https://irfu.cea.fr/Phocea/file.php?file=Seminaires/3142/Upgrade_phase_II_CMS_FF.pdf
Embedded reistors (previously mentione) A. Teixeira Micromegas Pad Resistive Read-Out with Embedded Protection Resistor Production, https://indico.cern.ch/event/356113/contributions/1766894

(embedded resistors previously mentioned)

Towards conclusions…

Just some slides shared between the different upgrades

FE Electronics

Experiment	Detector	Electronics
ALICE TPC	GEM	Sampa (1)
ATLAS NSW	MM	VMM3a (2)
CMS GE1/1, GE2/1, ME0	GEM	VFAT3 (3)
LHCb M2-M5	µRWELL	FATIC++ (4)

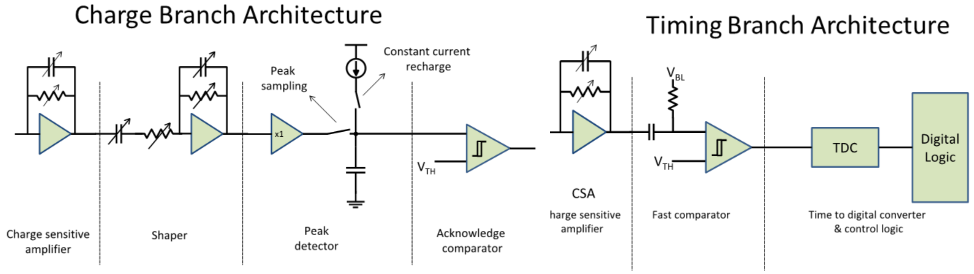

CSA features (High gain & 15 pF input capacitance):
- Dynamic ≈ 15 fC @ low gain; 60 fC @ High gain
- Peaking time ≈ 8ns
- Time jitter s ≈ 350ps with 6180e- (1fC input charge)
- ENC ≈ 18.5e-/pF*Cin+227.5e- (505e- Cin=15pF)
- Current consumption ≈ 1mA
- Technology node: 130nm

CSA settings:
- Input signal polarity: positive & negative • Gain: High ≈ 50mV/fC, Low ≈ 10 mV/fC
- Dynamic ≈ 15 fC @ low gain; 60 fC @ High gain
- Recovery time: adjustable

Shaper feature:
- Peaking time: 25ns, 50ns, 75ns, 100ns (polarity adj.)

Fast Comparator:
- Threshold from 0 to 76.5ke-, step 300e-

TDC resolution:
- 100ps (5 bits fine + 16 bits coarse)

(4) FATIC2: 32 chs ASIC (PRELIMINARY) F.Liciulli - G.De Robertis - INFN - Sezione di Bari, (pirvate comm. G. Felici LNF)

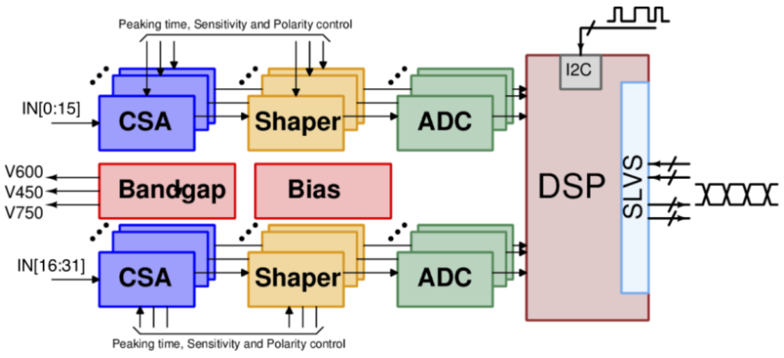

Figure 1. Sampa block diagram

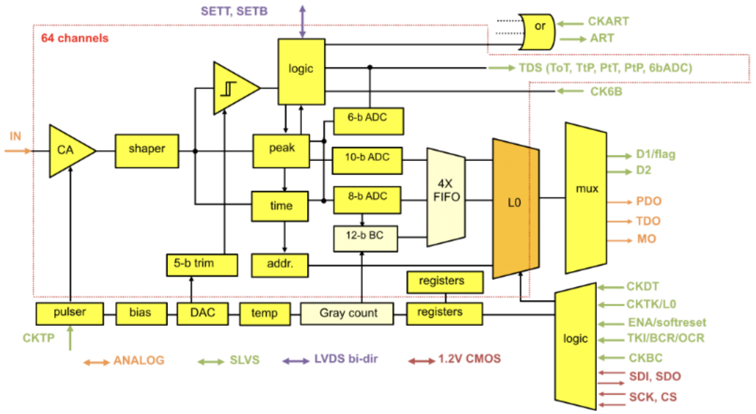

Figure 2. Architecture of the VMM.

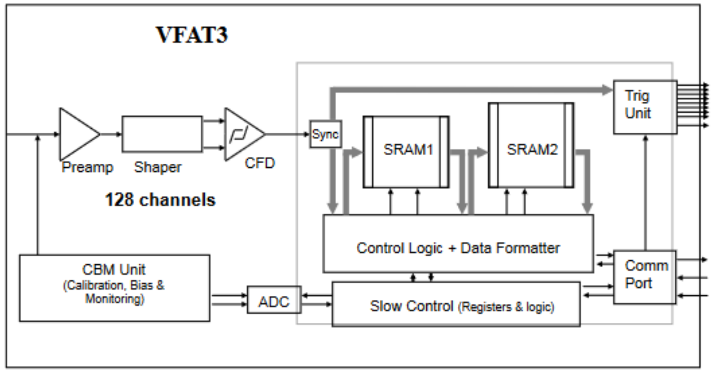

Figure 2: Block diagram of the VFAT3 ASIC

(1) https://indico.cern.ch/event/617831/attachments/1428015/2191906/TWEPP16_Bregant_minorRevised.pdf
Combines functions of the PASA (analog) and ALTRO (digital) chips currently being used

(2) https://iopscience.iop.org/article/10.1088/1742-6596/1498/1/012051/pdf

(3) DOI: 10.1109/NSSMIC.2018.8824655
Update of TOTEM VFAT2

MPGD (m^2)

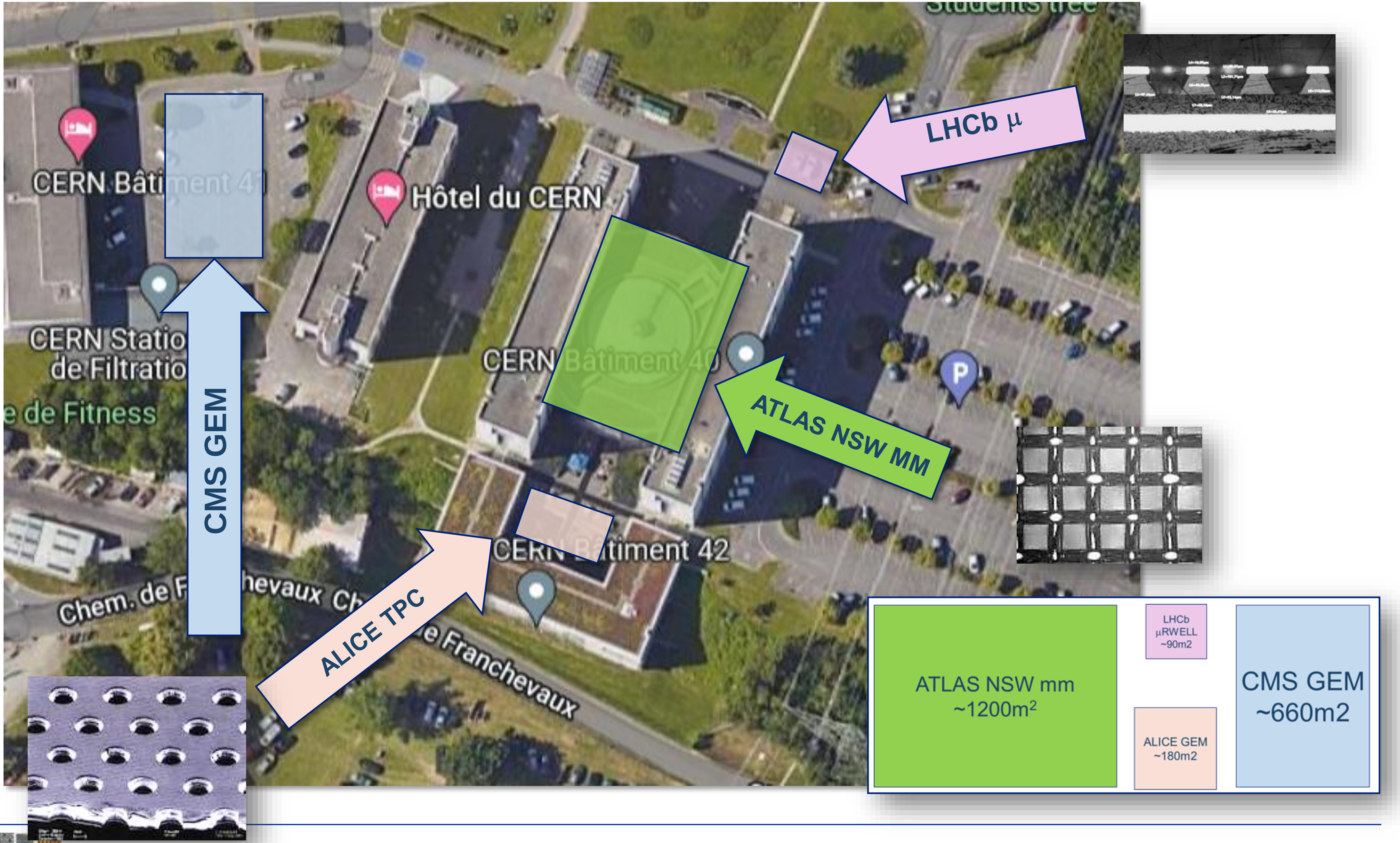

CERN Bâtiment 41
Hôtel du CERN
CERN Bâtiment 40
CERN Bâtiment 42
e de Fitness
Chem. de Franchevaux
CMS GEM
LHCb µ
ATLAS NSW MM
ALICE TPC
ATLAS NSW mm
~1200m²
LHCb
µRWELL
~90m2
ALICE GEM
~180m2
CMS GEM
~660m2

MPGD Productions for HL-LHC

	ALICE	ATLAS	CMS GEM	LHCb Muon
Detector	TPC	Muon tracking/triggering	Muon Tracking/Triggering	Muon Tracking
Station (# of aligned detectors)	1 (Single Station, no redundancy)	8 stations (+8sTGC)	2/2/6	16 (4 gaps in the 4 M-stations M2,M3, M4, M5)
Technology	GEM	Resistive MicroMegas	GEM	mRWELL
Area	32m2	1200m2	48/98/76 m2	~22m2
MPGD production area	32*4~120m2	1200m2	220*3~660m2	~90m2
N. Detector	36IROC+36OROC	128 detector (32x4 Modules)	144/72/216	576 gaps
Production	MPT	ELTOS/ELVIA (mm)	MPT/Korea/Techtra	MPT&ELTOS
Assembly & QA/QC	Sequential and distributed at different sites	Four main production chains connected to the four modules	Parallel and at different CMS sites	MPT&LNF

Timeline (Detector Installation)

Experiment	Detector	R&D Start	Installation
ALICE TPC	GEM	~2012	2021
ATLAS NSW	MM	~2007	2021
CMS GE1/1, GE2/1, ME0	GEM	~2009	2021/2024(5)/2026++
LHCb M2-M5	µRWELL	~2015	2026++

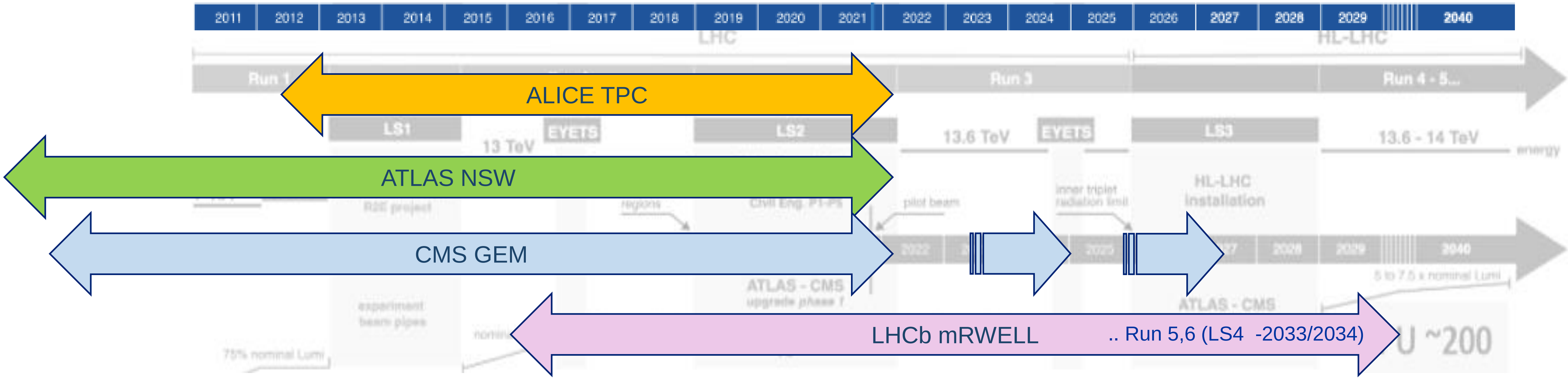

	ALICE TPC	ATLAS NSW	CMS GE1/1	CMS GE2/1	CMS ME0	LHCb
Technology	GEM (4)	Resistive Micromegas	GEM (3)	GEM(3)	GEM(3)	mRWELL
Requirements	50 kHz Pb-Pb rate; - Continuous TPC readout - Low IBF (<1-2%) and good energy resolution (12%@6keV)	Tracking/Triggering	Tracking/Triggering	Tracking/Triggering	Tracking/Triggering	Rate up to 1 MHz/cm^2 - Efficiency quadrigap >=99% within BX 25 ns
|η|			1.6–2.15	1.6–2.4	2.0–2.8	
Rate [Hz/cm2]	10 kHz/cm^2	<15 kHz/cm2	0.1 - 3 kHz/cm2	0.3 - 5 kHz/cm2	3-150 kHz/cm2	1 MHz/cm^2
Current Density	10 nC/(cm^2 s)					Up to 20 nA/cm2
Total Accumulated Charge	100 mC/cm^2	~ 0.5C/cm2	150 mC/cm2	150 mC/cm2 (M1, most exposed)	8C/cm2	1 C/cm^2 in 10 years for G=4000
Radiation	Flux of fast hadrons (> 20 MeV) at the TPC inner (outer) layer is expected to reach 3.4 kHz/cm 2 (0.7 kHz/cm2), including a safety factor of 2. TPC Electronics IR 2.1 krad.		1469 Hz/m2(hit rate) n~500,ph~850, e+/-~123	672Hz/m2 (hit rate) n~343,ph~273, e+/-~56	47510Hz/m2 (hit rate) n~5910,ph~33900, e+/-~7700	
Required Granularity	Pads (I: 0.4x0.75 cm2, O: 0.6x1cm2, 0.6x1.5cm2)					Pads, 1 cm2 in R1
Active Area	32 m2 72 (36IROC and 36OROC) readout chamber – 177m2 GEM	1200 m2 128 detector (32x4 Modules) Single unit detect: 2-3 m2	42m2 144 Chambers / 2 layers	97m2 72 chamber / 2 layers	76m2 216 Chambers / 6 layers	22 m2 corresponding to 90 m2 HR uRWELL detector units
Space Resolution	~250µm	<100um	200-340um	200-410um	160-390um	
Time Resolution	~ 100 ns	~ 10 ns	~ 8ns	~ 8ns	~ 8ns	5ns
Energy resolution	12 % (Fe55)					
Gain	2000		1-2e+4	1-2e+4	1-2e+4	4000
Efficiency	Min 50% transmission efficiency 1st GEM for energy resolution					quadrigap >=99% within BX 25 ns
S/N	20					
Gas	Ne-CO2-N2 90-10-5	Ar/CO2/iC4H10 93/5/2 (Ar/CO2 93/7)	Ar/CO2 70/30	Ar/CO2 70/30	Ar/CO2 70/30	Ar/CO2/CF4 45/15/40 - Ar/CO2/iC4H10 68/30/2
FE	waveform	Amplitude and time	VFAT3 (Binary)	VFAT3 (Binary)	VFAT3 (Binary)	FATIC++ (under development)

The PBC (physics beyond collider) Program @ CERN

Towards and during the HL-LHC era, but beyond the collider…

Physics Beyond Colliders

Annual Workshop: https://indico.cern.ch/event/1137276/timetable/#20221107.detailed

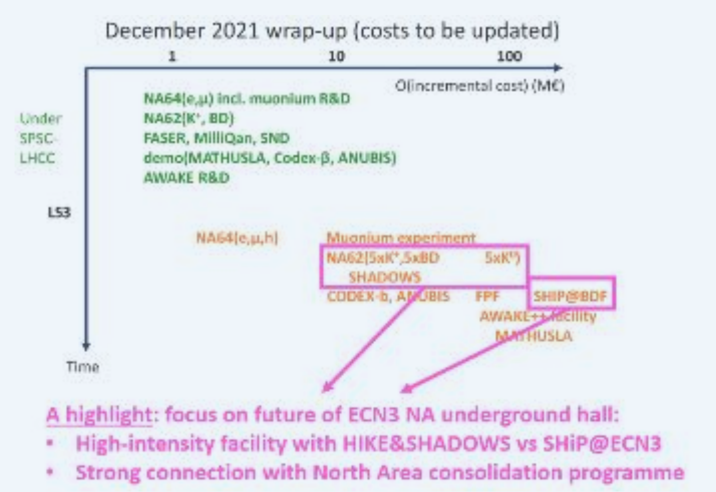

PBC BSM Landscape

- post-LS3 experiments in the North Area ECN3
- LHC Long-lived Particles (LLP, https://arxiv.org/ftp/arxiv/papers/1903/1903.04497.pdf)

PBC R&D Landscape

PBC QCD Landscape

- Fixed Target Experiments
- NA Ions

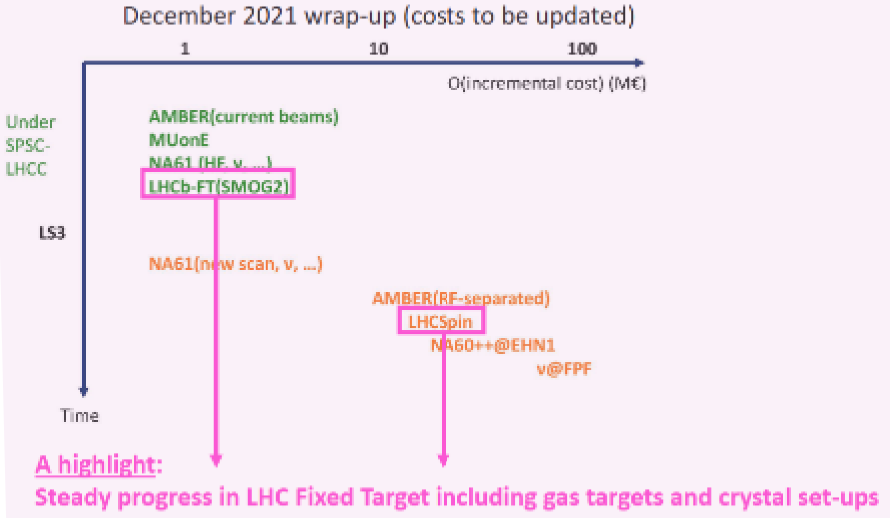

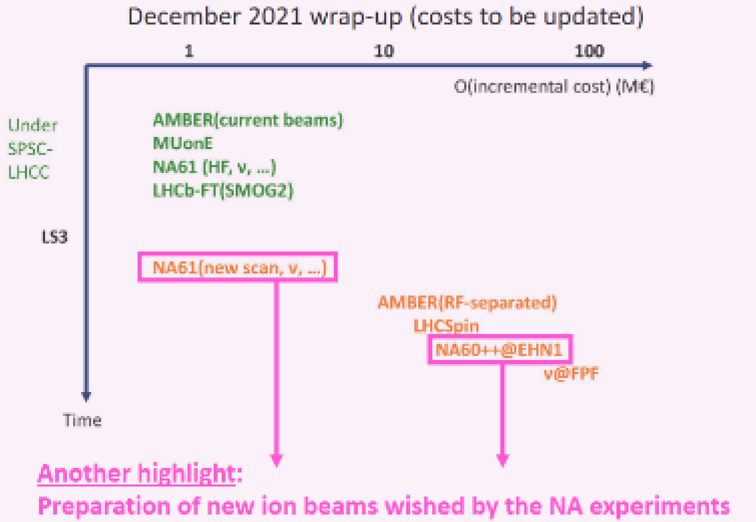

Introduction and scope of the workshop, C. Vallee, Physics Beyond Colliders Annual Workshop, Nov.2022, CERN, https://indico.cern.ch/event/1137276/contributions/4950647/attachments/2542101/4376929/PBC_introduction.pdf

Contribution @ MPGD 2022 of HL-LHC MPGD upgrades

- **Philip Hauer**, Gain Calibration of the Upgraded ALICE TPC

- **Giada Mancini**, Ready for LHC Run III - The ATLAS New Small Wheel and the MicroMegas chambers performances
- **Paolo Iengo**, The industrial production of Micro Pattern Gaseous Detector: experience from the ATLAS Micromegas
- **Mauro Iodice**, Towards Large Size Pixelized Micromegas for operation beyond 1 MHz/cm2
- **Paolo Iengo**, Accelerated longevity test of Resistive Micromegas detectors operated with and without small amount of hydrocarbons.

- **Piet Verwilligen**, GEM Detectors for the CMS Endcap Muon System: status of three new detector stations
- **Simone Calzaferri**, Study of discharges in the CMS GEM GE1/1 station with LHC beam
- **Antonello Pellecchia**, Michele Bianco, Production and characterization of random electrode sectorization in GEM foils

- **Marco Poli Lener**, The state of art of the µRWELL technology

Plus many contributions connected to the R&D performed for the upgrades or by the groups involved in the upgrades or for detectors considered for the upgrades…

(A Visual) summary

ALICE GEM-TPC

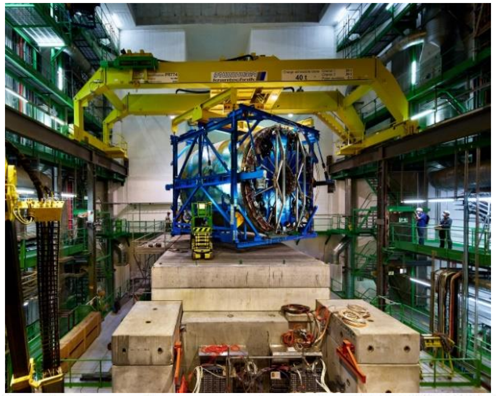

https://ep-news.web.cern.ch/upgraded-alice-tpc

ATLAS NSW

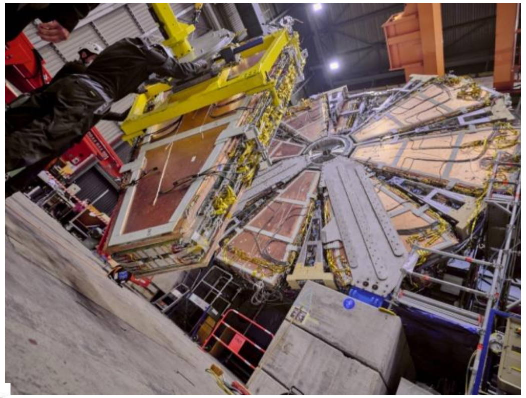

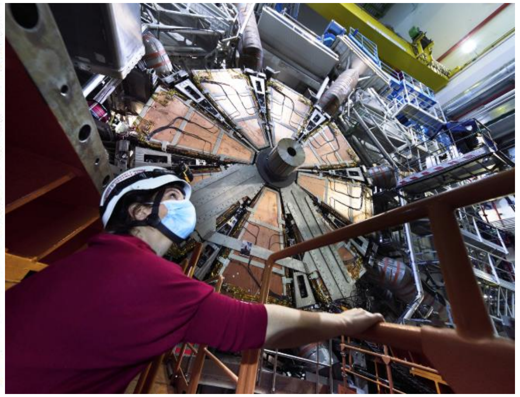

https://ep-news.web.cern.ch/content/atlas-new-small-wheel-upgrade-advances-0

CMS GEM

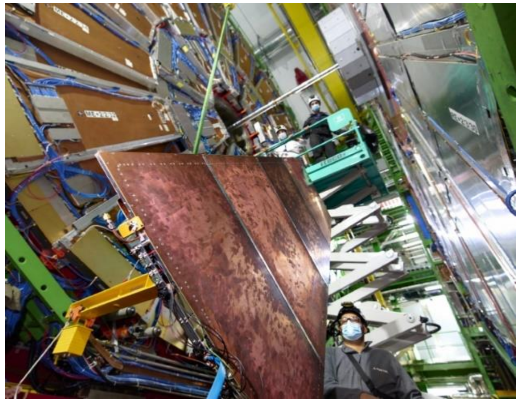

https://ep-news.web.cern.ch/content/demonstrating-capabilities-new-gem

LHCb µRWELL

A special thank to Chilo Garabatos, Gianfranco Morello, Giovanni Bencivenni, Giulietto Felici, Mauro Iodice, Michele Bianco, Paolo Iengo, Piotr Gasik, Robert Helmut Munzer for helping on collecting updated information

Backup

High Luminosity LHC (II)

Parameter	Nominal LHC	HL-LHC 25ns	HL-LHC 25ns (BCMS)	HL-LHC 50ns
Beam energy in collision [TeV]	7	7	7	7
N_b	1.15E+11	2.20E+11	2.20E+11	3.50E+11
n_b	2808	2748	2604	1404
Number of collisions in IP1 and IP5	2808	2736	2592	1404
N_{tot}	3.20E+14	6.00E+14	5.70E+14	4.90E+14
beam Current [A]	0.58	1.09	1.03	0.89
x-ing angle [μrad]	285	590	590	590
beam separation [σ]	9.4	12.5	12.5	11.4
β* [m]	0.55	0.15	0.15	0.15
ε_n [μm]	3.75	2.5	2.5	3
ε_L [eVs]	2.5	2.5	2.5	2.5
r.m.s. energy spread	1.13E-04	1.13E-04	1.13E-04	1.13E-04
r.m.s. bunch length [m]	7.55E-02	7.55E-02	7.55E-02	7.55E-02
IBS horizontal [h]	80->160	18.5	18.5	17.2
IBS longitudinal [h]	61->60	20.4	20.4	16.1
Piwinski parameter	0.65	3.14	3.14	2.87
Geometric loss factor R0 without crab-cavity	0.836	0.305	0.305	0.331
Geometric loss factor R1 with crab-cavity	-0.981	0.829	0.829	0.838
beam-beam / IP without Crab Cavity	3.1E-03	3.3E-03	3.3E-03	4.7E-03
beam-beam / IP with Crab cavity	3.8E-03	1.1E-02	1.1E-02	1.4E-02
Peak Luminosity without crab-cavity [cm-2 s-1]	1.00E+34	7.18E+34	6.80E+34	8.44E+34
Virtual Luminosity with crab-cavity: Lpeak*R1/R0 [cm-2 s-1]	1.18E+34	1.95E+35	1.85E+35	2.14E+35
Events / crossing without levelling and without crab-cavity	27	198	198	454
Leveled Luminosity [cm-2 s-1]		5.00E+34	5.00E+34	2.50E+34
Events / crossing (with leveling and crab-cavities for HL-LHC)	27	138	146	135
Peak line density of pile up event [event/mm] (max over stable beams)	0.21	1.25	1.31	1.2
Leveling time [h] (assuming no emittance growth)	8.3	7.6	18	
Number of collisions in IP2/IP8	2808	2452/2524	2288/2396	0/1404
N b at SPS extraction	1.20E+11	2.30E+11	2.30E+11	3.68E+11
n b / injection	288	288	288	144
N tot / injection	3.46E+13	6.62E+13	6.62E+13	5.30E+13
ε_n at SPS extraction [μm]	3.4	2	<2	2.3

Introduction to the HL-LHC Project Rossi , L (CERN) ; Brüning, O (CERN), Adv. Ser. Dir. High Energy Phys. 24 (2015) 1-17, The High Luminosity Large Hadron Collider, pp.1-17, DOI 10.1142/9789814675475_0001, https://cds.cern.ch/record/2130736/files/Introduction%20to%20the%20HL-LHC%20Project.pdf

High Luminosity LHC (II)

$$L = \gamma \frac{n_b N^2 f_{\text{rev}}}{4\pi \beta^* \varepsilon_n} R; \; R = 1 \Big/ \sqrt{1 + \frac{\theta_c \sigma_z}{2\sigma}}$$

γ is the proton beam energy in unit of rest mass;
n_b is the number of bunches in the machine: 1380 for 50 ns spacing and 2808 for 25 ns;
N is the bunch population. $N_{\text{nominal 25 ns}}$: 1.15×10^{11} p ($\Rightarrow$ 0.58 A of beam current at 2808 bunches);
f_{rev} is the revolution frequency (11.2 kHz);
β^* is the beam beta function (focal length) at the collision point (nominal design 0.55 m);
ε_n is the transverse normalized emittance (nominal design: 3.75 μm);
R is a luminosity geometrical reduction factor (0.85 at 0.55 m of β^*, down to 0.5 at 0.25 m);
θ_c is the full crossing angle between colliding beam (285 μrad as nominal design);
σ, σ_z are the transverse and longitudinal r.m.s. size, respectively (16.7 μm and 7.55 cm).

Introduction to the HL-LHC Project Rossi , L (CERN) ; Brüning, O (CERN), Adv. Ser. Dir. High Energy Phys. 24 (2015) 1-17, The High Luminosity Large Hadron Collider, pp.1-17, DOI 10.1142/9789814675475_0001, https://cds.cern.ch/record/2130736/files/Introduction%20to%20the%20HL-LHC%20Project.pdf

Physics Motivation for the High Luminosity LHC

Report on the Physics at the HL-LHC, and Perspectives for the HE-LHC
CERN-2019-007, HL/HE-LHC Workshop : Workshop on the Physics of HL-LHC, and Perspectives at HE-LHC, Geneva, Switzerland, 18 - 20 Jun 2018

The HL-LHC project will deliver (a) pp collisions at 14 TeV with an integrated luminosity of 3 ab−1 each for ATLAS and CMS and 50 fb−1 for LHCb, and (b) PbPb and pPb collisions with integrated luminosities of 13 nb−1 and 50 nb−1, respectively.

1. *Standard Model measurements*
2. *Studies of the properties of the Higgs boson*
3. *Searches for phenomena beyond the Standard Model*
4. *Flavour physics of heavy quarks and leptons*
5. *Studies of QCD matter at high density and temperature*

Physics Motivation for the High Luminosity LHC

Report on the Physics at the HL-LHC, and Perspectives for the HE-LHC(*)

CERN-2019-007, HL/HE-LHC Workshop : Workshop on the Physics of HL-LHC, and Perspectives at HE-LHC, Geneva, Switzerland, 18 - 20 Jun 2018

Standard Model physics at the HL-LHC and HE-LHC

Abstract

The successful operation of the Large Hadron Collider (LHC) and the excellent performance of the ATLAS, CMS, LHCb and ALICE detectors in Run-1 and Run-2 with *pp* collisions at center-of-mass energies of 7, 8 and 13 TeV as well as the giant leap in precision calculations and modeling of fundamental interactions at hadron colliders have allowed an extraordinary breadth of physics studies including precision measurements of a variety physics processes. The LHC results have so far confirmed the validity of the Standard Model of particle physics up to unprecedented energy scales and with great precision in the sectors of strong and electroweak interactions as well as flavour physics, for instance in top quark physics. The upgrade of the LHC to a High Luminosity phase (HL-LHC) at 14 TeV center-of-mass energy with 3 ab^{-1} of integrated luminosity will probe the Standard Model with even greater precision and will extend the sensitivity to possible anomalies in the Standard Model, thanks to a ten-fold larger data set, upgraded detectors and expected improvements in the theoretical understanding. This document summarises the physics reach of the HL-LHC in the realm of strong and electroweak interactions and top quark physics, and provides a glimpse of the potential of a possible further upgrade of the LHC to a 27 TeV *pp* collider, the High-Energy LHC (HE-LHC), assumed to accumulate an integrated luminosity of 15 ab^{-1}.

Higgs physics at the HL-LHC and HE-LHC

Abstract

The discovery of the Higgs boson in 2012, by the ATLAS and CMS experiments, was a success achieved with only a percent of the entire dataset foreseen for the LHC. It opened a landscape of possibilities in the study of Higgs boson properties, Electroweak Symmetry breaking and the Standard Model in general, as well as new avenues in probing new physics beyond the Standard Model. Six years after the discovery, with a conspicuously larger dataset collected during LHC Run 2 at a 13 TeV centre-of-mass energy, the theory and experimental particle physics communities have started a meticulous exploration of the potential for precision measurements of its properties. This includes studies of Higgs boson production and decays processes, the search for rare decays and production modes, high energy observables, and searches for an extended electroweak symmetry breaking sector. This report summarises the potential reach and opportunities in Higgs physics during the High Luminosity phase of the LHC, with an expected dataset of pp collisions at 14 TeV, corresponding to an integrated luminosity of 3 ab^{-1}. These studies are performed in light of the most recent analyses from LHC collaborations and the latest theoretical developments. The potential of an LHC upgrade, colliding protons at a centre-of-mass energy of 27 TeV and producing a dataset corresponding to an integrated luminosity of 15 ab^{-1}, is also discussed.

(*) https://cds.cern.ch/record/2315725/files/9999999_138-141.pdf

Physics Motivation for the High Luminosity LHC

Report on the Physics at the HL-LHC, and Perspectives for the HE-LHC

CERN-2019-007, HL/HE-LHC Workshop : Workshop on the Physics of HL-LHC, and Perspectives at HE-LHC, Geneva, Switzerland, 18 - 20 Jun 2018

Beyond the Standard Model physics at the HL-LHC and HE-LHC

Abstract

This is the third out of five chapters of the final report [1] of the Workshop on *Physics at HL-LHC, and perspectives on HE-LHC* [2]. It is devoted to the study of the potential, in the search for Beyond the Standard Model (BSM) physics, of the High Luminosity (HL) phase of the LHC, defined as $3\ \mathrm{ab}^{-1}$ of data taken at a centre-of-mass energy of 14 TeV, and of a possible future upgrade, the High Energy (HE) LHC, defined as $15\ \mathrm{ab}^{-1}$ of data at a centre-of-mass energy of 27 TeV. We consider a large variety of new physics models, both in a simplified model fashion and in a more model-dependent one. A long list of contributions from the theory and experimental (ATLAS, CMS, LHCb) communities have been collected and merged together to give a complete, wide, and consistent view of future prospects for BSM physics at the considered colliders. On top of the usual *standard candles*, such as supersymmetric simplified models and resonances, considered for the evaluation of future collider potentials, this report contains results on dark matter and dark sectors, long lived particles, leptoquarks, sterile neutrinos, axion-like particles, heavy scalars, vector-like quarks, and more. Particular attention is placed, especially in the study of the HL-LHC prospects, to the detector upgrades, the assessment of the future systematic uncertainties, and new experimental techniques. The general conclusion is that the HL-LHC, on top of allowing to extend the present LHC mass and coupling reach by $20 - 50\%$ on most new physics scenarios, will also be able to constrain, and potentially discover, new physics that is presently unconstrained. Moreover, compared to the HL-LHC, the reach in most observables will generally more than double at the HE-LHC, which may represent a good candidate future facility for a final test of TeV-scale new physics.

Opportunities in **flavour physics** at the HL-LHC and HE-LHC

Abstract

Motivated by the success of the flavour physics programme carried out over the last decade at the Large Hadron Collider (LHC), we characterize in detail the physics potential of its High-Luminosity and High-Energy upgrades in this domain of physics. We document the extraordinary breadth of the HL/HE-LHC programme enabled by a putative Upgrade II of the dedicated flavour physics experiment LHCb and the evolution of the established flavour physics role of the ATLAS and CMS general purpose experiments. We connect the dedicated flavour physics programme to studies of the top quark, Higgs boson, and direct high-p_T searches for new particles and force carriers. We discuss the complementarity of their discovery potential for physics beyond the Standard Model, affirming the necessity to fully exploit the LHC's flavour physics potential throughout its upgrade eras.

Future physics opportunities for **high-density QCD** at the LHC with heavy-ion and proton beams

Abstract

The future opportunities for high-density QCD studies with ion and proton beams at the LHC are presented. Four major scientific goals are identified: the characterisation of the macroscopic long wavelength Quark-Gluon Plasma (QGP) properties with unprecedented precision, the investigation of the microscopic parton dynamics underlying QGP properties, the development of a unified picture of particle production and QCD dynamics from small (pp) to large (nucleus–nucleus) systems, the exploration of parton densities in nuclei in a broad (x, Q^2) kinematic range and the search for the possible onset of parton saturation. In order to address these scientific goals, high-luminosity Pb–Pb and p–Pb programmes are considered as priorities for Runs 3 and 4, complemented by high-multiplicity studies in pp collisions and a short run with oxygen ions. High-luminosity runs with intermediate-mass nuclei, for example Ar or Kr, are considered as an appealing case for extending the heavy-ion programme at the LHC beyond Run 4. The potential of the High-Energy LHC to probe QCD matter with newly-available observables, at twice larger center-of-mass energies than the LHC, is investigated.

ALICE GEM TPC: Common mode, Ion Tail

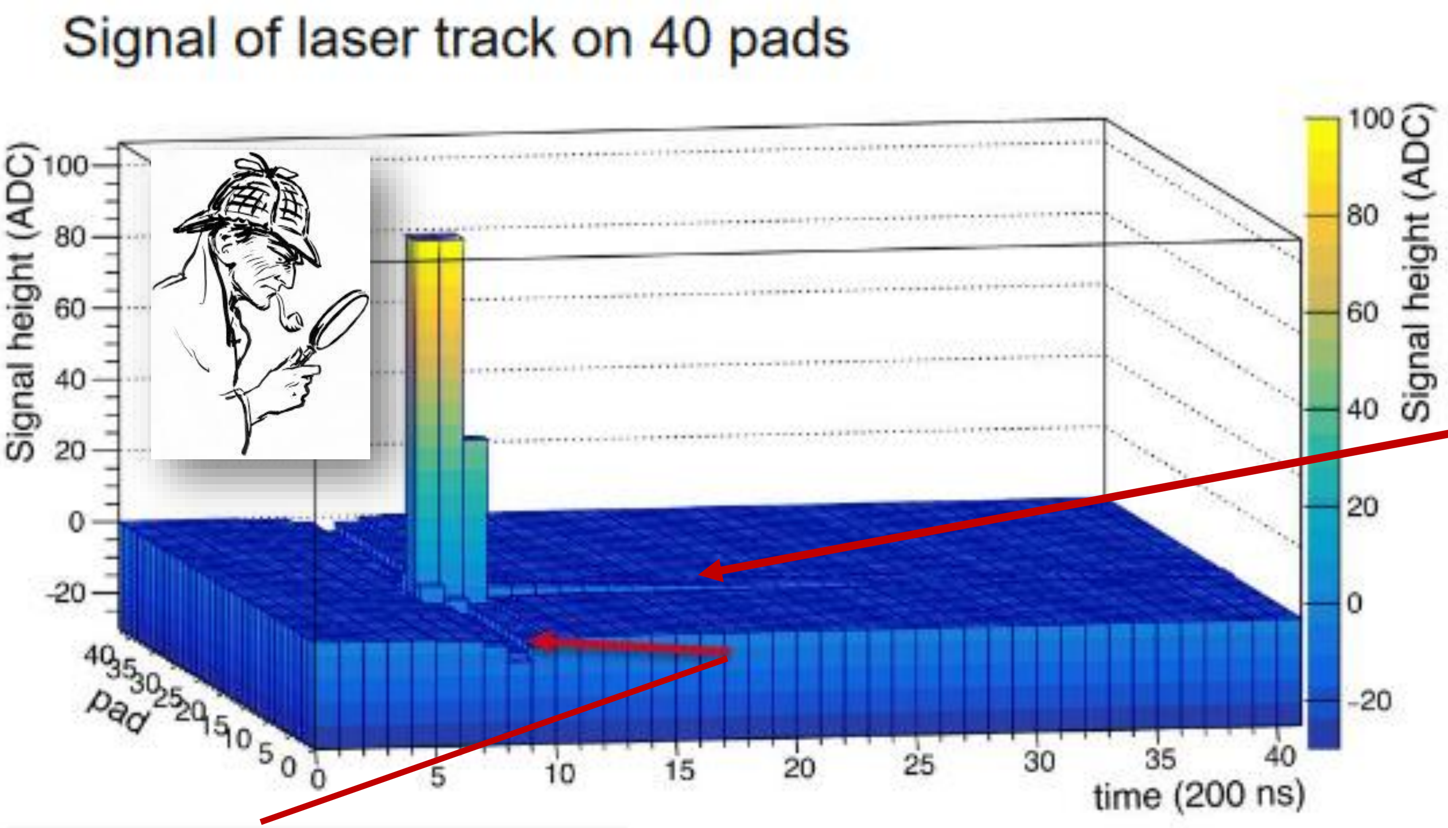

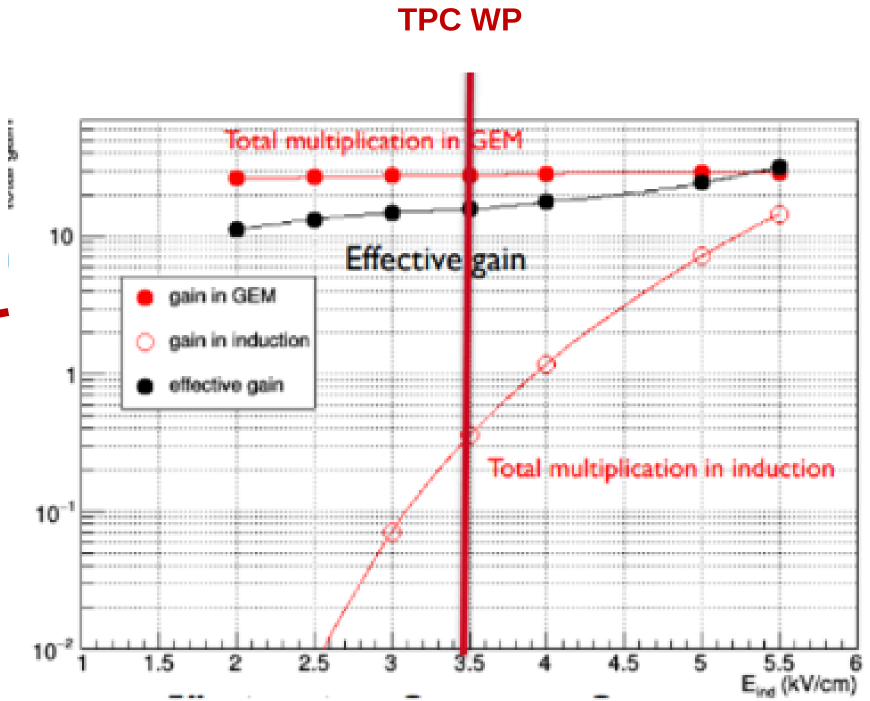

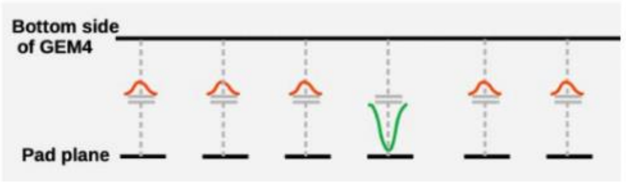

R. H. Munzer, Continuous data taking with the upgraded ALICE GEM-TPC, CERN EP Detector Seminar, 24/6/2022, https://indico.cern.ch/event/1172978/

ALICE GEM TPC: Magnetic Field

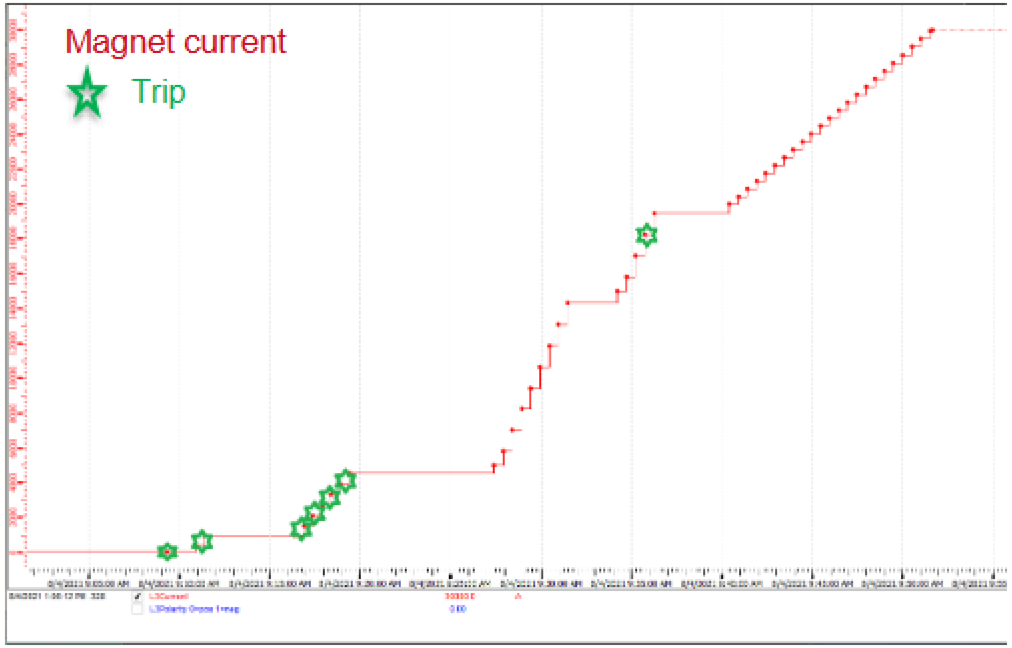

Instabilities during magnet ramp observed as well in CMS GEM and ATLAS NSW MM

Hypothesis:
- *Ramping up or down of E and B fields may cause dust particles to move, if they carry charge*
- *Dust particles on electrodes, moving inside GEM holes, either melts (short+ trip) or evaporates (only trip)*

Solution:
- *Keep GEMs at full voltage while magnet is ramping Trip rate during magnet ramp reduced over time; not much dust on GEMs*
- *No further issue observed with this procedure*

R. H. Munzer, Continuous data taking with the upgraded ALICE GEM-TPC, CERN EP Detector Seminar, 24/6/2022, https://indico.cern.ch/event/1172978/

RPC Upgrade for HL-LHC

The challenge of making the chambers compatible with operation at higher hit rates is addressed by:

- *a **reduction of the gas gain** (or charge per count) …*
- *a reduction of gas gaps from 2 to 1 mm (less voltage, thinner chamber, from about 1.1 ns to 0.4 ns **time resolution**, improved avalanche transfer efficiency (**better S/N**))*
- *a simultaneous **increase of the sensitivity and signal-to-noise ratio of the front-end electronics**, preserving the RPC fast timing capability...*

*The new-generation RPCs have an **increased rate capability by an order of magnitude**, a decreased total chamber weight and thickness, and **operate at around half the working voltage**. They are **compatible with the use of low-GWP mixtures**.*

Reduce the gain

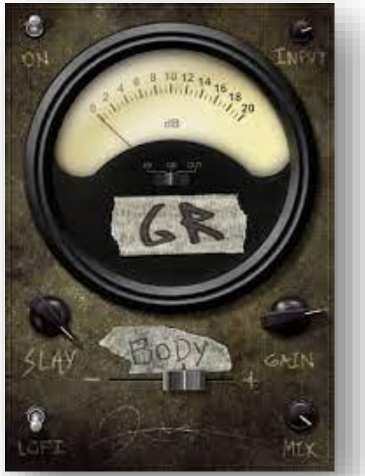

Optimize the signal

CERN-LHCC-2017-017 ; ATLAS-TDR-026, Technical Design Report for the Phase-II Upgrade of the ATLAS Muon Spectrometer, http://cds.cern.ch/record/2285580/

CMS Muon Spectrometer Upgrade

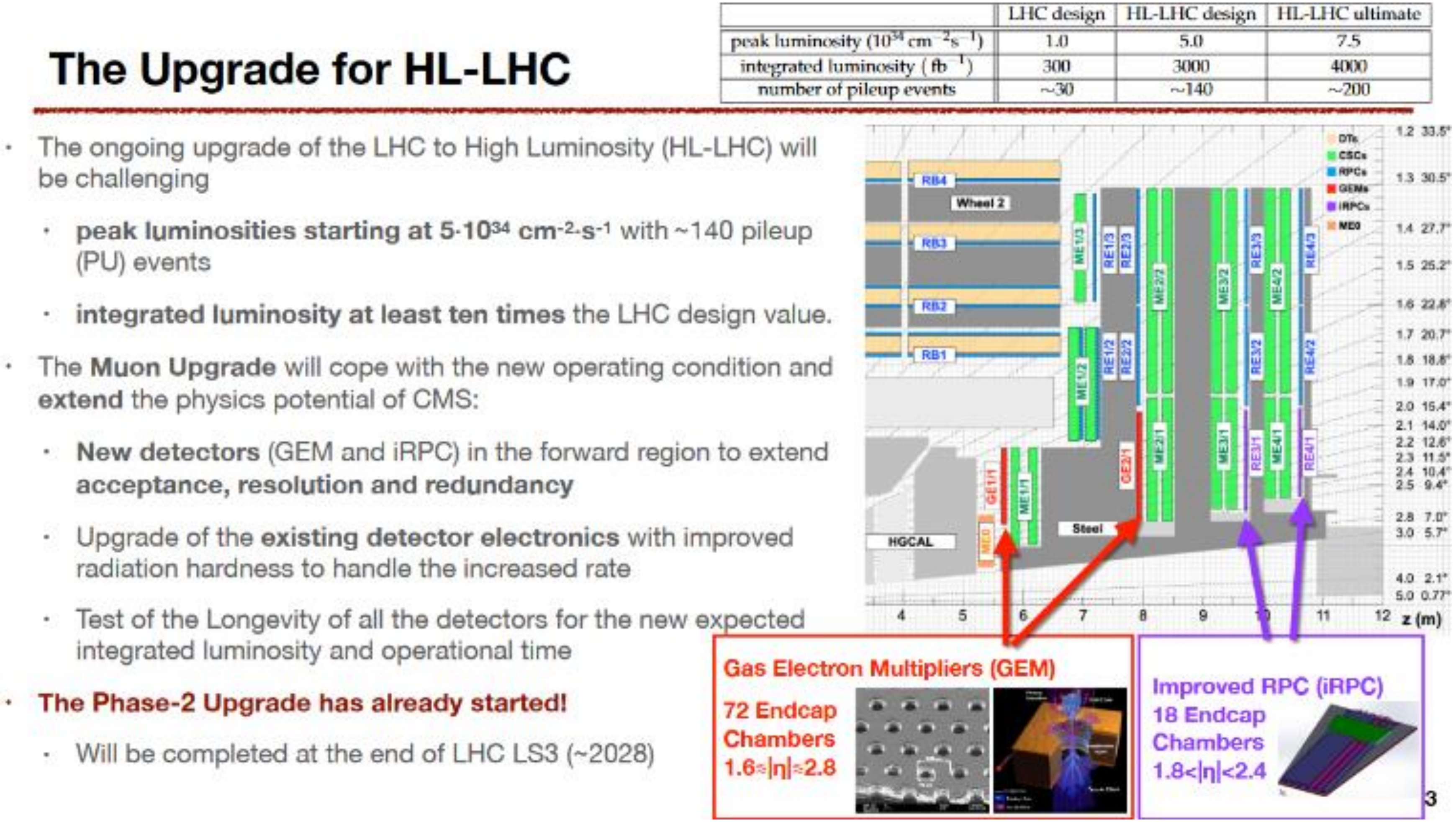

The Upgrade for HL-LHC

	LHC design	HL-LHC design	HL-LHC ultimate
peak luminosity (10^{34} cm^{-2}s^{-1})	1.0	5.0	7.5
integrated luminosity (fb^{-1})	300	3000	4000
number of pileup events	~30	~140	~200

- The ongoing upgrade of the LHC to High Luminosity (HL-LHC) will be challenging
  - **peak luminosities starting at 5·10^{34} cm^{-2}·s^{-1}** with ~140 pileup (PU) events
  - **integrated luminosity at least ten times** the LHC design value.
- The **Muon Upgrade** will cope with the new operating condition and **extend** the physics potential of CMS:
  - **New detectors** (GEM and iRPC) in the forward region to extend **acceptance, resolution and redundancy**
  - Upgrade of the **existing detector electronics** with improved radiation hardness to handle the increased rate
  - Test of the Longevity of all the detectors for the new expected integrated luminosity and operational time
- **The Phase-2 Upgrade has already started!**
  - Will be completed at the end of LHC LS3 (~2028)

- Existing Detectors compatible with HL-LHC expected rates and dose
- New detectors to extend acceptance and resolution (GEM and RPC)
- Electronics changed to improve trigger

D. Fasanella, The CMS Muon Spectrometer Upgrade, https://indico.cern.ch/event/868940/contributions/3813866/attachments/2080933/3495211/ICHEP_Fasanella.pdf

CMS Muons (GE1/1, GE2/1, ME0)

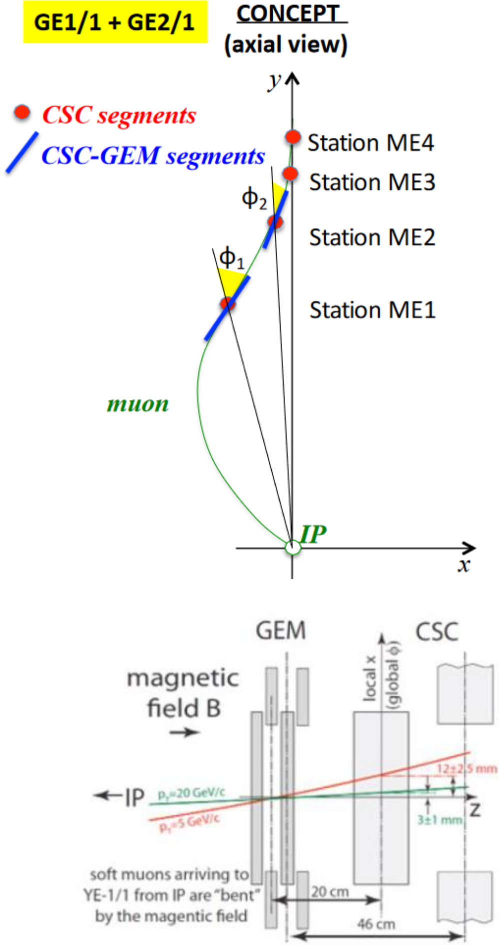

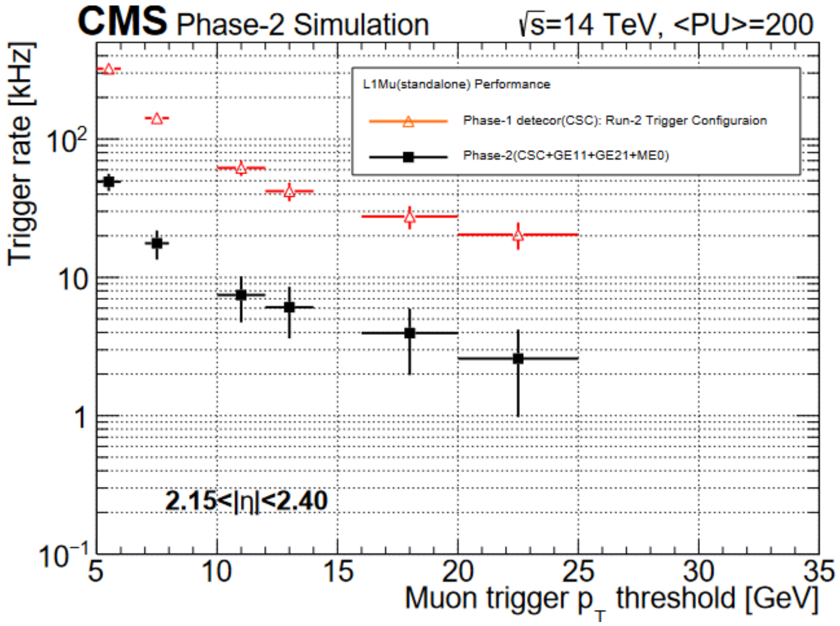

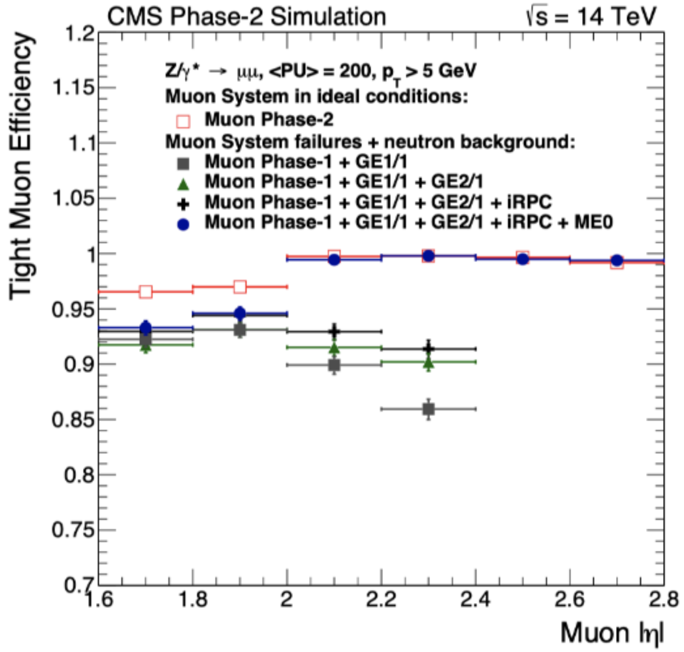

ME0 extends acceptance into 2.4 < |η| < 2.8.
The increased muon acceptance is fully covered by the new Phase-2 inner silicon tracker

M. Bianco, The GEM detectors within the CMS Experiment, CERN EP Detector Seminar, 8/7/2022, https://indico.cern.ch/event/1175363/

CMS

The iRPC Project

Specification	RPC	iRPC
$\|\eta\|$ coverage	0-1.8	1.9-2.4
Max. expected rate (safety factor 3 included)	600 Hz/cm^2	2 kHz/cm^2
Max. Integrated charge (safety factor 3 included)	~ 0.8 C/cm^2	~ 1 C/cm^2
High Pressure Laminate thickness	2 mm	1.4 mm
Number and thickness of gas gap	2 and 2 mm	2 and 1.4 mm
Resistivity (Ωcm)	1 - 6 x 10^{10}	0.9 - 3 x 10^{10}
Charge threshold	150 fC	50 fC

- Installation of 72 iRPC with **increased rate capability** by a factor of ~3:
  - **Lower Electrodes thickness**: 1.4mm
    - Reduce the **recovery time**
    - Increase in efficiency of extracting the pickup charge from the avalanche charge.
  - Decrease **Gas Gap thickness** to 1.4mm
    - **reduces the fast growth of pickup charge** of the ionization avalanches
    - lowers the operational high voltage making system more robust than before
      - less chance of ageing.
  - **Electronic Thresholds at 50 fC**
    - Lower threshold electronic helps to provide better sensitivity to reduce charge
- Improved performance providing **measurements in 2D**
  - strips are readout from both ends
- **Services are being installed in L2**
- Installation possible before LS3 in a YETS 23/24

Fiber optics box installed back of YE-3 and Y+3


Gas impedance boxes


RE4.1 Cooling

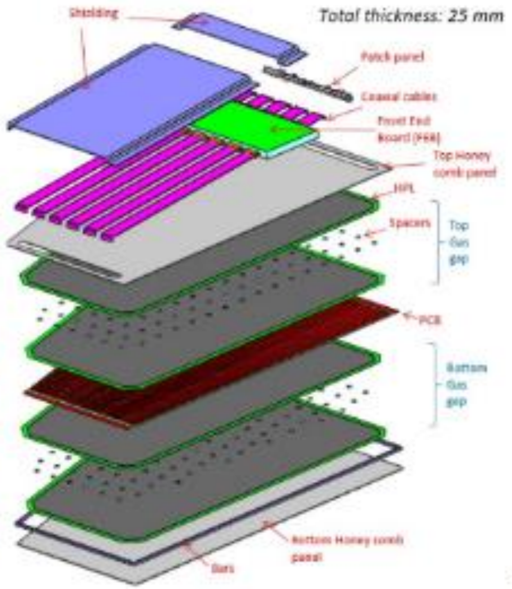

12

D. Fasanella, The CMS Muon Spectrometer Upgrade , https://indico.cern.ch/event/868940/contributions/3813866/attachments/2080933/3495211/ICHEP_Fasanella.pdf

µRWELL (PEP)

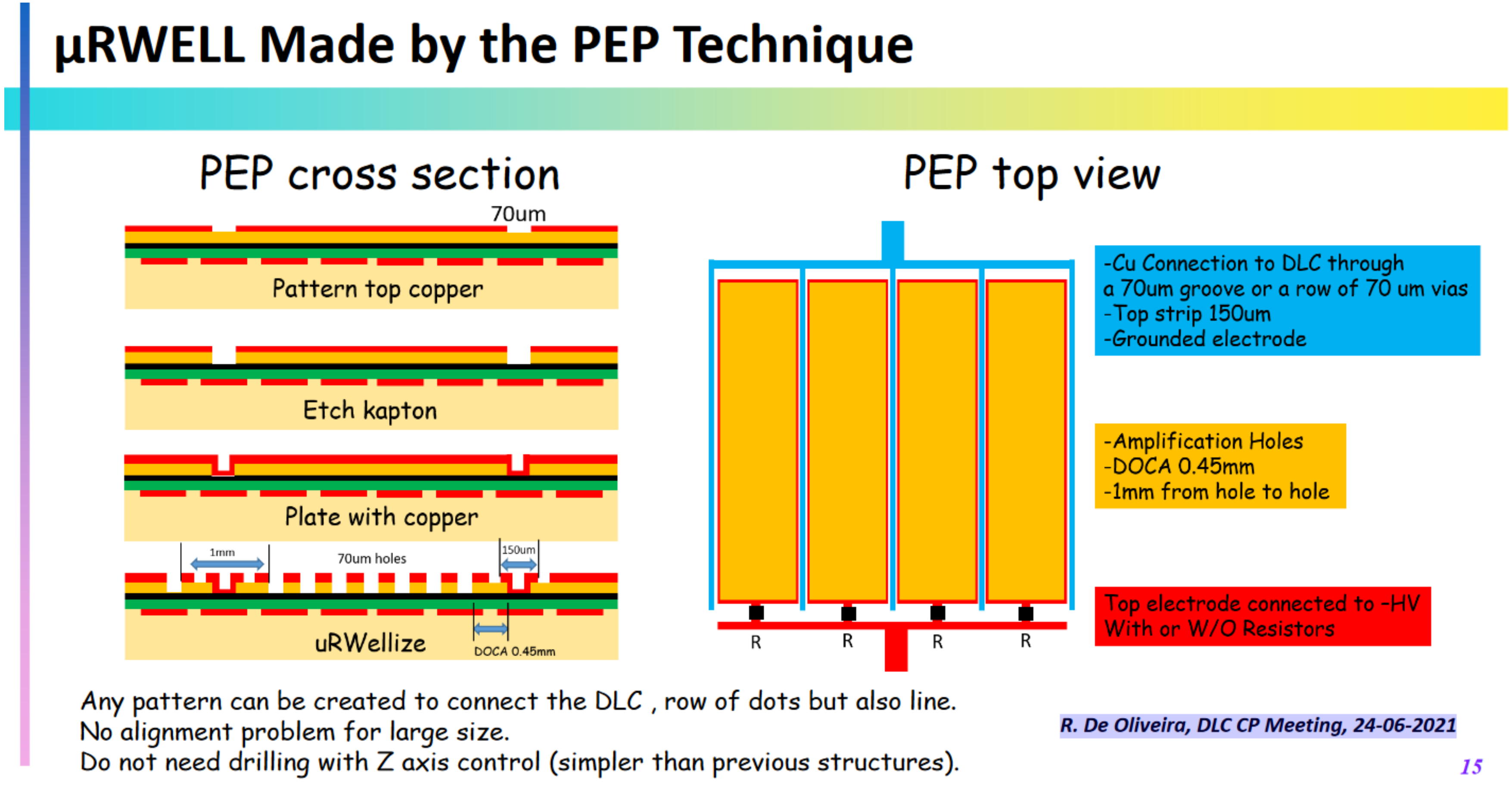

Resistive Detectors with Diamond-Like Carbon(DLC), Yi Zhou, The 10th Symposium on Large TPCs for Low-Energy Rare Events Detection https://indico.cern.ch/event/852331/contributions/4611238/
Resistive MPGD Processes and problems, Rui de Oliveira 12/02/2020, CERN RD51 mini-week https://indico.cern.ch/event/872501/contributions/3723342/

Main References

- *Rossi , L (CERN) ; Brüning, O (CERN), Introduction to the HL-LHC Project, Adv. Ser. Dir. High Energy Phys. 24 (2015) 1-17, The High Luminosity Large Hadron Collider, pp.1-17, DOI 10.1142/9789814675475_0001*
- *B. Schmidt 2016 J. Phys.: Conf. Ser. 706 022002 https://iopscience.iop.org/article/10.1088/1742-6596/706/2/022002/pdf*
- *C. Lacasta, Detector Upgrades for the HL-LHC, XIII CPAN DAYS, March 2022, Huelva, https://indico.ific.uv.es/event/6457/contributions/17779/attachments/10004/13374/Detector.Upgrades.CPAN22.pdf*
- *CERN-LHCC-2017-017 ; **ATLAS-TDR-026**, Technical Design Report for the Phase-II Upgrade of the ATLAS Muon Spectrometer, http://cds.cern.ch/record/2285580/*
- *CERN-LHCC-2013-006; **ATLAS-TDR-020**, Technical Design Report New Small Wheel, https://cds.cern.ch/record/1552862/*
- *T. Vafeiadis, The New Small Wheel project of ATLAS, CERN EP Detector Seminar 17/6/2022, https://indico.cern.ch/event/1168778/*
- *CERN-LHCC-2017-012 ; **CMS-TDR-016**, The Phase-2 Upgrade of the CMS Muon Detectors, https://cds.cern.ch/record/2283189/files/CMS-TDR-016.pdf*
- *R. H. Munzer, Continuous data taking with the upgraded ALICE GEM-TPC, CERN EP Detector Seminar, 24/6/2022, https://indico.cern.ch/event/1172978/*
- *M. Bianco, The GEM detectors within the CMS Experiment, CERN EP Detector Seminar, 8/7/2022, https://indico.cern.ch/event/1175363/*
- *CERN-LHCC-2013-022 ; **LHCB-TDR-014**, LHCb PID Upgrade Technical Design Report, https://cds.cern.ch/record/001624074*
- *CERN-LHCC-2017-003, **Expression of Interest for a Phase-II LHCb Upgrade**: Opportunities in flavour physics, and beyond, in the HL-LHC era, https://cds.cern.ch/record/2244311/*
- *CERN-LHCC-2021-012 ; LHCB-TDR-023, **Framework TDR for the LHCb Upgrade II** - Opportunities in flavour physics, and beyond, in the HL-LHC era, https://cds.cern.ch/record/2776420/*
- *G. Morello, The micro-RWELL detector for the LHCb Muon system phase-2 upgrade, ICHEP 2022, https://agenda.infn.it/event/28874/contributions/169584/*
- *CERN-LHCC-2013-020 ; **ALICE-TDR-016,** Upgrade of the ALICE Time Projection Chamber, https://cds.cern.ch/record/1622286*
- …

home.cern